



**Aalto University
School of Chemical
Technology**

**School of Chemical Technology
Degree Programme of Materials Science and Engineering**

Sini Eskonniemi

**TECHNICAL TESTING AND APPLICABILITY OF A X-RAY FLUORESCENCE
DEVICE FOR METAL RECYCLING**

**Master's thesis for the degree of Master of Science in Technology submitted for
inspection, Espoo, 24 March, 2015.**

Supervisor

Professor Kari Heiskanen

Instructors

Lic.Sc. Jyri Talja

M.Sc. Tiina Malin

Author Sini Orvokki Eskonniemi

Title of thesis TECHNICAL TESTING AND APPLICABILITY OF A X-RAY FLUORESCENCE DEVICE FOR METAL RECYCLING

Department Department of Materials Science and Engineering

Professorship Mechanical Processing and Recycling **Code of professorship** Mak-46

Thesis supervisor Professor Kari Heiskanen

Thesis advisors Lic.Sc.(Tech.) Jyri Talja and M.Sc.(Tech.) Tiina Malin

Date 24.3.2015

Number of pages 81 + 32

Language English

Abstract

The automatic sensor-based sorting is a developing branch of non-contact technologies, which can be utilized in the sorting of material streams. Different technologies and applications are overviewed in the literature part. The technologies differ from each other in the used wavelength range of the electromagnetic radiation or on the measured physical variable. X-Ray fluorescence technology (XRF) is introduced in more detail both in the theory and in the experimental part. XRF is based on the differences in the characteristic fluorescence emissions of materials when exposed to X-radiation. The measurable elements range from sodium to uranium.

In the experimental part, the objective was to test the functionality of a XRF sorting device with selected metal samples. The device was built and designed together with VTT Technical Research Centre of Finland Ltd. The objectives were the sorting of two different steel grades, the sorting of brass from more pure copper and analysing the gold coated copper-nickel circuit board. The results were examined by comparing the actual recovery with different variables.

The results showed that the consistency between the detectors is very good. Furthermore, it was found that the actual recovery of materials differs from the theoretical recovery. The factors limiting the final sorting result in practice are the functionality of the camera and the success of the ejection. In addition, the shape and size of the samples affect both the measurement and the sorting results. The measured pulse values of the small sized samples showed more deviation than the larger samples. The sample width and the relation of sample width and mass affect the ejection. Both the sorting of the steel samples and the sorting of copper and brass showed promising results. The examination of the gold coated circuit board sample was stopped due to the limitations of the camera since the sorting of flat shaped particles is not possible on this equipment. The tested XRF equipment was found suitable for sorting multiform particles sized over 40 mm.

Keywords Sensor-Based Sorting, X-Ray Fluorescence, Metal Recycling, Kuusakoski Oy

Tekijä Sini Orvokki Eskonniemi

Työn nimi RÖNTGENFLUORESENSSILAITTEISTON TEKNINEN TESTAUS JA SOVELTUVUUS METALLIEN KIERRÄTYKSEEN

Laitos Materiaalitekniikan laitos

Professuuri Mekaaninen prosessointi ja kierrätys **Professuurikoodi** Mak-46

Työn valvoja Professori Kari Heiskanen

Työn ohjaajat TkL Jyri Talja ja DI Tiina Malin

Päivämäärä 24.3.2015**Sivumäärä** 81 + 32**Kieli** englanti

Tiivistelmä

Automaattinen sensoripohjainen lajittelu on kehittyvä teknologiahaara, jota voidaan hyödyntää kierrätysmateriaalivirtojen lajittelussa ja rikastamisessa. Työn kirjallisessa osiossa esitellään yleisesti erilaisia sensoripohjaisia erotteluteknologioita ja niiden käyttökohteita. Teknologiat eroavat toisistaan käytettävän elektromagneettisen säteilyn aallonpituuden tai mitattavan fyysikaalisen suureen perusteella. Röntgenfluoresenssiteknologiaan (XRF) tutustutaan tarkemmin niin teoriassa kuin XRF -laitteiston kautta. Röntgenfluoresenssi perustuu eroihin materiaalien karakteristisessa fluoresenssisäteilyssä, kun ne altistetaan röntgensäteilylle. Mitattavat alkuaineet vaihtelevat jaksollisessa järjestelmässä natriumista uraaniin.

Työn tarkoituksen oli tutkia kokeellisesti XRF -laitteiston toiminnallisuutta sekä soveltuvuutta kolmelle eri metallinäytteelle. Laitteisto on suunniteltu ja kehitetty yhdessä VTT:n kanssa. Tarkoituksena oli kahden eri teräslaadun lajittelu molybdeenipitoisuuden perusteella, kuparin ja messingin erottelu sekä kultapinnoitetun kupari-nikkelipiirilevyn analysointi. Materiaalien lajittelutulosta tarkasteltiin vertailemalla toteutunutta talteenottoa eri muuttujiin.

Tulokset osoittivat, että detektorien toimivuuden välillä esiintyy hyvin vähän eroja. Lisäksi huomattiin, että materiaalien toteutunut talteenotto eroaa teoreettisesta. Käytännössä lopullista lajittelutulosta rajoittavat eniten kameran näkökyky sekä puhallustapahtuman onnistuminen. Kappaleen muoto ja koko vaikuttavat sekä mittaus- että lajittelutulokseen. Pienten kappaleiden mittaustuloksissa esiintyi enemmän hajontaa kuin suuremmilla kappaleilla. Kappaleen leveys sekä leveyden ja massan suhde vaikuttavat puhallustapahtuman onnistumiseen. Teräslaatuojen lajittelu toisistaan sekä kuparin ja messingin erottaminen osoittivat lupaavia tuloksia. Kultapinnoitetun piirilevyn analysointi keskeytettiin, koska litteiden levymäisten kappaleiden lajittelu ei ole mahdollista tällä laitteistolla. Tutkittu XRF laitteisto soveltuu hyvin yli 40 mm monimuotoisten kappaleiden lajitteluun.

Avainsanat Sensoripohjainen lajittelu, Röntgenfluoresenssi, Metallien kierrätys, Kuusakoski oy

Preface

This master's thesis has been made for Kuusakoski Oy, in Ekopark Lahti. First of all, I would like to thank Jyri Talja, the Vice President of Technology at Kuusakoski Oy, for instructions and support as well as giving me an opportunity to work with this interesting topic and for the chance to work independently. I would also like to express my gratitude to the supervisor of my thesis, Professor Kari Heiskanen from Aalto University, for all the good advice during this work as well as my studies.

I would like to show my thanks to R&D Engineer Tiina Malin for instructors and giving valuable academic perspective. Even though this project proved to be very challenging, it was also very educational. I was allowed to become acquainted with several interesting technologies and learned about comprehensive project management. Special thanks belong to the original designer and implementer of the project, Jouko Viitanen. Thank you for the good practical hints in operation of Poly-XRF. Thanks also to my colleagues Juha Hietamäki, Arsi Saukkola, Pekka Vainio and Leena Tuominen for help and expertise. I also want to thank my good friend Juha Nikkola (D.Sc.) for giving feedback to my text.

Finally, I want to thank my parents, Paula and Kalevi Eskonniemi, for all the love and support that you have given me. Also my friends earn huge thanks for being there for me when I needed you and for bringing so much joy and light into my life.

Espoo, 24th March, 2015

Sini Eskonniemi

Abbreviations

Poly-XRF	Multi-Channel X-Ray Fluorescence Device Used in the Master's Thesis at Kuusakoski Oy
XRF	X-Ray Fluorescence
EDXRF	Energy Dispersive X-Ray Fluorescence
WDXRF	Wavelength Dispersive X-Ray Fluorescence
HMS	Heavy Media Separation
DE-XRT	Dual Energy X-Ray Transmission
EMS	Electromagnetic Sensor
CCD	Charge-Coupled Device
CMOS	Complementary Metal-Oxide-Semiconductor
VIS	Visual Light Spectroscopy
NIR	Near-Infrared Spectroscopy
MIR	Middle-Infrared Spectroscopy
HIS	Hyper Spectral Imaging
LIBS	Laser-Induced Breakdown Spectroscopy
PLC	Programmable Logic Controller
TH	Threshold Value

Table of Contents

1 Introduction	1
I Literature part	3
2 Sensor-Based Sorting Technologies	3
2.1 Different Sensor-Based Sorting Technologies in General	3
2.2 Equipment Used in Sensor-Based Sorting	5
3 X-Ray Fluorescence Technology (XRF)	7
3.1 General Principles	7
3.2 Analytical Methods	10
3.2.1 Radiation Sources	12
3.2.2 Detectors	14
3.3 Material Requirements and Factors Affecting the Analysis	15
3.4 Applications of XRF in Recycling Industry	16
4 Other Sensor-Based Technologies Used in Recycling	19
4.1 X-Ray Transmission Spectroscopy (XRT)	19
4.2 Electromagnetic Sensor (EMS)	20
4.3 Visual Sensor Technology	21
4.4 Infrared Spectroscopy (IR)	22
4.5 Laser Detection	24
4.6 Technologies under Research	25
5 Sensor-Based Equipment on the Market	28
II Experimental Part	31
6 Poly-XRF Sorting Equipment	31
6.1 General Working Principle	32
6.2 Equipment Specifications and Main Adjustments	34

6.3 Classification Principles	37
7 Test Materials.....	38
7.1 Test Material 1.....	38
7.2 Test Material 2.....	40
7.3 Test Material 3.....	42
8 Experiments.....	43
8.1 Preparation for Experiments	43
8.2 Experimental Procedures	44
9 Results	46
9.1 Detector Consistency.....	46
9.2 Sorting Results of Test Material 1	49
9.2.1 Recovery Rates.....	50
9.2.2 Recovery and Grade.....	54
9.3 Sorting Results of Test Material 2	56
9.3.1 Recovery	56
9.3.2 Grade	58
9.4 Sorting Results of Test Material 3	59
10 Discussion.....	61
11 Conclusions	68
12 Suggestions for Further Research	70
References.....	72
Appendices.....	82

List of Tables

Table 1. Summary of sensor-based technologies used in recycling industry	6
Table 2. Sensor-based equipment on the market	29
Table 3. Poly-XRF equipment specifications	34
Table 4. Test materials used in the thesis experimental part.....	38
Table 5. Iron and Molybdenum content in test material 1.....	40
Table 6. Copper and Zinc content in test material 2.....	41
Table 7. Test systems used during the experiments.....	43
Table 8. Literature values for emission lines	44
Table 9. Calculated Grade and Recovery values	54
Table 10. Recognition degree of the camera on each detector line	58
Table 11. Zinc and copper grade of Eject.....	58
Table 12. Zinc and copper grade of Drop.....	59
Table 13. Comparison of Poly-XRF and Kuusakoski Works Heinola XRF	65
Table 14. The masses of test material 1 samples	83
Table 15. Test material 1, element composition analysis, part 1	83
Table 16. Test material 1, element composition analysis, part 2	84
Table 17. The masses of test material 2 samples	85
Table 18. Test material 2, element composition analysis, part 1	85
Table 19. Test material 2, element composition analysis, part 2	86
Table 20. Test material 3, element composition analysis.....	111
Table 21. The results of pre-tests of test material 3.....	112
Table 22. The peak data of test material 3, sample 1 spectrum (5 s).....	113
Table 23. The peak data of test material 3, sample 1 spectrum (0.3 s).....	113

List of Figures

Figure 1. General working principle of a sensor-based sorting device.....	5
Figure 2. Electromagnetic radiation.....	8
Figure 3. Formation of the fluorescence radiation. a) Primary X-radiation releases an electron. b) Filling of vacant electron position and formation of fluorescence radiation	8
Figure 4. The transitions of electrons	9
Figure 5. The spectra of Copper, Zinc, Lead and Brass	10
Figure 6. Two different spectrometer types a) EDXRF and b) WDXRF	11
Figure 7. Simple ED-XRF arrangement	12
Figure 8. Working principle of a general X-Ray tube	13
Figure 9. A radiation shielded side window X-Ray tube	13
Figure 10. Working principle of a general solid-state detector	15
Figure 11. XRF spectrum of stainless steel EN 1.4432 (AISI 316).....	17
Figure 12. Working principle of the X-Ray camera	19
Figure 13. NIR spectra of different polymer types.....	23
Figure 14. The principle of LIBS analysis	25
Figure 15. Eriez / TORATEC EcoTowerSort®	28
Figure 16. Poly-XRF test system	32
Figure 17. Functional principle of Poly-XRF.	33
Figure 18. The measuring geometry	36
Figure 19. Test material 1, samples 1 - 5	39
Figure 20. Test material 1, samples 6 - 10	39
Figure 21. Test material 2	41
Figure 22. Test material 3	42
Figure 23. The pulse frequencies of test material 1 on detector 1	47
Figure 24. The pulse frequencies of test material 1 on detector 2.	47
Figure 25. The pulse frequencies of test material 2 on detector 1	48
Figure 26. The pulse frequencies of test material 2 on detector 2	48

Figure 27. Actual and theoretical recovery at threshold values 8 and 11.....	50
Figure 28. Effect of Mo-content on Recovery.....	51
Figure 29. Effect of a sample mass on Recovery.....	51
Figure 30. Effect of sample width on Recovery	52
Figure 31. Effect of sample width over mass ratio on Recovery	52
Figure 32. The pulse frequencies of test material 1, Sample 1 on all detectors	53
Figure 33. Test material 1, Sample 1.....	53
Figure 34. The pulse frequencies of test material1, Sample 4 on all detectors	53
Figure 35. Test material 1, Sample 4.....	53
Figure 36. Theoretical Grade-Recovery Curve and actual Grade and Recovery.....	54
Figure 37. Effect of Threshold value on Recovery	55
Figure 38. Actual and theoretical recovery at threshold value 5	56
Figure 39. The pulse frequencies of test material 2, Sample 3 on all detectors	57
Figure 40. Test material 2, Sample 3.....	57
Figure 41. The pulse frequencies of test material 2, Sample 4 on all detectors	58
Figure 42. Test material 2, Sample 4.....	58
Figure 43. Spectrum of test material 3, sample 1. Measuring time 5s.....	60
Figure 44. Spectrum of test material 3, sample 1. Measuring time 0.3s.....	60
Figure 45. Test material 3, showing an example of the different angles	60
Figure 46. A calibration result of Poly-XRF sorting equipment.....	87
Figure 47. The pulse frequencies of test material 1 on detector 3	88
Figure 48. The pulse frequencies of test material 1 on detector 4	88
Figure 49. The pulse frequencies of test material 1 on detector 5	89
Figure 50. The pulse frequencies of test material 1 on detector 6	89
Figure 51. The pulse frequencies of test material 2 on detector 3	90
Figure 52. The pulse frequencies of test material 2 on detector 4	90
Figure 53. The pulse frequencies of test material 2 on detector 5	91
Figure 54. The pulse frequencies of test material 2 on detector 6	91
Figure 55. The pulse frequencies of test material 1, Sample 3 on all detectors	98
Figure 56. Test material 1, Sample 3.....	98

Figure 57. The pulse frequencies of test material 1, Sample 4 on all detectors	98
Figure 58. Test material 1, Sample 4.....	98
Figure 59. The pulse frequencies of Sample 5 on all detectors	99
Figure 60. Test material 1, Sample 5.....	99
Figure 61. The pulse frequencies of Sample 6 on all detectors.....	99
Figure 62. Test material 1, Sample 6.....	99
Figure 63. The pulse frequencies of test material 1, Sample 7 on all detectors	100
Figure 64. Test material 1, Sample 7.....	100
Figure 65. The pulse frequencies of test material 1, Sample 8 on all detectors	100
Figure 66. Test material 1, Sample 8.....	100
Figure 67. The pulse frequencies of test material 1, Sample 9 on all detectors	101
Figure 68. Test material 1, Sample 9.....	101
Figure 69. The pulse frequencies of test material 1, Sample 10 on all detectors	101
Figure 70. Test material 1, Sample 10.....	101
Figure 71. The pulse frequencies of test material 2, Sample 1 on all detectors	108
Figure 72. Test material 2, Sample 1.....	108
Figure 73. The pulse frequencies of test material 2, Sample 2 on all detectors	108
Figure 74. Test material 2, Sample 2.....	108
Figure 75. The pulse frequencies of test material 2, Sample 5 on all detectors	109
Figure 76. Test material 2, Sample 5.....	109
Figure 77. The pulse frequencies of test material 2, Sample 6 on all detectors	109
Figure 78. Test material 2, Sample 6.....	109
Figure 79. The pulse frequencies of test material 2, Sample 7 on all detectors	110
Figure 80. Test material 2, Sample 7.....	110
Figure 81. The pulse frequencies of test material 2, Sample 8 on all detectors	110
Figure 82. Test material 2, Sample 8.....	110

1 Introduction

The Earth's natural resources are decreasing while the material use is growing rapidly. There are several ways the resource efficiency can be improved and one is to recycle the resources and materials. [1] This means that a well-functioning recycling system producing pure products is needed. As well as improvement of new technologies, such as sensor-based sorting is essential in achieving this target. [2] The use of sensor technologies may replace manual sorting and lead to higher levels of automation and increasing recovery and purity. In addition to sorting based on material-specific characteristics and analysis, sensors can be applied in the process control and selective extraction of materials. [3, 4] The sensor-based sorting methods can also replace conventional unit processes, such as heavy media separation (HMS), which consumes large quantities of water and expensive additives [5].

X-Ray fluorescence technology (XRF) may be utilized in sensor-based sorting [6]. The method is based on the characteristic fluorescence radiation emitted by the material, when it is first exposed to primary X-radiation. All elements in the periodic table have different energies and they may be separated based on it. The measurable elements range from sodium to uranium [7]. The most important advantage of the method is its applicability to metals of all colours. For example, grey metals with different chemical composition may be distinguished. [5]

Kuusakoski Oy processes different waste materials in an industrial scale and it has been necessary to develop new efficient recycling solutions. The XRF sorting device was built and designed together with VTT Technical Research Centre of Finland Ltd and there was a need for the technical testing of the device.

The main objective of the thesis was to test the functionality and applicability of a XRF sorting device for metal sorting. The consistency between the detectors was set as an

indicator of the device functionality. In addition, the factors affecting the ejection of the particles were observed. Three different process samples were chosen for the performing of tests. The objectives were to sort two different steel grades from each other, brass from more pure copper and to analyse the gold coated copper-nickel circuit board. Larger scale pilot tests as well as the study of the economic potential of the device for the enrichment of material streams were excluded from this work. The sorting results were analysed by comparing the actual recovery with different variables. The conclusions on the applicability of the device for metal sorting are drawn on the basis of the sorting results.

I Literature part

2 Sensor-Based Sorting Technologies

The following chapters provide literature review concerning sensor-based technologies used in recycling industry. X-Ray Fluorescence technology is reviewed a little more carefully, since the sorting equipment used in the thesis experimental part is based on it. Furthermore, other technologies and equipment on the market are presented. A summary of the different methods is presented at the end of Chapter 2.

2.1 Different Sensor-Based Sorting Technologies in General

The term *sensor-based sorting* refers to contact-free detection used for individual particle separation, where the input material is fed as a monolayer. [8] It is a developing and growing technology branch, which utilizes different sensing technologies; for example colour analysis, X-Ray transmission, X-Ray fluorescence and other spectroscopic methods. The technologies differ from each other on the basis of the used wavelength of the electromagnetic radiation or on the measured physical properties such as conductivity, atomic density, elemental composition, colour or shape [8, 9]. The suitable size range is estimated to be from millimetre size up to several hundred millimetres, depending on the equipment configuration, the manufacturer and the detected variable [10, 11]. In addition to recycling industry, also mining and food industries utilize separation methods based on sensor technology [11]. By automating the process stages, a high and more constant degree of purity can be guaranteed to the product. Furthermore, automatic sorting can substitute hand sorting and reduce labour costs and improve safety at work. [12, 13] It is important to realize that manual sorting may have negative impact on human health [13].

There are several motivations to use sensor-based technologies for recycled materials. First of all, the use of secondary materials instead of primary sources is sustainable and

environmentally friendly. [9] In addition, it can lower the total energy costs. For example, in the case of Aluminium, the production of secondary raw materials uses only approximately 10 per cent of the energy consumed in the primary production. A growing problem in the use of recycled materials is the accumulation of impurities (tramp elements), which apply to all material streams in recycling. At the moment the most common ways to use recycled materials are dilution with primary material and downcycling, where materials are transformed into lower value products. Thus, sensor-based technologies can be used for upgrading the product quality by physically separating impurity elements. [14]

The accumulation of copper (Cu) and tin (Sn) in the steel structure is a good example, because they have negative impact on the mechanical properties of steel. Their solubility in steel is very high and they cannot be removed with common pyrometallurgical processes. The main sources of copper are the shredder scrap from the End of Life Vehicles (ELV) and large household appliances. The copper parts are attached to steel components, e.g. small electric motors. The other major source is scrap from higher Cu-containing steels, where copper is in solid solution with steel. The main sources for tin are tin plate scrap from packages, cans and coatings. [9, 14] This harmful accumulation could be reduced with the pre-enrichment of shredder scrap with appropriate sensor-based sorting technologies [14, 15].

In addition to metals, the sensor technology is well suited for sorting recycled wood and plastics. NIR-technology, for example, can be used for separating different types of plastics from each other and thus give more opportunities for further processing stages. Alternatively, components containing harmful compounds, such as flame-retardants in plastics and impregnated wood can be removed. [11, 16] The flame-retardants and chemicals used in the wood pressure treatment have been classified as hazardous wastes [17].

2.2 Equipment Used in Sensor-Based Sorting

Sensor-based sorting equipment commonly consists of a feeder, conveyor belt, the selected detector or a combination of detectors and the material collection [9]. A general equipment configuration is shown in Figure 1. Usually, it is possible to divide the input material into two product fractions (*drop* and *eject*). [11] The detected materials that meet certain criterion (e.g. right colour) are separated by compressed air jets, controlled through the computer-based automation system. Either the valuable particles or the waste can be selected for ejection. [18] The block of air valves can be placed either above or below the material stream depending on the equipment configuration [11, 19]. Other separation methods are mechanical flaps and robot arms, which are more suitable for large and heavy particles [13, 18]. A summary of sensor-based technologies used in recycling industry is presented in Table 1.

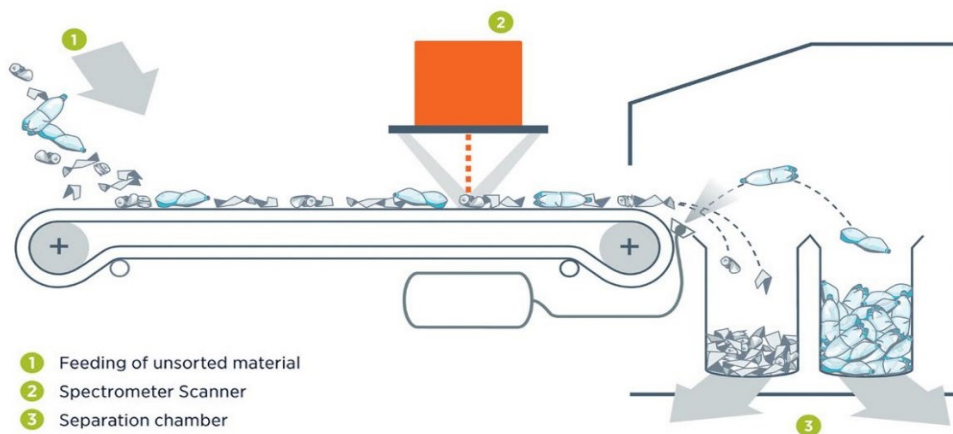


Figure 1. General working principle of a sensor-based sorting device [11].

It is impossible to create completely pure material fractions with any commercial sorting method; they just improve the quality of the product. At the moment of separation, the behaviour of the particle can be predicted with the help of the probability distribution. If a particle consists of several different materials, separation based on physical properties will be still more problematic. It is possible to get closer to the desired purity level by combining different methods. Often a compromise is made between the quality of the product and the recovery. If one wants to maximize

the quality, the recovery will remain small. Usually, only a small part of the input feed is clean and liberated. If lower quality is accepted, a larger part of the wanted material will be recovered. The liberation behaviour of materials in recycling processes may be complex. The liberation has a major effect on the quality of the product. If a large part of the material is poorly liberated, only weak quality can be attained. [9]

Table 1. Summary of sensor-based technologies used in recycling industry

Sensor Technology	Detected Property	Applications
X-Ray Fluorescence (XRF) [7]	Characteristic fluorescence radiation	Heavy metals, stainless, steel and copper
X-Ray Transmission (XRT) [20]	Atomic density	Al, precious and heavy metals (Cu, Brass, Zn etc.). Flame retardants in plastics
Electromagnetic Sensor (EMS) [11, 21]	Electromagnetic properties (conductivity and permeability)	Separation of metals from non-metals
Colour Line Camera [11]	Colour properties (green, red and blue)	Sorting materials by colour
Visual Spectroscopy (VIS) [11]	Visible spectrum	Transparent and opaque materials
Near Infra-Red (NIR) [11]	Reflection, absorption	Sorting of plastics by type
Middle Infra-Red (MIR) [22]	MIR spectrum	Sorting of polymers and wood, also black coloured
Laser [23]	The reflected laser beam	Material size, shape, structure, location
Laser induced breakdown spectroscopy (LIBS) [24]	Atomic emission	Metals and plastics
Terahertz technology (THz) [25]	Reflection, absorption	Plastics, also black

3 X-Ray Fluorescence Technology (XRF)

XRF technology is studied in more detail throughout this Chapter. At first, in Chapter 3.1, general principles and theory are presented. Chapter 3.2 tells about the differences between the analytical methods and introduces the main components of XRF spectrometers. Eventually the material requirements and applications in recycling industry are presented in Chapters 3.3 and 3.4.

3.1 General Principles

The X-Ray fluorescence is a quick measuring method and it does not destroy the sample. For this reason, it is suitable for a qualitative or semi-quantitative determination of the elemental composition of a wide range of different materials. It is utilized in various industrial applications, e.g. in metal and mining industries as well as in the fields of environment and recycling. [7, 26] The method is particularly suitable for the analysis of metals and alloys, because of their high atomic number and density. These material properties affect the way that response of high intensity fluorescence is obtained even if a low energy source was used. [27]

The X-Ray fluorescence analysis is based on the electromagnetic radiation having a wavelength range about 0.1 - 10 nm. This wavelength range corresponds to energies between 0.125 - 125 keV. The wavelength of the X-radiation is inversely proportional to its energy according to Equation 1:

$$E = \frac{hc}{\lambda} \quad (1)$$

Where E is the energy [keV]
 λ is the wavelength [nm]
 H is Planck's constant, 6.6262×10^{-34} [Js]
 c is the speed of light [m/s].

In other words the shorter the wavelength, the higher energy of the radiation. In practice, the measurable elements range from Sodium¹¹ to Uranium⁹². The electromagnetic radiation in different wavelength regions is shown in Figure 2. [7, 28]

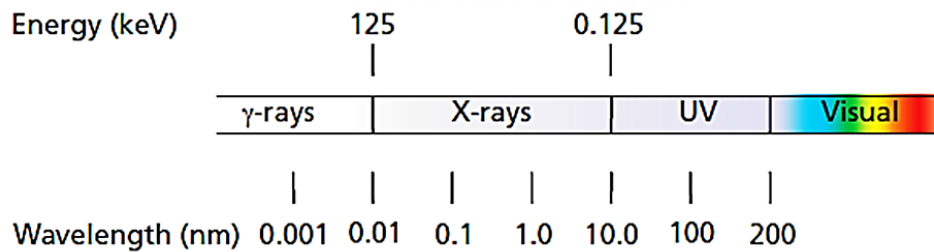


Figure 2. Electromagnetic radiation [7].

The X-Ray fluorescence in the material is achieved by directing primary X-radiation to the examined sample. All elements in the periodic table produce fluorescence radiation with characteristic wavelengths. When the atom is exposed to X-radiation, the electron on its inner shell is released (Figure 3a). Thus a new electron from outer shell will fill the resulting vacant position (Figure 3b). [29]

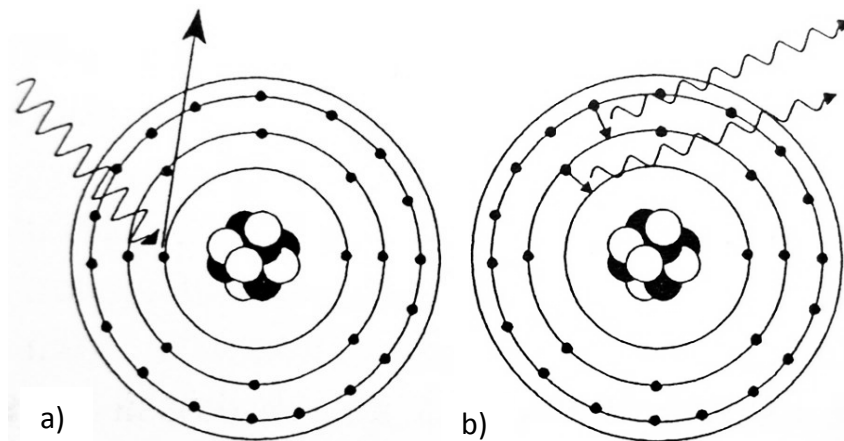


Figure 3. Formation of the fluorescence radiation. a) Primary X-radiation releases an electron. b) Filling of vacant electron position and formation of fluorescence radiation. [29]

The element and the transition of a specific electron, for example $Fe_{K\alpha}$, are presented according to a certain way. For example, the K_{α} line originates from the energy that is generated when an electron from L-shell is transferred to K-shell. Correspondingly, the K_{β} line comes from the energy of the electron, which has been transferred from M-shell to K-shell. The L_{α} and L_{β} lines come from the displacements of electrons from shells M and N, to L-shell. The transitions of the electrons are illustrated in Figure 4. [29]. Furthermore, the atom shell has several orbitals, which can be labelled with α_1 , α_2 or β_1 and β_2 and so on. [26]

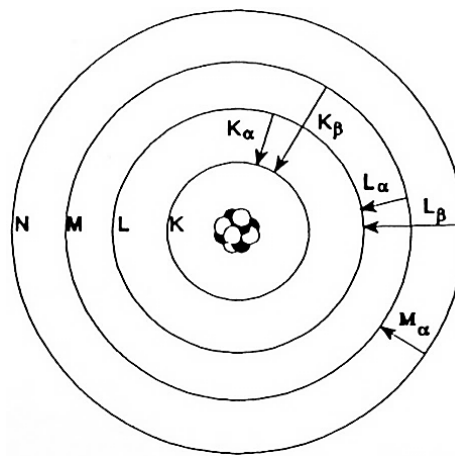


Figure 4. The transitions of electrons [29].

The energy of resulting fluorescence radiation depends on the energy difference between the atomic shells. An electron from outer shell has higher energy than an electron from inner shell. In case the electron moves from L-shell to K-shell, excess energy is released as fluorescence radiation. Usually more than one type of energy is released from an atom since several electron vacancies are released and replaced. This resulting collection of energy lines (*fingerprint*) is characteristic of every element. [7]

An example of XRF-spectrum is presented in Figure 5. The x-axis indicates the energy and the y-axis the number of pulses or counts per energy channel. First the spectra of pure elements, here Copper, Lead and Zinc, are analysed. Then these results can be used for the qualitative analysis of metal alloy, here Brass, which mainly consists of these three elements. Both copper and zinc give strong K_{α} lines. The intensities of the

lines give information about the quantities of the elements. The spectrum of Brass is given in the logarithmic scale so that the small peaks can be observed better. [30]

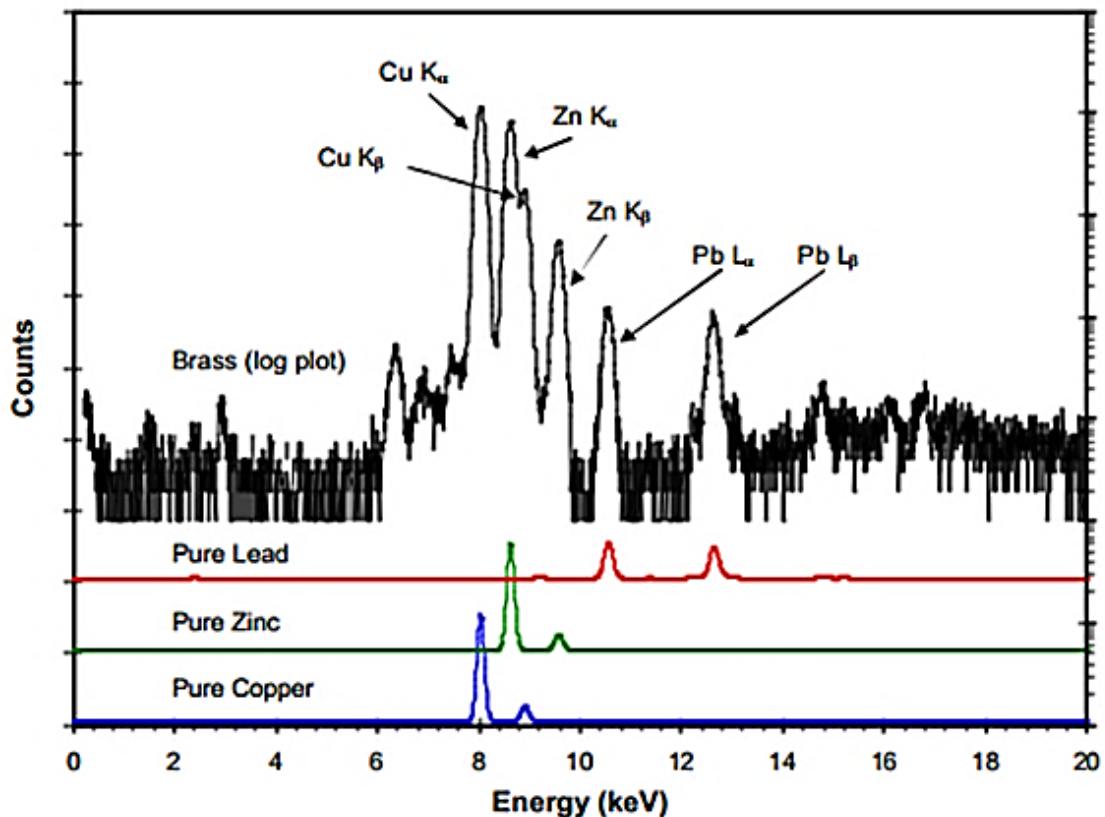


Figure 5. The spectra of Copper, Zinc, Lead and Brass [30].

3.2 Analytical Methods

In this paragraph, the structure of XRF spectrometers and main components as well as functional differences between the main detection systems, energy dispersive and wavelength dispersive, are briefly described. Energy dispersive analysers are normally used in the online sorting devices.

First of all, two fundamentally different spectrometer types appear. The difference of energy dispersive XRF (EDXRF) and wavelength dispersive XRF (WDXRF) is in their measuring geometric arrangement, which has been illustrated in Figure 6 [31]. In the EDXRF system, the sample is excited with an X-Ray tube [32]. The characteristic radiation of all the elements in the sample is measured by the detector [7, 32].

The radiation is dispersed and sorted qualitatively according to the energies that correspond to different elements. Also quantitative or semi-quantitative analysis is done when the number of X-Ray photons per second for each energies are determined. [7, 21, 32] The advantages of EDXRF technique are its possibility to simultaneously analyse a wide area of elements and to obtain the results in short time [6, 7, 31].

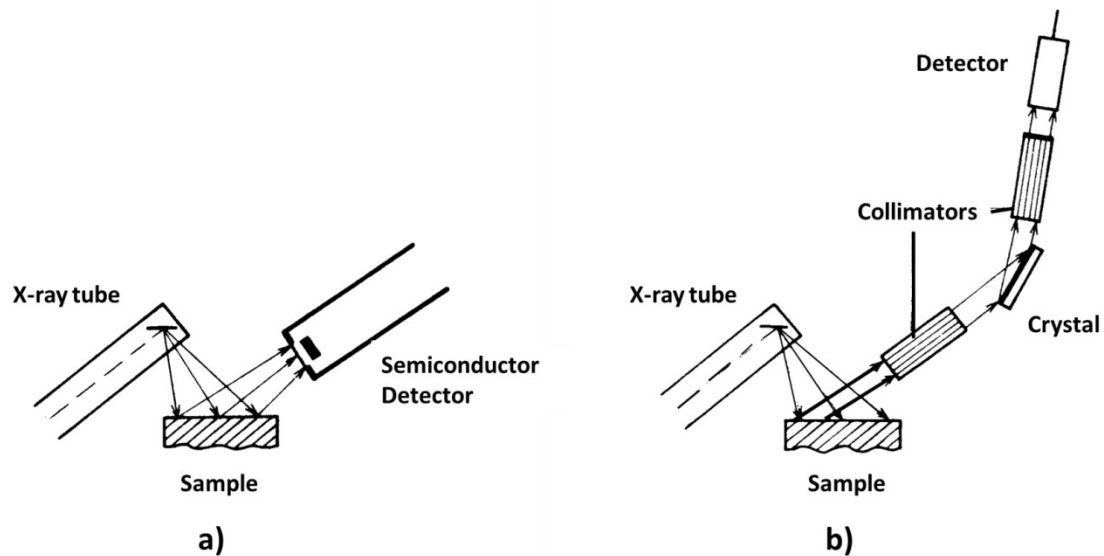


Figure 6. Two different spectrometer types a) EDXRF and b) WDXRF [31].

The working principle of wavelength dispersive XRF (WDXRF) technique is very similar to EDXRF, only the analysis of the characteristic radiation from the sample is done with the help of a crystal. When the radiation from the sample hits the crystal, it separates the wavelengths with different energies from each other. Then the detector analyses individually only the radiation which is directed to it. [7, 32] Different wavelengths are measured as sequences, with a movable detector or with a set of fixed detectors. The concentrations of different elements in the sample can be determined with the help of the intensities of the radiation. The advantages of WDXRF technique are the very accurate analysis of the radiation and the suitability to analyse lighter elements. The measurable elements range from Be^4 to U^{92} . [6, 7]

A simple arrangement of EDXRF system is shown in Figure 7. A general measuring system, spectrometer, always consists of a radiation source (1), a sample (2), a dispersion device and detector (3). But also signal processing electronics (4), a microprocessor and computer with analysis software (5) are needed. [32, 33] The principle and the components are described throughout this chapter.

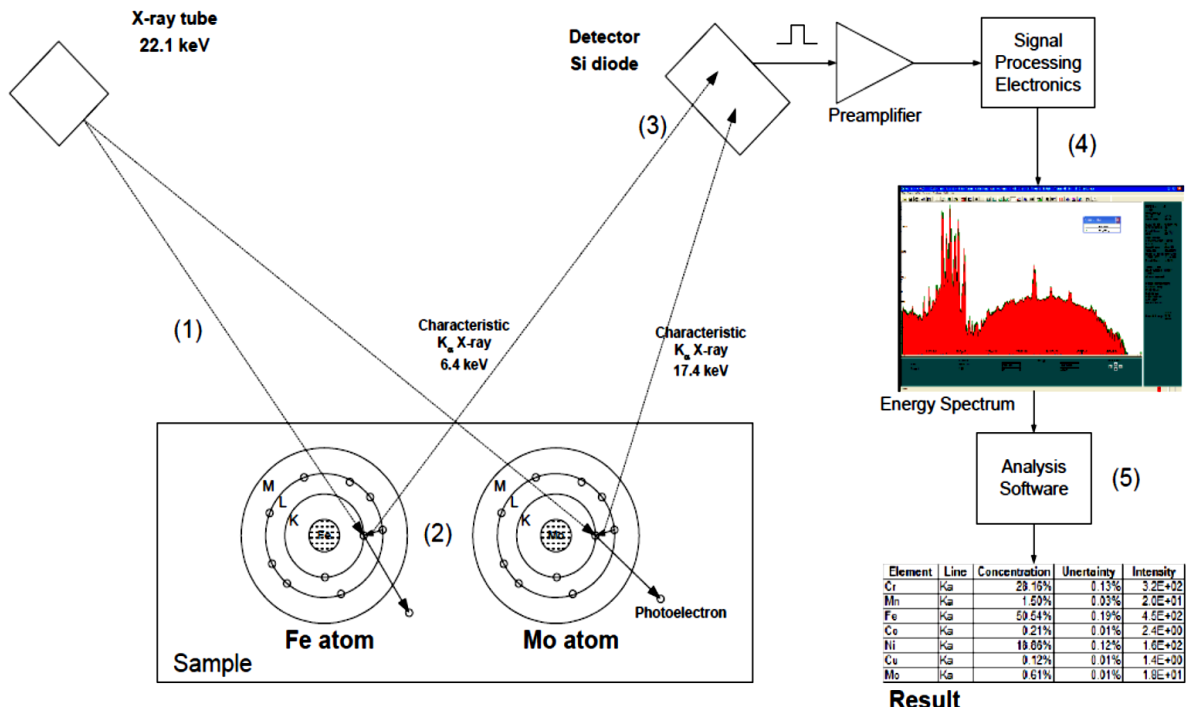


Figure 7. Simple ED-XRF arrangement [33].

3.2.1 Radiation Sources

The radiation source can be an X-Ray tube, a radioactive source or a synchrotron [5]. In this work, only the X-Ray tubes are discussed. Figure 8 illustrates the working principle of an X-Ray tube in general and Figure 9 shows a radiation shielded side window X-Ray tube from Oxford Instruments. Inside the X-Ray tube, in vacuum environment, there is a filament which works as a cathode and certain target material working as an anode. The filament is usually made of tungsten. The electric current heats the filament, from where electrons are released. [6, 7] The energy range of 35 – 50 keV is applied [21]. The electrons are accelerated with high voltage, after which they hit the target material and generate decelerating radiation, so called "Bremsstrahlung" [7, 31].

Furthermore, part of the electrons hit the atoms of the target material and release some electrons from it. This results in radiation that is characteristic to the target material and can be seen in the background spectrum. [7, 31] There are a wide range of target materials to choose, e.g. Ag, Au, Co, Cr, Cu, Fe, Mo, Pd, Rh, Ti, W [34]. The anode material defines the X-Ray tube's characteristic spectrum [35].

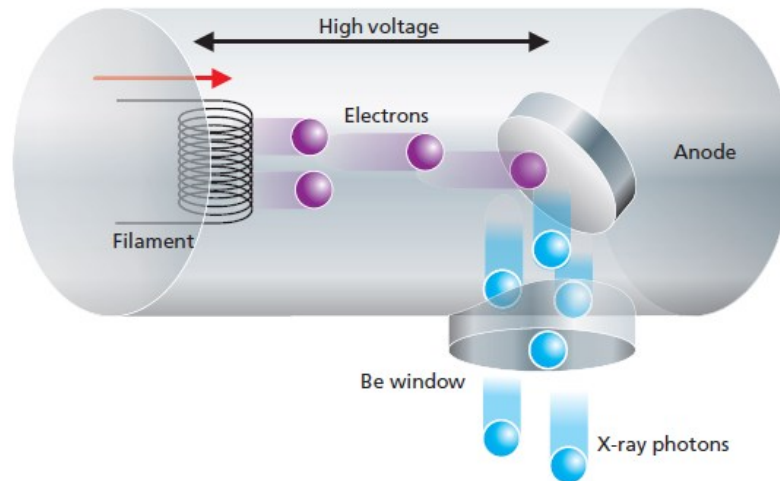


Figure 8. Working principle of a general X-Ray tube [7].

The X-Ray photons that have high enough energy pass through the tube's Beryllium window. The energy of the photons is determined by the high voltage. Depending on the equipment configuration, a secondary target or a filter can be used between the source and the sample. The filters reduce the intensity of the disturbing lines and background at the energies of interest. Also the signal to noise ratio is improved. [7]



Figure 9. A radiation shielded side window X-Ray tube [34].

3.2.2 Detectors

The use of different detector types between EDXRF and WDXRF can be divided roughly. EDXRF systems typically utilise solid-state detectors, as they are able to measure a wide range of elements with high efficiency. WDXRF systems utilise gas-filled detectors, with analysis area roughly from Beryllium to Copper and scintillation detectors that measure elements from Copper to Uranium. [7, 36]

The basic working principle is that when a photon arrives at the detector, it causes an electrical pulse. The pulse height is proportional to its energy. Furthermore, the voltage signal is amplified and the multi-channel analyser (MCA) calculates the number of pulses formed in each height interval and provides the corresponding energy intensity. [7, 36]

The most important features of the detector are resolution, sensitivity and dispersion. Resolution indicates how well the detector is able to distinguish between different levels of energy from each other. The sensitivity, in turn, is the relation between calculated pulses and the incoming photons. Finally, the dispersion ability is linked to the detector's ability to distinguish between the different energetic X-Rays from each other. [7]

The solid state detectors are most commonly produced of silicon, germanium or other semiconducting material. Also, compound semiconductors are manufactured [6, 36]. For example, Amptek Inc. provides XRF spectrometers with different semiconductor detectors, such as Silicon Drift Detectors (SDD) and Si-PIN or CdTe detectors. [37] The general working principle of a detector is illustrated in Figure 10 below. The detector has a Beryllium window which allows the X-Ray photons to enter the detector where they form electron-hole pairs. The number of incoming photons determines the number of formed electrons i.e. the higher the energy more electrons are produced. Due to the high voltage, the electrons are transported to the back of the detector and when they reach it, the potential drops which occur as a negative pulse. The height of the pulse is dependent on the number of electrons. [7] In addition to the detector's ability to simultaneously analyse a wide range of X-Rays, the main advantages are the

insensitivity of the measuring geometry. The energy analysis is not dependent on the diffraction or the orientation of the radiation. This means that the setting between the sample and the detector does not have that much impact on the measurement. [36]

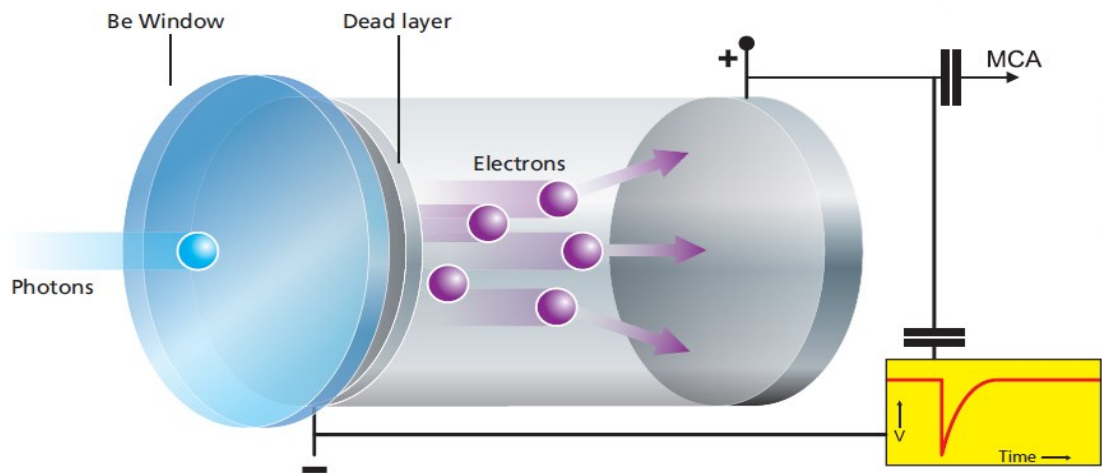


Figure 10. Working principle of a general solid-state detector [7].

3.3 Material Requirements and Factors Affecting the Analysis

The qualitative XRF analysis does not set great demands for the analysed material, e.g. in sample preparation, also no chemicals are needed. In addition to solid particles, the laboratory analysers also make the analysing of powders and fluids possible. [38] XRF is a surface measurement method; therefore the surface must represent the whole examined material. The qualitative analysis means that the element composition of the sample is determined, in which case the locations of the peak tops indicate the occurrence of a certain element in the sample. The peak areas, however, correspond to their intensity. If the analysed material is an alloy, some overlapping of peaks may be found in the EDXRF spectrum. Then, if the strongest peak of the searched element is overlapped by another peak, then the peak with a weaker signal is used in the analysis. [7]

The intensity of the X-Ray signal depends on the amount of the elements, but also on the quality and amount of primary radiation. In other words, the power of the X-Ray tubes, their distance to the sample, amount of collimation and filtration, affect the

accuracy of the XRF-analysis. The intensity of the radiation decreases in relation to the square of distance. Also the interactions of the different elements in the sample affect each other and the accuracy of the measurement. For example, if the emission energies of different elements are very near to each other. Furthermore, the measurement time and distance affect the accuracy. [39]

The XRF analysis is a surface measurement technique, in which case the cleanness of the surface has a great effect on the validity of the result. The average measuring depth is about 100 μm . The surface properties such as roughness or contaminations like paint and dust are the most common sources of errors and they have greater impact on light elements like magnesium [39]. Generally, light elements require a longer measurement time and higher concentrations to be detected [6].

The overall error that affects the results is caused by several issues including the repeatability of the measurements. The repeatability is proportional to the measuring time and it weakens when the time is shortened. In automatic measurement of moving scrap particles, further sources of errors are the settling of the particle with respect to primary X-radiation and detectors, the heterogeneity and particle size of material and furthermore, the calibration error. [39]

3.4 Applications of XRF in Recycling Industry

In online measurement, the particle is moving either on a conveyor or in free fall when it is measured. Therefore it stays a very short time under the X-Rays and detectors. The commercial sorting devices often operate with 2 - 3 m/s belt speed, which means that the measurement time is very short, less than a second. [6] This sets high demands for the sensitivity and resolution of the detectors.

XRF technology has a lot of potential and possibilities in the sorting of recycled materials. [6] Traditional separation methods are often based on the differences in the physical properties of materials. For example, the sink-and-float process which is based on differences in the densities, and in addition consumes a lot of water and additives. [9, 12] Also, more traditional sensor-based devices such as metal detector and the

camera have their own limitations. If the equipment for example has a combination of these sensors, most of the grey metals will end up in the same fraction, because the sorting criterions are metal or non-metal and the colour. Thus XRF technology has its advantages compared with these more traditional sensors and technologies, including manual sorting. The XRF technology is based on the differences in the chemical composition of the samples and thus there are no restrictions with the colour, for example and the grey metals can be separated from each other. [5]

A good example of sorting grey metals is the sorting of different stainless steels by their quality. The material streams can be enriched and better commercial value obtained for them. For example, in Kuusakoski Works Heinola, the stainless steel material stream is sorted for acid proof (EN 1.4432; AISI 316) and common stainless steel (EN 1.4301; AISI 304) fractions with a self-built XRF-system, similar to the equipment used in the experimental part of this thesis. The materials can be separated on the basis of their molybdenum content. Figure 11 shows a typical XRF spectrum of AISI 316 steel [40]. The sorting of this material was also tested in the thesis experimental part.

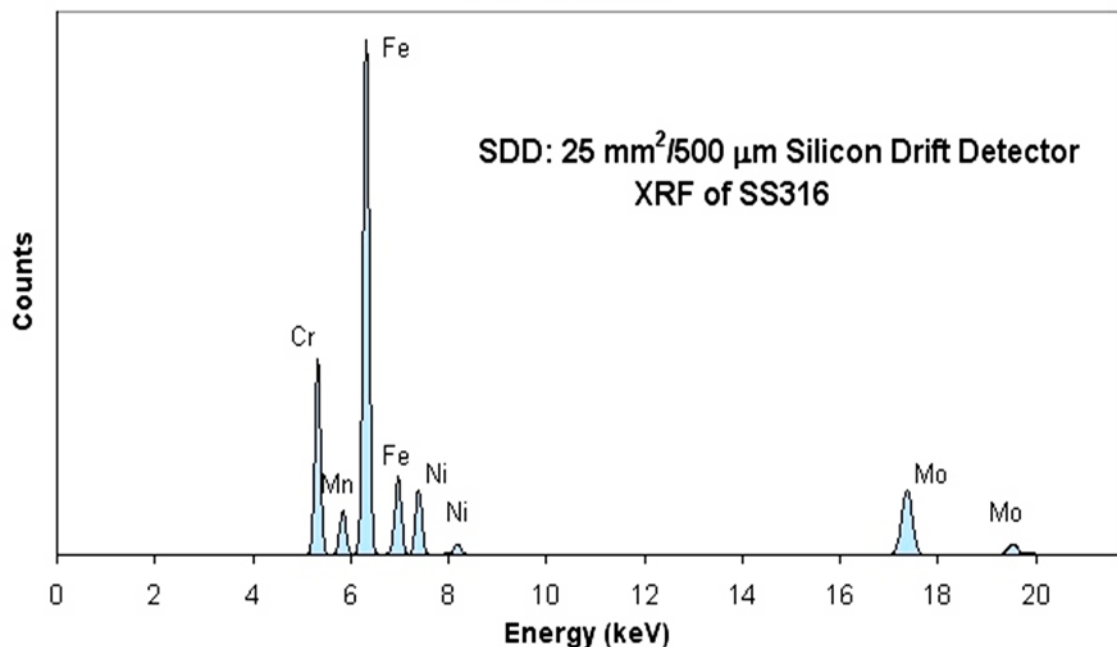


Figure 11. XRF spectrum of stainless steel EN 1.4432 (AISI 316) [40].

There are several sorting equipment manufacturers on the market, for example Tomra Sorting Recycling, STEINERT Elektromagnetbau GmbH and Redwave. They all have their own versions of XRF sorting devices which can be modified to suit the customer's process keeping in mind e.g. the capacity demands and particle sizes. RedWave, for example has originally developed XRF technology for sorting of the recycled glass; more precisely separation of heat-resistant and leaded glass from recyclable glass cullet. Later they have also expanded their XRF portfolio to the sorting of minerals and recycled metals. [5]

One application with great potential is the reducing of impurities from recycled steel. Tomra Recycling, for example, offers XRF technology for this purpose. Steel is one of the most recycled metal alloys and it must answer certain quality requirements e.g. the copper content should be less than 0.25%. Copper often appears as clean copper or copper alloys but it is entangled with a piece of steel e.g. copper coils and electric motors; called meatballs. The removal of impurities increases the purity and economic value of the product. [15, 41]

Another important area of XRF technology is the handheld analysers. They are widely used in the scrap yards for on-site alloy identification for both incoming and outgoing scrap, also at Kuusakoski Oy. They are easy to use and the key elements analysis is performed in a simple point-and-shoot method. [42] The element compositions of the test samples used in the theses experimental part were measured with a handheld XRF analyser more specifically the Oxford Instruments X-MET 7500.

The different sensing technologies can be combined with each other to increase the using possibilities and add the versatility of the sorting device. XRF technology can be combined, for example, with an electromagnetic sensor as in Tomra X-Tract sorting device, to help determine the positions and sizes of the particles before the XRF analysis. [20] Combining with other sensors is not necessary, since XRF is usually used for such material streams that have gone through several treatment stages. Thus the feed material is quite clean and not too heterogeneous. [43]

4 Other Sensor-Based Technologies Used in Recycling

Chapter 4 introduces other sensor-based sorting technologies used in recycling industry processes. Also few technologies that may have potential as online sorting method in the future are presented.

4.1 X-Ray Transmission Spectroscopy (XRT)

X-Ray transmission technology can be used for identifying differences between the specific atomic densities of materials [20]. It is the only sensor, which provides information on the internal material compositions, not just the surface. The principle of XRT is that X-radiation with certain initial intensity penetrates the material; part of the radiation is absorbed and part goes through. The passed radiation with reduced intensity is measured. Materials with different densities and thicknesses absorb different amounts of radiation. [44] The energy range of used X-Rays is between 90 and 200 keV [21].

In the Dual Energy X-Ray Transmission (DE-XRT), the detectors combine information from two different energy levels that have different spectral sensitivities (high and low) [20]. This is illustrated in Figure 12.

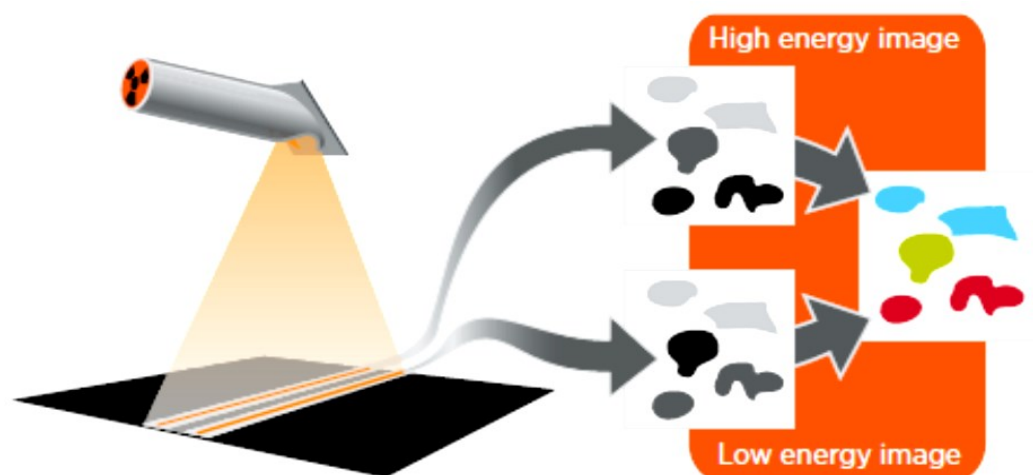


Figure 12. Working principle of the X-Ray camera [20].

The intensity from each pixel is converted to electrical signals and thus into grey scale pictures. Different grey scale intervals correspond to certain colour classes and false colour pictures are created with the help of the software. [44]

The advantage of DE-XRT is that the measurement is not affected by surface contaminations e.g. dust, moisture etc. since the measurement is independent of the surface [20]. Problems may occur if objects with different densities and thicknesses are measured. This means that thin particle with high density and thick particle with lower density may have similar results. The appearance of the problem can be reduced using two different wavelengths. [44]

The applications vary from aluminium and magnesium removal from heavy metals to removal of brominated flame retardants containing plastics or PVC from mixed plastics. [20, 45] In addition, one interesting application is found in minerals processing, where diamonds are recovered from gangue with the help of XRT [46].

4.2 Electromagnetic Sensor (EMS)

Electromagnetic Sensor (EMS) detects materials through their conductivity and permeability [11]. The metal detectors are widely used for sorting metals from non-metals or from heterogeneous feed. It is a relatively low cost and effective technology. [11, 47] The electromagnetic sensors utilize the Eddy-current principle [21]. It detects the differences between the electrical properties of metals and an alternating magnetic field [47]. The EMS contains two main parts, transmitter and receiver coils. In the transmitter coil, an electrical current is achieved by inducing conductive material. This produces the magnetic field around the current and interacts with metal particles. The receiver coil measures this interaction. [21, 47] The sensors utilize three different principles: a beat frequency oscillator, induction balance, and pulse induction [21]. Usually, the metal detectors are placed under the conveyor belt [48].

Two different types of receiver coils exist; a sensor that recognizes all metals from the input material and produces conductive and non-conductive product fractions. The other type is a selective detector. It can identify, if the measured signal is originated

from weakly conductive metal e.g. stainless steel or lead or from metals with higher conductivity, non-ferrous metals for example. [48] Coatings or other surface contaminations do not disturb the identification [47]. The main applications of the inductive sensors are the recovery of metals from shedder residues that have already gone through magnetic and eddy current separation [48].

4.3 Visual Sensor Technology

Visual sensing technology includes all the detection systems applied in the visual range of electromagnetic radiation (390 - 780 nm). Both the colour camera and VIS spectroscopy belong to this group. [49] This Chapter deals only the colour cameras. VIS spectroscopy is a special application of visual sensors [49]. According to discussion with Hinterseer the VIS spectroscopy is not utilized in sensor-based sorting devices. The colour cameras are commonly used. [43] Although, Tomra utilizes VIS spectroscopy in recognizing transparent and opaque objects, such as PET bottles [11].

The colour camera technology is applied when materials are sorted based on their colour. In addition to visual light, cameras may utilize infrared and ultraviolet wavelengths. The colour line scan cameras have high resolution and colour selectivity. The information from the camera can be processed digitally to achieve precise location at pixel level. At present the used light sources are light emitting diodes (LED). The detected material properties include colour, shape, brightness and size. [11, 50]

The conventional line scan cameras utilize Charged-Coupled Devices (CCD) [21]. However, the Complementary Metal-Oxide-Semiconductor (CMOS) sensors have been replacing CCD sensors, because they are faster, cheaper and have lower power consumption [48, 51]. The readers are requested to look more detailed information on the operating principle, the components and colour models in the proceedings Sensor Technologies: Impulses for the Raw Materials Industry by Nienhaus et al. (2014) in more detail in Chapter 4.5 Principles of VIS by Berwanger & Maul [49].

The colour based sorting can be applied for cleaning mixed metals into cleaner mono fractions, electronic scrap e.g. recovering copper or together with EM sensor, for example recovering cables. [50]. One common application is the sorting of recycled shredded metals, which have first gone through magnetic separation, eddy current and HMS stages. The output stream is very mixed and can be sorted by the colour; Copper as red colour metal, brass as yellow metal and zinc, lead etc. as grey metals. [5]

Limitations of the technology are for example that grey metals cannot be sorted from each other based only on the colour. As already talked in Chapter 3.4, the grey metals can be further processed with XRF, for example. In addition all the surface contaminants such as paint or rust cause measuring errors, since the colour sorting purely analyses the surface characteristics. [5]

4.4 Infrared Spectroscopy (IR)

Infrared light is part of the electromagnetic spectrum and the wavelength ranges approximately from 0.7 μm to 1000 μm . The sorting devices usually utilize near infrared (NIR) region that is closest to the visible light. [52] The sensors are furthermore divided into NIR1 and NIR2 regions that correspond roughly to the areas of 700 – 1098 nm and 1100 – 2498 nm [53, 54].

In the NIR spectroscopy, materials can be recognized based on their specific spectral properties of reflected or transmitted light [52, 54]. The radiation hits the material surface causing the vibrational transitions of components such as C-O, O-H, N-H or C-H [52, 55]. Furthermore a characteristic spectrum of absorption bands is created. An example of NIR spectra (700 – 2500 nm) of different common plastics are given in Figure 13. [55]

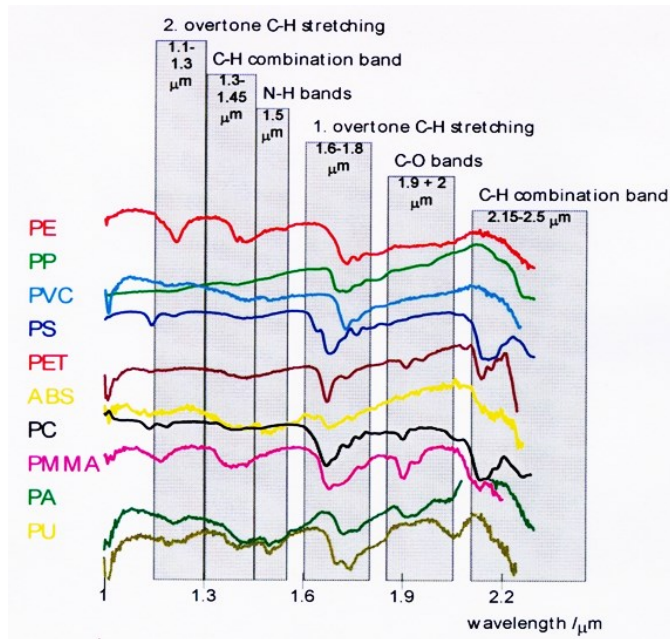


Figure 13. NIR spectra of different polymer types [55].

The latest NIR camera technology utilizes Hyper Spectral Imaging (HSI), which provides images that contain a full spectrum on each pixel [21, 56]. The advantage of HSI over common NIR technology is that the data from the spectroscopic analysis is detected simultaneously, not from a single spot and then processed with a high-resolution line camera [57]. A generated image shows different components by giving colours to different pixels based on the characteristic wavelengths [52]. The sensors usually contain a two dimensional array, thus one dimension provides the spectral resolution and the other gives information on the spatial resolution [21]. The disadvantage of NIR technology is that black materials that are coloured with carbon black pigments cannot be analysed. All radiation is totally absorbed by the material. [22, 52]

In the recycling industry, NIR technology can be applied in plastic sorting by different polymer type. Other applications vary from removing paper from a mixed stream to waste wood sorting. [16, 54] A study on waste wood purification with NIR imaging technique was performed by Pigorsch et al. They found that it suits this purpose extremely well and most of the organic chemical contaminations paint, coatings and glues etc. could be detected. [16]

In addition to recycling applications, a very interesting example of HSI technology used in food industry was investigated by Schenker et al in automatic wine grape sorting. They applied two HSI cameras; one with visual/NIR spectrum (400 – 1000 nm) and another with short wave IR (1000 – 2500 nm) to acquire images from berries. In wine production, the qualitative sorting of valuable grapes from rotten grapes and other impurities such as rocks, beetles and other bugs play an important role. HSI imaging was used for analysing the differences in sweetness. The analysed grape varieties were Pinot Noir, Pinot Blanc and Riesling. [58]

4.5 Laser Detection

Laser detection can be used when information on the material size, shape, structure or location is needed [11]. The Laser Detection and Ranging known as LADAR technology operates within infrared spectrum. A laser light beam is emitted towards the object, and then the reflected laser beam is detected by a CCD element. The distance between the source and object can be calculated, using the position of the light point. [23, 59]

2D and 3D images can be produced when the process is repeated in sequences in multiple angles. Two analysing principles appear; the first measures the time for the laser pulse to travel from the light source to the sample and back. The second utilizes a continuous wave and the phase difference of the emitted and received wave is measured. A laser scanner includes four main parts; a laser light source, optics, mirrors and a photodiode receptor. In addition to the measured distance of the object, the returned pulse contains information on the material. Different elements reflect the infrared light in different quantities and therefore it can be identified. [23] The readers are requested to look up more detailed information about the subject in the proceedings *Sensor Technologies: Impulses for the Raw Materials Industry* by Nienhaus et al. (2014) in more detail in Chapter 4.10 Principles of Laser Detection and Ranging by Neumann and Hahn [23] or directly from the web pages of the sensor manufacturer, such as Micro-Epsilon [59].

4.6 Technologies under Research

This Chapter introduces some technologies under research, which may be expected to be commercialized in the near future. The first technology (LIBS) is suitable also for the identification of metals and the second example concentrates on the identification problem of black plastics.

Laser-Induced Breakdown Spectroscopy (LIBS) utilizes atomic emissions spectroscopy. The principle of the measurement is introduced in Figure 14 [24]. Very powerful lasers are used as excitation sources. The radiation pulse is aimed at the sample surface, where plasma is generated having temperature of 10000 – 25000 K. A small amount of surface atoms vaporize. The temperature of the plasma decreases between the pulses. The emission spectrum of the material is measured and the result is a qualitative elemental composition. The LIBS technology is suitable for all elements in the periodic table as well as solids, gases or liquids. [24, 60]

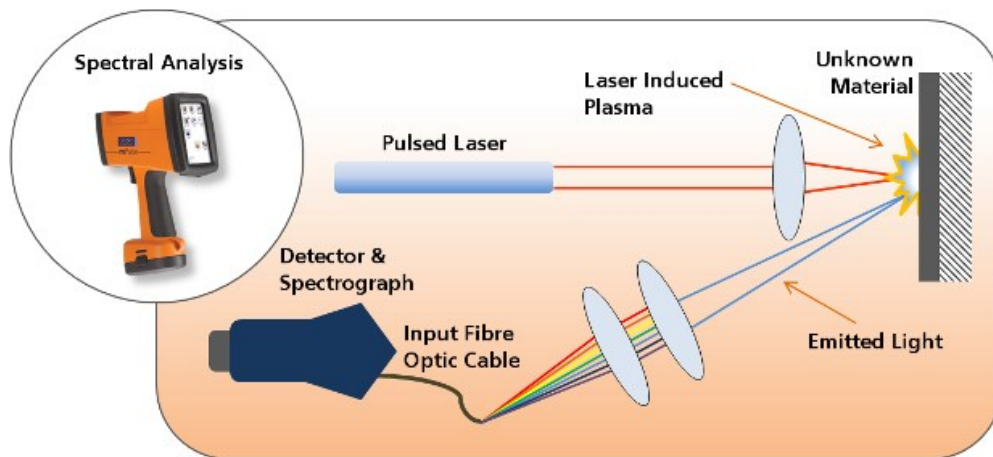


Figure 14. The principle of LIBS analysis [24].

The advantages of the method are that no sample preparation is needed and it is suitable for materials of all kind. Chemical or physical factors such as varying moisture content may limit the analysis. The applications areas of LIBS have been increasing recently. [60] In recycling industry, the applications include for example scrap metal analyses. Furthermore, it can replace the hand-held XRF analysers since there is no risk of X-radiation exposure. [24]

The fast development of the technology is well described when according to Gaastra and Küch (2014) LIBS technology does not yet exist as a reliable and efficient online analysis method [60]. But according to Feierabend (2014), Secopta GmbH has developed an online LIBS analyser, which may have potential in analysing and sorting of recycled materials e.g. aluminium as well as quality assurance and process monitoring applications in the manufacturing industry. [61, 62]

One problem area of sorting processes has been the identification of black objects, such as black plastics and wet wood. The NIR technology that has usually been used in the sorting of plastics, is not suitable for analysing black particles since all radiation is absorbed into the material, as it has been discussed already in Chapter 4.4. The suitability of several technologies has been studied in recent years and two of them are mentioned in this context; middle-Infrared (MIR) and terahertz technologies.

Kassouf et al. had examined successfully the use of MIR ($4000 - 600 \text{ cm}^{-1}$) in the identification of packaging plastics where some of the samples were black. The study was conducted in laboratory conditions. The used IR method utilizes an ATR crystal, where the sample is clamped to the crystal. A non-contact detection method is needed in order to apply MIR technology in online sorting. [22]

Another technology under an active study is the Terahertz technology (THz). The wavelength area of THz is between the infrared waves and the microwaves. The wavelength is from $30 \mu\text{m}$ to 3 mm which means that its energy content is very low. [63] The restrictions of the technology have been the difficulty of detecting the radiation and the high cost of full spectroscopic sensors [63, 64].

THz technology has several applications ranging from the medical sector where it has been used for detection and imaging of mutated tissues like cancer to safety sector, where the most common use is the full-body scanners. There are not so many examples of the use of THz in the raw materials industry. [63] However Hein et al. from

the Fraunhofer Institut have utilized THz technology in identifying different polymers, also black coloured. [25] As a conclusion both of these techniques, MIR and THz, may have potential in solving the identification problem of the black polymers in the future.

5 Sensor-Based Equipment on the Market

This Chapter introduces some of the equipment suppliers that make sorting machines for the needs of the recycling industry. A summary of equipment suppliers and sorting machines is given in Table 2 at the end of the Chapter. The readers are requested to look at more exact information and more examples directly from the manufacturers' websites.

Usually, the sorting equipment contains a feeder system, a conveyor belt, material detection and separation with the help of compressed air jets into two product fractions. An example of this type of equipment was given in Chapter 2.2 in Figure 1. [11] The devices can also be built in a way that more than two output streams are produced, as for example the Eriez/TORATEC EcoTowerSort machine (Figure 15). More decks can be added when needed and this way repeated material feeding can be prevented. [65]

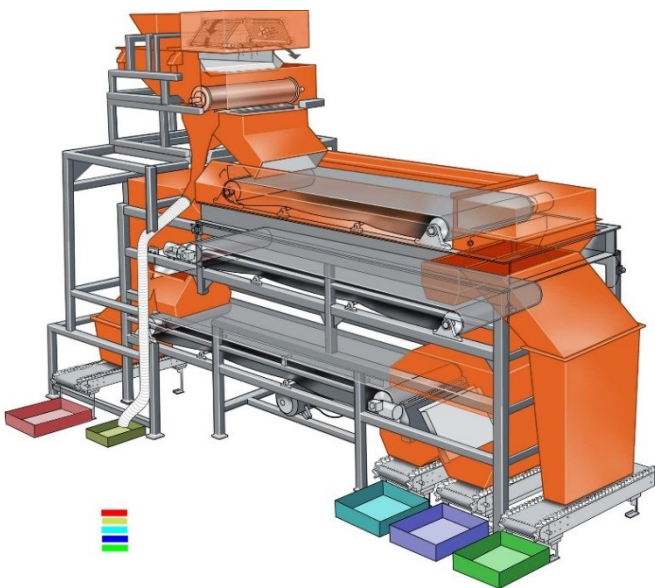


Figure 15. Eriez / TORATEC EcoTowerSort® [65].

In addition to other sorting technologies, a Finnish company called ZenRobotics Ltd, represents a different philosophical approach to material sorting. The beauty of their technology is that it utilizes machine learning. Also the sorting takes place with the help of robotic arms and this way the number of product fractions is not limited. [13]

Table 2. Sensor-based equipment on the market

Supplier	Sorting Equipment	Additional information
TOMRA, Sorting Solutions, Recycling [11]	TITECH autosort	Sensor options NIR1, NIR2, VIS
	TITECH combisense	Sensor options colour line scan camera (CRGB), EM
	TITECH finder	Sensor options EM, NIR1
	TITECH x-tract	Sensor options XRT or XRF (with EM)
STEINERT Elektromagnetbau GmbH [10]	STEINERT ISS	Induction based sorting (EM)
	STEINERT KSS	Combined sorting system; EM, XRT, Colour
	STEINERT XSS F	XRF sensor
	STEINERT XSS T	XRT sensor
	UNISORT C	Colour camera
	UNISORT Flake	Colour camera, NIR
	UNISORT PR	NIR-HSI
IMRO Maschinenbau GMBH [66]	IMRO DiscoveryLine	Sensor options / combination EM, NIR, VIS/Camera, X-Ray
	IMRO DSS	Sensor options / combination EM, NIR, VIS/Colour, X-Ray
Redwave [19]	Redwave C	Colour camera
	Redwave NIR & NIR / C	NIR sensor and NIR with colour camera
	Redwave M	Induction based sorting (EM)
	REDWAVE XRF-M	EDXRF
Eriez [65]	Eriez / TORATEC EcoTowerSort	A vertical-stack design. EM or NIR combined with rare earth and eddy current separators
PELLENC ST [67]	Mistral	Technologies : NIR, VIS Color
	Fine sort	Technologies: NIR, VIS color. For small sized materials, 4mm – 15mm
	Xpert	Technologies : XRT

S+S Separation and Sorting Technology GmbH [68]	VARISORT C / M / N / CMN / COMPACT	Single sensors: Colour / Metal detection / NIR / All sensors combined / For fractions 5 – 40 mm
	WEEE-SORT C / M / N / CM / CMN	For E-Scrap Recycling. Colour / Metal detection / NIR / Combinations
	FLAKE PURIFIER C / M / N	For purifying plastic flake fractions. Colour / Metal detection / NIR
BLU BOX [69]	BLUBOX Plug & Recycle	Mixed lamp and flat panel display recycling
Zen Robotics Ltd. [13]	ZenRobotics Recycler (ZRR)	Advanced machine learning technology with multiple sensors VIS spectrum cameras / NIR / 3D laser scanners / haptic sensors etc.
MSS INC. [70]	CIRRUS™	Combined NIR, Colour & Metal sorting systems
	L-VIS™	Colour sorting system for small particles
	MetalSort™	Induction base true all-metal sensor
	Sapphire™	Full spectrum near infrared (NIR) sensor

II Experimental Part

The main objectives of the experimental part were testing of the Poly-XRF sorting equipment with selected samples. Information was obtained from the parallel measurements of one spectrometer, as well as between all six spectrometers. The sorting was not necessarily intended to produce 100% pure fractions, but rather to enrich material streams, or alternatively, to reduce the concentration of undesired substances.

Chapter 6 introduces the Poly-XRF sorting device with its main components and adjustments as well as its working principle. Chapter 7 presents the test materials. Preparation and performance of experiments are described in Chapter 8 and results in Chapter 9. At the end of the thesis, the results are analysed and discussed together with conclusions and recommendations for further study in Chapters 10, 11 and 12, respectively.

6 Poly-XRF Sorting Equipment

The equipment used in the experimental part of the master's thesis, Poly-XRF, is a result of long research collaboration between Kuusakoski Oy and VTT Technical Research Centre of Finland Ltd. The physical structure of the device was built by Kuusakoski's own metal workshop RecTec and the software was designed by VTT. The Poly-XRF is a prototype sorting equipment for metal recyclates with estimated throughput around 1 ton an hour. It is designed for sorting materials that contain the following elements; iron (Fe), chromium (Cr), manganese (Mn), copper (Cu), zinc (Zn), molybdenum (Mo), nickel (Ni), lead (Pb), gold (Au) and bromine (Br). One type of material can be ejected at the time from the feed material.

The Poly-XRF device is presented in the Figure 16. The whole sorting system can be divided into three main units marked in the figure; the *Feeding unit*, the *Detection unit* and the *Separation unit*. The Feeding unit consists of a Transport belt, a Vibratory feeder and a Detector belt. The Detection unit consists of a Camera, Laser line projector, X-Ray Tubes (3 pieces) and Detectors (6 pieces), which are placed under protective lead cover. The Separation unit consists of a block of Air Valves and collection bins for both dropped and ejected materials.

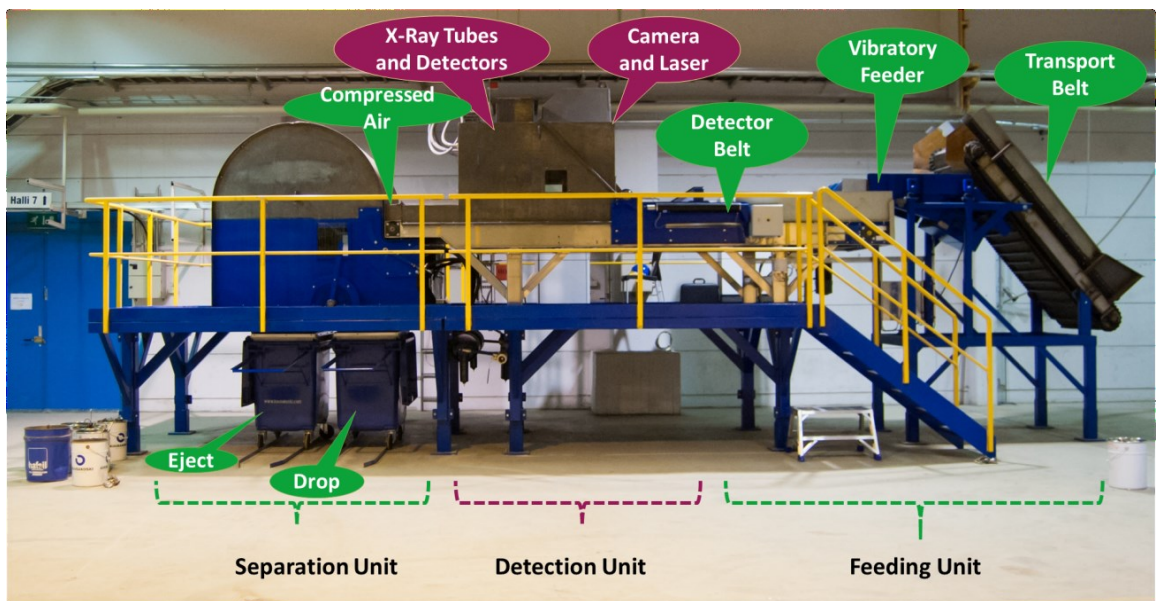


Figure 16. Poly-XRF test system.

6.1 General Working Principle

The functional principle of Poly-XRF is presented in the Figure 17. At first, in the *Feeding unit*, unsorted metal recyclates are fed onto the Transport belt, which drops the material on the Vibratory feeder. It divides the material into six fractions and creates a so called queuing system for the particles. This makes the particles to form an even feed when they are dropped onto the Detector belt with the working width of 1400 mm. The purpose of the queuing system is to prevent too many particles from entering the *Detection unit* at the same time. When particles reach the Laser line and

3D-camera, information of their location and size is transmitted to the automation system. Based on this positional information, particles are exposed to the primary X-Ray radiation coming from three X-Ray Tubes. [71]

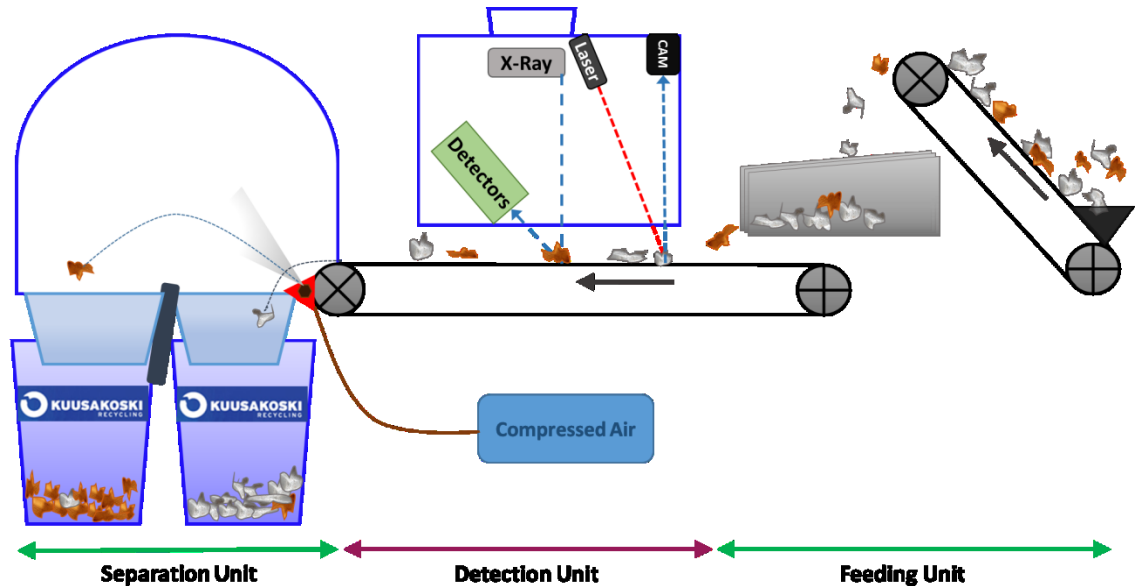


Figure 17. Functional principle of Poly-XRF.

The particles emit fluorescent X-Rays that are detected by the spectrometers using Silicon Drift Detectors (SDD) [72]. The X-Rays are converted to voltage pulses in the detectors. The amplitudes of the pulses correspond to the energies of the X-Ray photons and the spectrometer has the facility to discriminate the pulses at selected energy regions. If the energy of a pulse falls within a desired region, then one digital counting pulse is sent to the programmable logic controller (later PLC). Three such regions can be defined for each spectrometer for the comparative analysis of XRF spectral features. [71]

The actual classification decision is executed via PLC, where the information on classification limits is transmitted from recipes. The classification of a passing particle is based on the counts per second value in a specific energy interval, which is compared with a threshold value pre-defined by the operator. At the beginning of the tests, a

sophisticated guess of the threshold value is set and it may be changed later according to the actual Pulse Value Results. If the set threshold value is exceeded, a command from the PLC is sent to activate appropriate air valves from the ejection unit. Therefore, the particle is ejected with the jet of compressed air. In the *Separation unit*, the feed material is divided into two fractions, eject and drop. [72]

6.2 Equipment Specifications and Main Adjustments

The equipment consists of a variety of adjustable settings that need to be separately optimized for each input material. Some of the adjustments are mechanical and they are adjusted around the device. While others, are programmed in the software and can be modified in the user interface. The equipment also contains some fixed components. The main specifications and adjustments are briefly presented both in Table 3 and in the text below.

Table 3. Poly-XRF equipment specifications [72]

Parameters	Values
Working width	1400 mm
Detector Belt Speed	0 – 2 m/s
X-Ray Sources (3 pieces)	50 kV, 1.0 mA, Ag target
Collimator slit width	1.4; 2.0; 3.1; 4.7 mm
Thickness of the X-Ray tube Al-filter	0.29 mm or 1 mm
Detector distance from the conveyor	~70 – 200 mm
Resolution of detectors	140 eV
Air valve nozzles	104 pcs, \varnothing 2.5 mm
Nozzle distance	12.5 mm
Compressed air pressure	7 bar
Gap size of divider	0.05 – 0.8 m

The speed range of the detector conveyor belt is from 0 - 2 m/s, while the estimated operating speed ranges from 0.2 – 1.2 m/s. The speed can be adjusted from the user interface and it can be higher for larger particles, since they provide larger amount of pulses for the detectors. In addition to this, the speed of the transport belt and the power of the vibrating feeder can be adjusted. [72]

The X-Ray sources of the Poly-XRF are situated perpendicularly towards the detector belt and the distance is 0.8 m [72]. Silver (Ag) had been selected as target material for the X-Ray tubes. The anode material determines the pattern of the characteristic background radiation created from the X-Ray tubes. The characteristic line which is created from silver does not disturb the analysis of iron, molybdenum, copper or zinc for example because it is placed on a higher energy region. [35]

The width of the X-Ray beam can be adjusted by changing the width of the collimator slit. There is a mechanical control with four different widths and two different aluminium filtering thicknesses. The size of the X-Ray beam is selected to correspond to the particle size of the input. [72] The width must not be too large, since then the detectors can observe the fluorescence radiation from more than one specimen. Also the amount of background scattering can get too high causing measuring errors. On the other hand, a too narrow X-Ray beam can reduce the pulse frequency and thus requires the use of a slower conveyor speed. [71]

Usually, a filter is put in front of the X-Ray tube to reduce the backscatter in the most interesting energy areas [33]. The thicker aluminium filtering is chosen if there is a strong, dominating line in the low-energy region of the spectrum. [72] For example, if the input contains plenty of iron; its signal strength can be reduced with the help of the thicker Al filtration. This may help to identify weaker lines from the spectrum. [71]

All six detectors have been set inside a movable protection case, which is set at 55 degree angle with respect to the conveyor [72]. The measuring geometry of the equipment is illustrated in Figure 18.

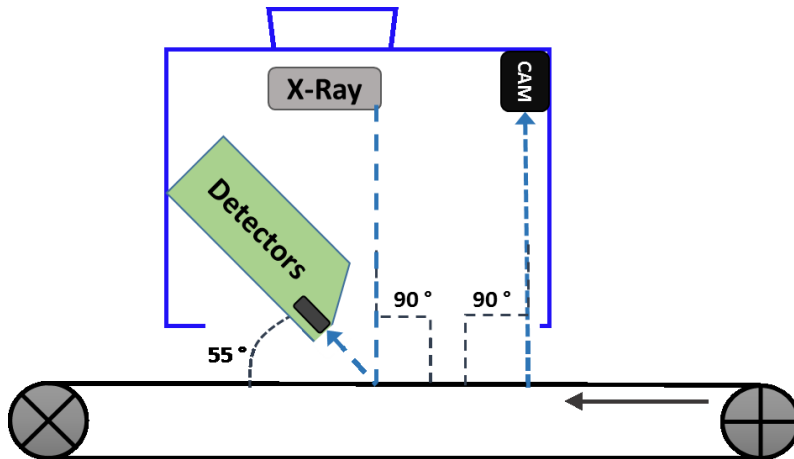


Figure 18. The measuring geometry.

The distance of the Detectors from the conveyor is mainly selected according to the particle size and content of the input material. In order to provide sufficient amount of pulses from small-sized particles, detectors must be set as close to the belt as possible. [71] Then one must, however, keep in mind that when the detectors are closer to the conveyor, their area of vision will narrow. In that case the good functionality of the queuing system will be more critical and more important.

Inside the *Separation unit*, there is a divider, between the two product fractions. The Gap size corresponds to the width of the opening between the air valve block and the divider. Both the speed of the Detector belt and the particle size of the input affect the selection of the width. [72]

Some of the equipment components are fixed, for example the line laser and camera, and the operator cannot make any adjustments related to these. In addition, the compressed air pressure and valve type are fixed. The operator is able to modify the timing of the air jets, but neither on the number of active valves nor the time how long one exhaust takes place. Information is received from the camera and PLC. [72]

6.3 Classification Principles

The classification principle can be either *absolute* or *relative*. Absolute classification is chosen in situations in which there is no relevant reference spectrum, or concentrations of different elements vary. The absolute classification principle is suitable when the particle size distribution of the input is very narrow. It favors large particles and may neglect small pieces completely. In absolute classification, the range of emission energy values is set only for the searched element in the Channel 1. [72]

In relative classification, pulses from two different channels (*Channel 1* and *Channel 2*) are compared with each other. The counts are presented in the user interface as Pulse Ratio Values, which change in the range of 0 – 100%. The emission energy range for the searched element is set to Channel 1, similar to absolute classification. The reference region of the spectrum, including the emission area of Channel 1, is set in the Channel 2. [72]

An *emission line chart* [73] can be used as help when choosing emission values. In addition, known reference samples can be measured with the software of the spectrometer manufacturer (Amptek), where the emission limits can be checked from the spectrum. At the same time, appropriate minimum measurement time may be evaluated. The relative classification is suitable and recommended for most situations and it also fits sorting particles with varying sizes [71].

7 Test Materials

The Poly-XRF sorting equipment was tested with three test materials, which are shortly presented in Table 4. The selection criteria and composition of the test materials are discussed in the following chapter. All of the samples were characterized by weighing with a laboratory scale (METTLER TOLEDO, NewClassicMS) and analysing their element composition with a handheld XRF analyser (OXFORD INSTRUMENTS, X-MET 7500). The characterization results are presented in the Appendices I, II and X.

Table 4. Test materials used in the thesis experimental part

Test material no.	Detected element	Things to consider
Test material 1	Molybdenum (Mo)	Mo-concentration is easy to identify
Test material 2	Zinc (Zn)	Identifying zinc-alloys from copper
Test material 3	Gold (Au)	The shape of the specimens

7.1 Test Material 1

Material 1 contains altogether ten samples (Figures 19 & 20), seven pieces of acid proof (EN 1.4432; AISI 316) steel having approximately 2 % of molybdenum (Mo) and three pieces of common stainless steel (EN 1.4301; AISI 304). The material is originated from the Kuusakoski Oy Heinola Works, where the End of Life Vehicles (ELV) and large household appliances are crushed and processed. The material undergoes several unit processes, for example washing, screening, magnetic separation and specific weight based separation, also known as sink-and-float. In addition, copper, brass, zinc and lead are removed by *Titech Combisense* and hand sorting stages. At the moment, the remaining stainless steel fraction is sorted for acid proof stainless steel separation with an older, similar type XRF-system, with smaller expected capacity than that of the Poly-XRF. In the thesis experimental part, this same material stream is used for testing the Poly-XRF. The motivation for sorting is that a better commercial value is gained for higher Mo-concentration. Both product fractions are sold to steel smelters for the production

of new steel. An identification criterion for material 1 is the high enough concentration of molybdenum, which is easy to characterize from the spectrum.



Figure 19. Test material 1, samples 1 - 5.



Figure 20. Test material 1, samples 6 - 10.

The iron (Fe) and molybdenum (Mo) contents of test material 1 samples are presented in Table 5. The wider characterization results of element composition are presented in Appendix I.

Table 5. Iron and Molybdenum content in test material 1

No.	Stainless Steel Type	Fe [%]	Mo [%]
Sample 1	1.4432; AISI 316	68	2.0
Sample 2	1.4432; AISI 316	69	1.9
Sample 3	1.4432; AISI 316	68	2.1
Sample 4	1.4432; AISI 316	69	2.5
Sample 5	1.4432; AISI 316	64	2.4
Sample 6	1.4432; AISI 316	71	2.0
Sample 7	1.4432; AISI 316	68	2.6
Sample 8	EN 1.4301; AISI 304	70	0.26
Sample 9	EN 1.4301; AISI 304	71	0.17
Sample 10	EN 1.4301; AISI 304	71	0.05

7.2 Test Material 2

The second material (Figure 21) is originated from the same process as material 1. It is the remaining fraction of the *Titech Combisense* sorting process. In addition to copper and brass, the material stream contains lead and zinc etc. In this experiment, 3 pieces of brass and 3 pieces of copper were taken from the real process stream that has particle sizes ranging from 40 to 120 mm. In addition, one sample of pure zinc (> 95 %) was included as a reference sample. The objective was to separate brass from more pure copper. This would result in better commercial terms of the cleaned fractions. An identification criterion is the high enough concentration of zinc. The characterization from the spectrum may not be easy, because the energy emission lines of copper and zinc are very close to each other. The removal of other metals is not studied here.



Figure 21. Test material 2.

The copper (Cu) and zinc (Zn) contents of test material 2 samples are presented in Table 6. The wider characterization results of element composition are presented in Appendix II.

Table 6. Copper and Zinc content in test material 2

No.	Cu [%]	Zn [%]
Sample 1	85	10
Sample 2	56	38
Sample 3	61	35
Sample 4	50	50
Sample 5	0.17	99
Sample 6	95	0.47
Sample 7	95	0.61
Sample 8	96	0.50

7.3 Test Material 3

The third material is a radio frequency (RF) circuit board from a GSM base station (Figure 22). It was chosen due to its economic significance. The copper nickel circuit board is coated with a very thin gold layer ($< 0.1 \mu\text{m}$). A big RF-board was cut into eight parts, which were marked with numbers and arrows similar to materials one and two. The objective was to examine if the Poly-XRF is able to identify the energy that gold emits, when the measurement time in on-line measurement is rather short. Copper and nickel may interfere in the detection of gold.

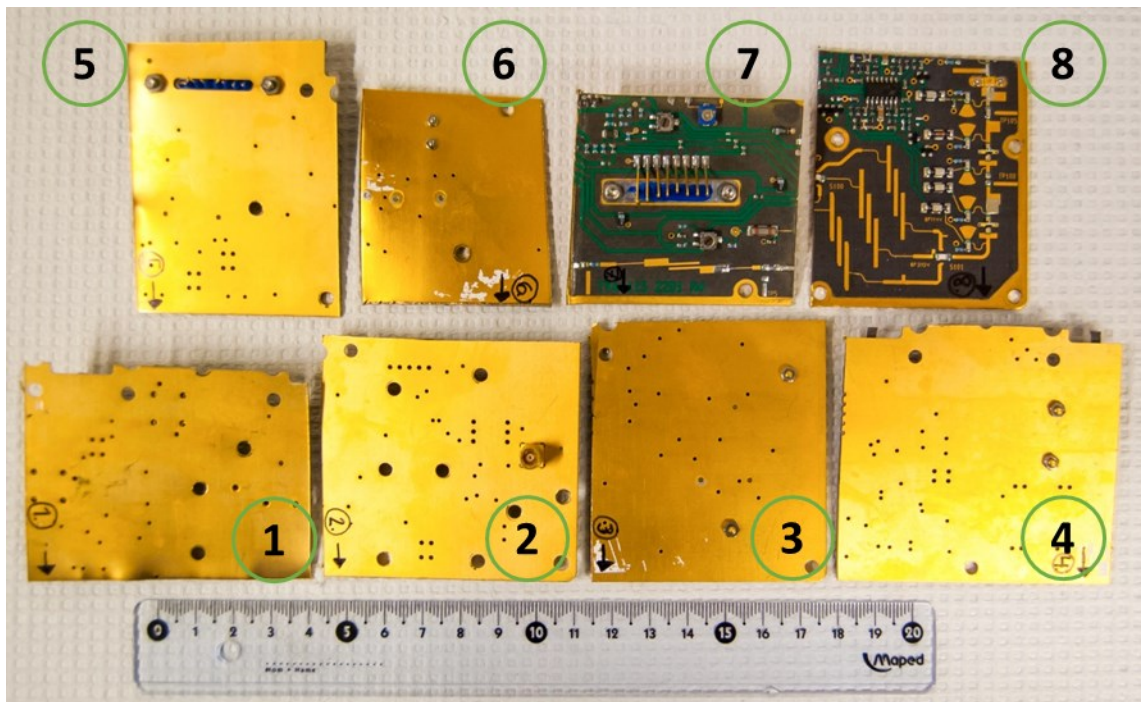


Figure 22. Test material 3.

8 Experiments

8.1 Preparation for Experiments

All three test materials were prepared for actual experiments. The samples were weighed and the contents were measured with a handheld XRF analyser (Chapter 7 and Appendices I, II and X). In addition, they were marked with numbers and arrows to present their feeding order and direction in the tests. All three chosen test materials differ from each other and their analysis criteria are very different. Thus, before the actual experiments, the suitable measuring parameters had to be chosen and the recipes for the user interface created. The used test systems are presented in Table 7. Choosing of the adjustments is discussed in Chapter 6, where Poly-XRF, its operating principle, main specifications and classification principles were introduced (cf. Chapters 6.1, 6.2 and 6.3).

Table 7. Test systems used during the experiments

Parameters	Test material 1	Test material 2	Test material 3
Detector distance from the conveyor [mm]	140	100	70
Detector Belt Speed [m/s]	0.4	0.2	0.2
Collimator slit width [mm]	3.1	2.0	2.0
Thickness of the X-Ray tube Al-filter [mm]	1	0.29	0.29
Classification principle	Relative	Relative	Absolute
Channel 1 [keV]	17.12 – 17.82	8.30 – 8.75	9.59 – 11.72
Channel 2 [keV]	6.17 – 17.82	7.75 – 9.2	-
Threshold value	8 / 11	5	-
Belt length offset [mm]	-45	-50	-
Gap size of divider [m]	0.17	0.14	-

Since the performance of Poly-XRF was not tested earlier, the maximum operating speed is not known. In the thesis, the emphasis was on studying the measuring reliability and consistency. Therefore, relatively low speed of the Detector belt was used in the experiments. The emission energy literature values for the elements dealt in the experiments are presented in Table 8. The values marked with brackets were not needed.

Table 8. Literature values for emission lines [73]

Element \ Emission Line	K_α [keV]	K_β [keV]	L_α [keV]	L_β [keV]
Iron (Fe)	6.40	(7.06)	(0.70)	(0.72)
Molybdenum (Mo)	17.48	(19.61)	(2.29)	(2.40)
Copper (Cu)	8.05	8.9	(0.93)	(0.95)
Zinc (Zn)	8.64	9.57	(1.01)	(1.03)
Gold (Au)	(68.79)	(77.97)	9.71	11.44
Nickel (Ni)	7.48	8.26	(0.85)	(0.87)

8.2 Experimental Procedures

The actual experiments were performed with the same principle to all tested materials. The samples were fed on the detector belt by hand in numbered order, with varying distances (15 - 100 cm). With every six detectors, 30 repetitions were measured and their measuring order was chosen randomly. Before the experiments, the energy scale of spectrometers were calibrated using a stainless steel plate that contains molybdenum and the background was measured with an empty detector belt. An example of the calibration result is presented in Appendix III.

Pulse values [counts/s] or Pulse Ratio Values [%] depending on the chosen classification principle, are registered in the user interface. From there, they can be copied to Excel worksheet for example, for analysing the results. The purpose is that the variation of measurement results can be compared within one detector and with all detectors.

The success of the ejection was monitored in the cases of test materials 1 and 2. A statistical note is not registered in the user interface, thus the data is based on the operator's observations. Furthermore, the samples were collected and calculated manually from two product fractions, eject and drop.

9 Results

All the measurement results are presented in Chapter 9. First the consistency between detectors was evaluated with the help of the results of materials 1 and 2, since the same sample population was measured with each six detector. Furthermore, the effect of different variables on the recovery and the differences in particle sizes and shapes on the pulse frequency distributions were observed. In addition, an estimate for the product grade is given to the materials 1 and 2. The test material 3 was studied in a little different way than materials 1 and 2.

9.1 Detector Consistency

The functionality was tested by comparing the detectors with the help of test materials 1 and 2. The consistency has been illustrated in Figures 23 - 24 where the results are from the detectors 1 and 2. Each detector measured the same sample population. The *x-axis* indicates the Pulse Ratio Values [%] and the *y-axis* their frequency. Furthermore, due to simplification all samples with similar chemical composition were marked with the same colour; samples of AISI 316 (7 pcs) with violet and AISI 304 (3 pcs) with green. The results from detectors 3 - 6 can be found in Appendix IV, in Figures 47 - 50.

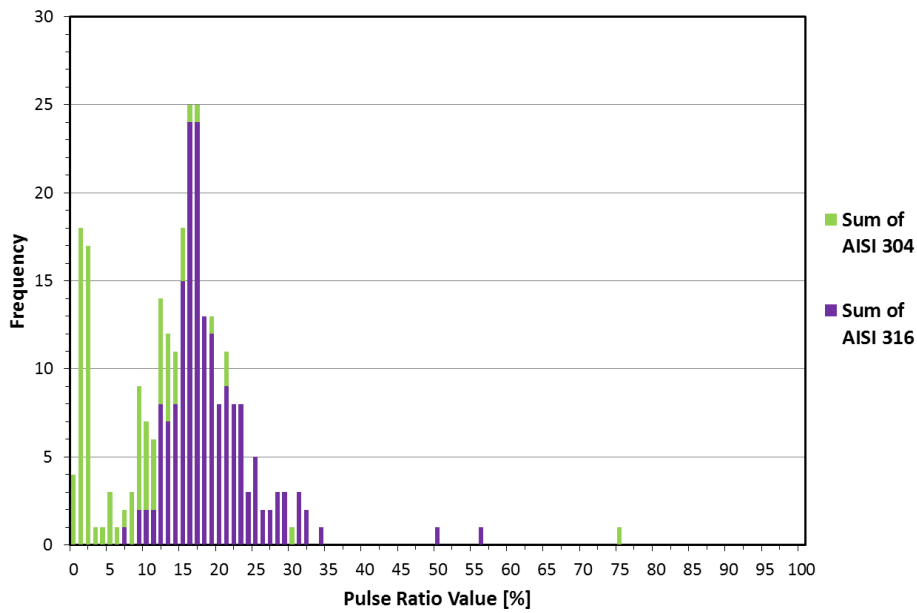


Figure 23. The pulse frequencies of test material 1 on detector 1.

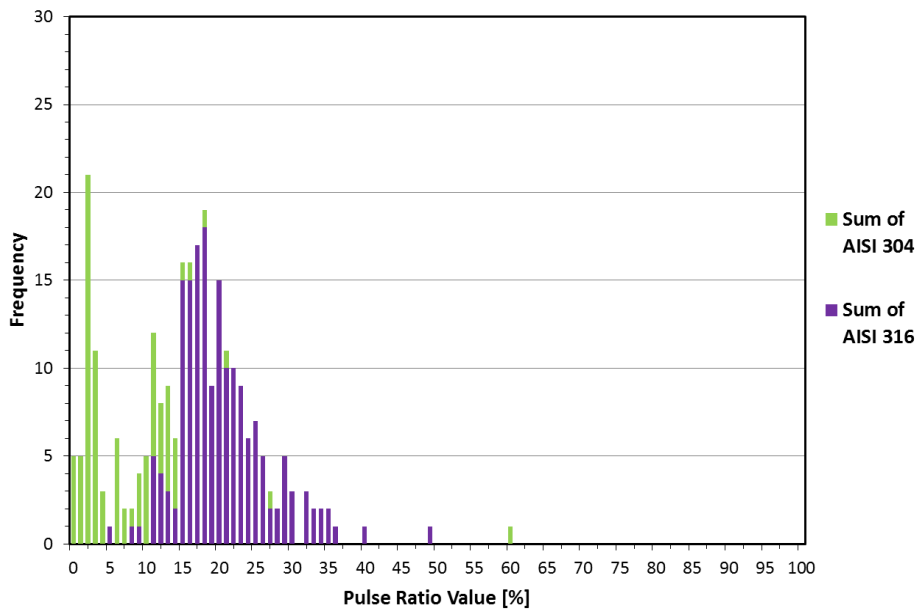


Figure 24. The pulse frequencies of test material 1 on detector 2.

The detector consistency was also tested with test material 2, as can be seen in Figures 25 and 26. All the copper alloys with less than 0.7 % of zinc were marked with light green (3 pcs), zinc (more than 95 % of Zn) with light blue (1 pcs), brass sample with app. 10 % of zinc with black (1 pcs) and the rest of the brass samples, that had zinc

content ranging from ~35 – 50 %, with fuchsia (3 pcs). The results from detectors 3 - 6 can be found in Appendix V, Figures 51 - 54.

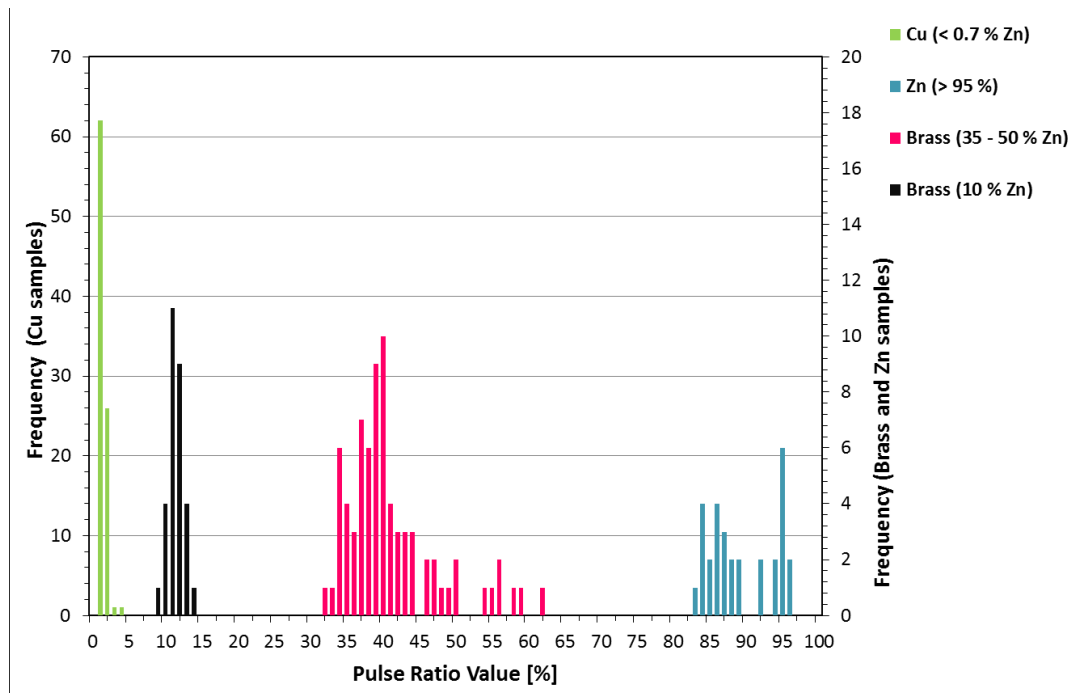


Figure 25. The pulse frequencies of test material 2 on detector 1.

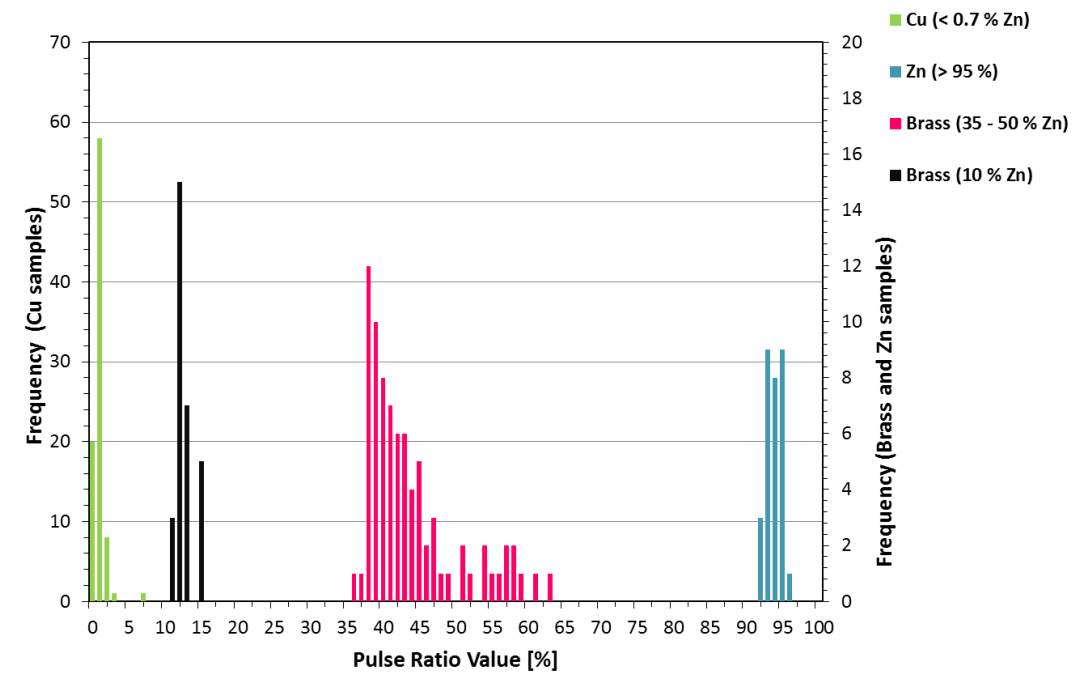


Figure 26. The pulse frequencies of test material 2 on detector 2.

9.2 Sorting Results of Test Material 1

The measurement data of test material 1 is presented in Appendix VI. There the results have been divided in six parts according to the number of the detector. Altogether 30 similar series were measured with every detector. The numerical values in the tables are Pulse Ratio Values [%] and it has been marked either under Drop or Eject, depending on which product fraction the sample ended up in. On the basis of the first ten measurement results, the threshold value was increased from eight to eleven.

By changing the operating parameters of the sorting device for each material, the desired fraction can be separated out, optimising either the total yield or the quality of the product. The terms recovery and grade are used as they are described. These terms are commonly used when the concentration of metallic ores is described and they are also suitable for describing the enrichment process of recycled metals. In ore-dressing, the recovery is the percentage of the total metal contained in the ore, which is recovered into the concentrate. For example a recovery of 90 % means that 90 % of all metals in the ore is recovered into the concentrate (here eject) and 10% is lost in the tailings (here drop). [18] In the case of processing recycled metals, recovery is the percentage of the total metal content of the feed that is recovered in the concentrate (eject).

The grade usually refers to quality, i.e. the content of the marketable product in the material, e.g. in metallic ores it refers to the per cent of metals. The grade can also be given as parts per million (ppm) or grams per ton (g/t). [18] In the case of recycled metals, the grade illustrates the per cent of the metals which define the market price of the saleable product. In this work, the grade was only calculated for molybdenum to make it simpler.

9.2.1 Recovery Rates

The result of the actual recovery of each sample was compared with theoretical recoveries, at threshold values eight and eleven. This is shown in Figure 27 below. The possible reasons for the difference between actual and theoretical values are examined throughout this Chapter.

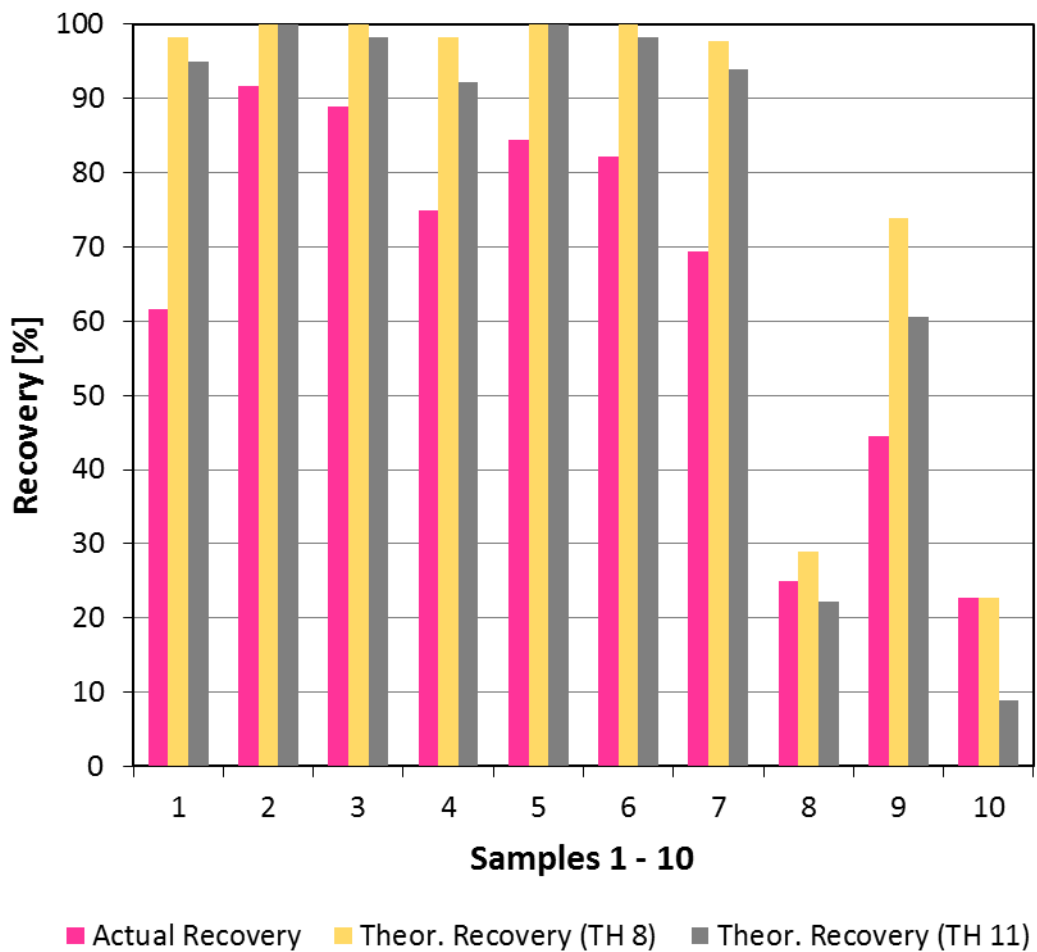


Figure 27. Actual and theoretical recovery at threshold values 8 and 11.

The actual separation was examined by comparing the effect of different variables on the actual recovery. These variables were molybdenum content of a sample, mass, sample width, and sample width – mass ratio. These are presented in Figures 28 – 31.

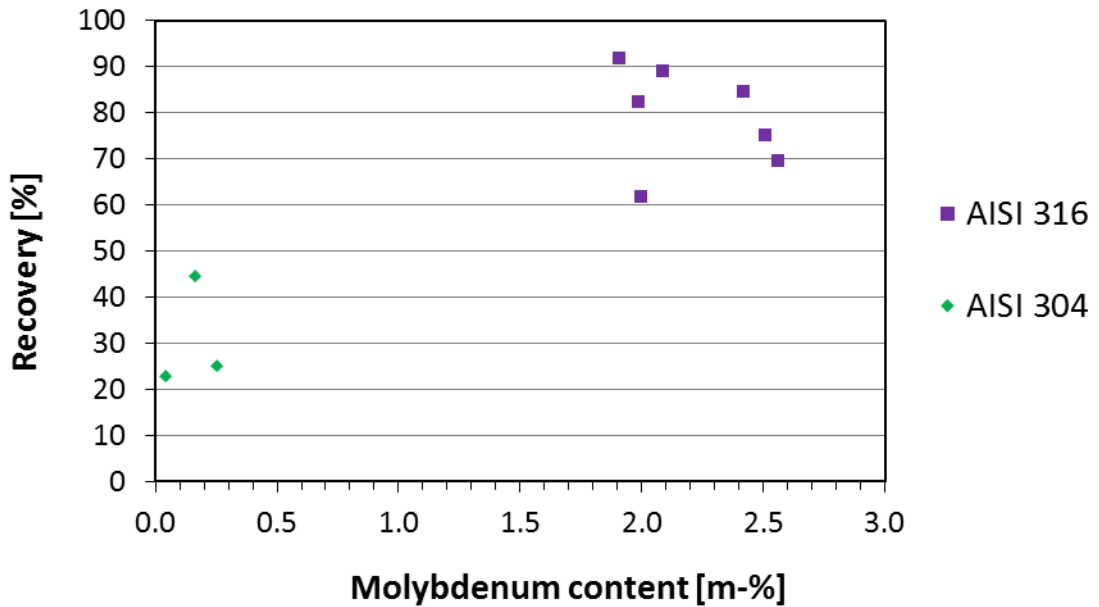


Figure 28. Effect of Mo-content on Recovery.

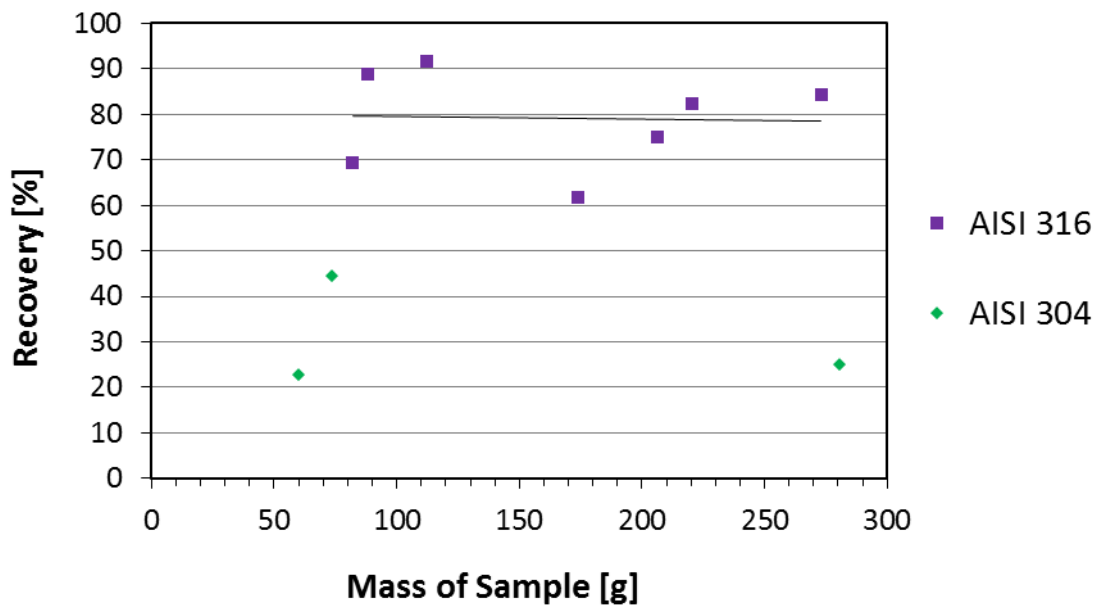


Figure 29. Effect of a sample mass on Recovery.

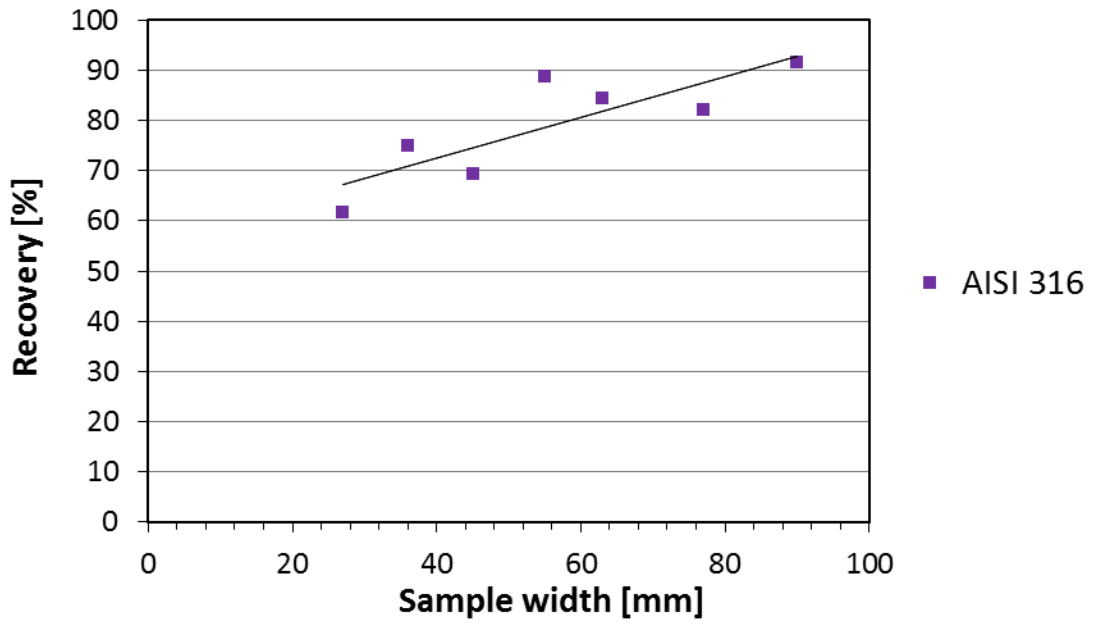


Figure 30. Effect of sample width on Recovery.

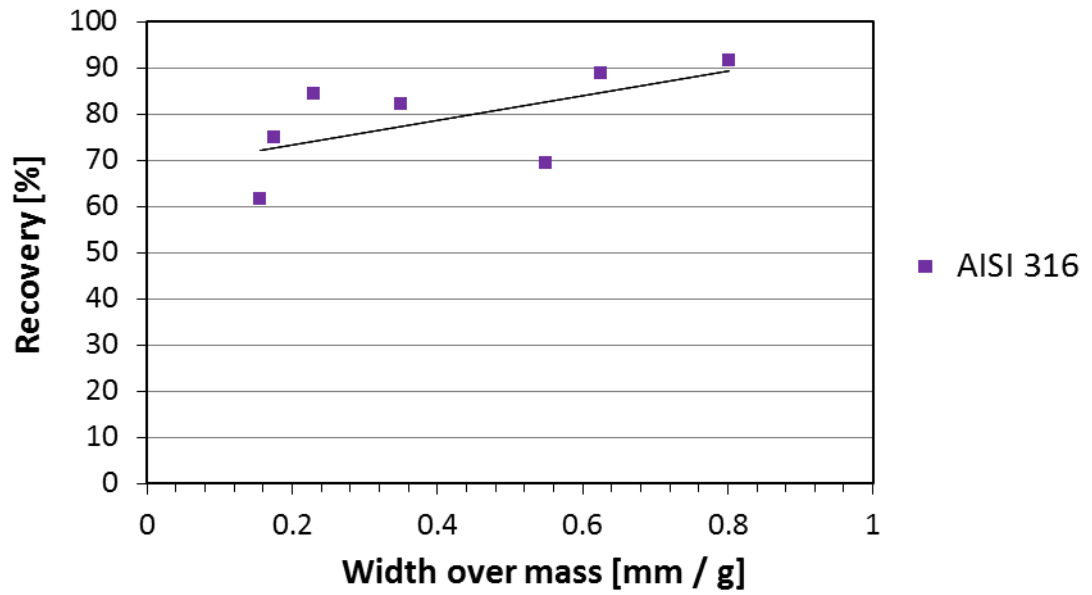


Figure 31. Effect of sample width over mass ratio on Recovery.

The effect of shape and size of the samples with constant chemical composition were studied with comparing the variation of pulse frequencies between different samples. As an example, frequency distributions of Pulse Ratio Values of samples 1 and 2 are given in Figures 32 - 35. The results for the rest of the samples are given in Appendix VII.

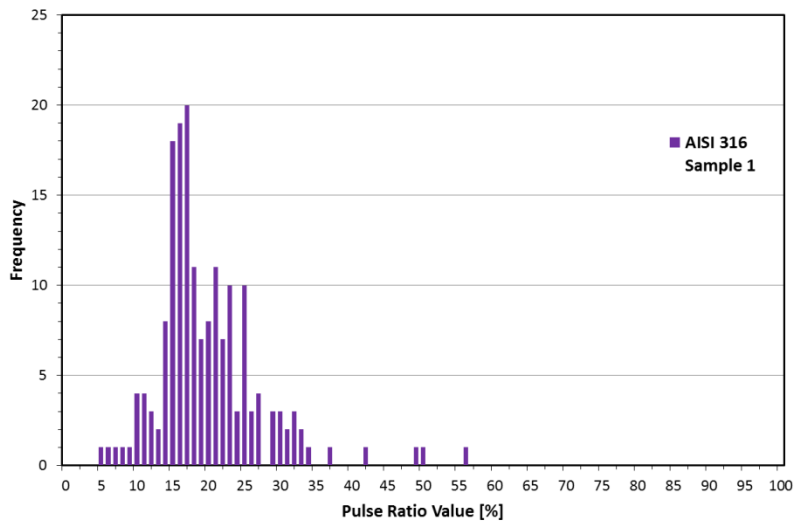


Figure 32. The pulse frequencies of test material 1, Sample 1 on all detectors.



Figure 33. Test material 1, Sample 1.

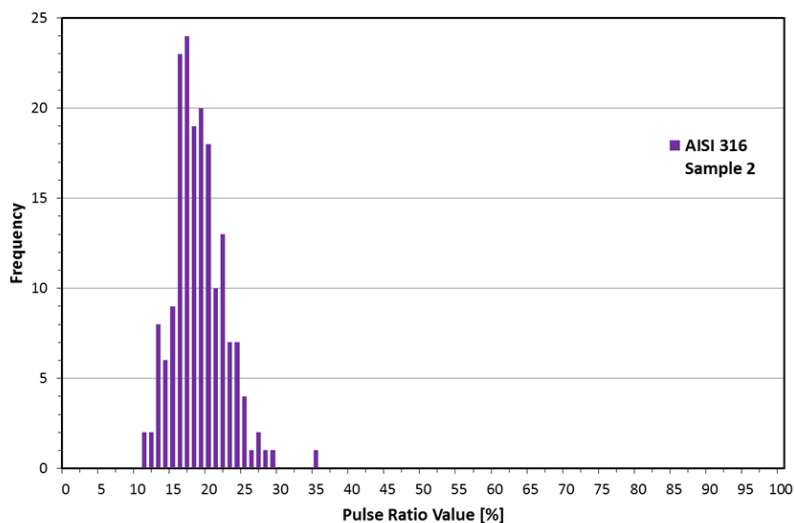


Figure 34. The pulse frequencies of test material 1, Sample 4 on all detectors.



Figure 35. Test material 1, Sample 4.

9.2.2 Recovery and Grade

The result of the actual grade and recovery was compared with theoretical values. This has been plotted in Figure 36. The grade-recovery curve was calculated with different threshold values; the numbers are given in Table 9. In addition, the effect of threshold value on theoretical recovery was illustrated in Figure 37.

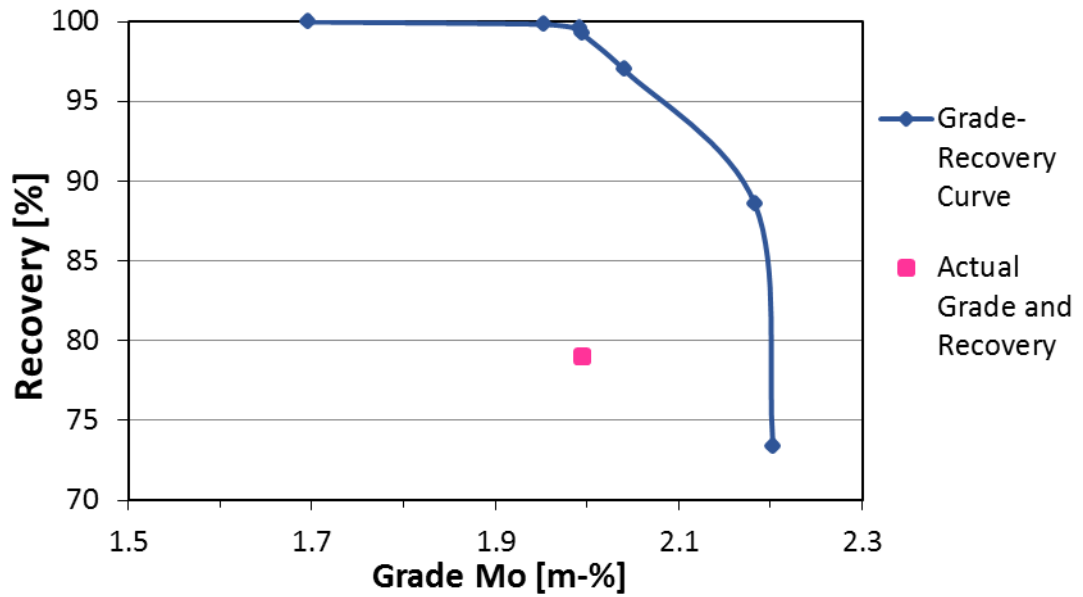


Figure 36. Theoretical Grade-Recovery Curve and actual Grade and Recovery.

Table 9. Calculated Grade and Recovery values

Threshold value	Grade of Molybdenum [m-%]	Recovery [%]
Feed	1.7	100.0
5	2.0	99.8
7	2.0	99.6
8	2.0	99.3
11	2.0	97.0
15	2.2	88.5
17	2.2	73.0
Actual	2.0	79.0

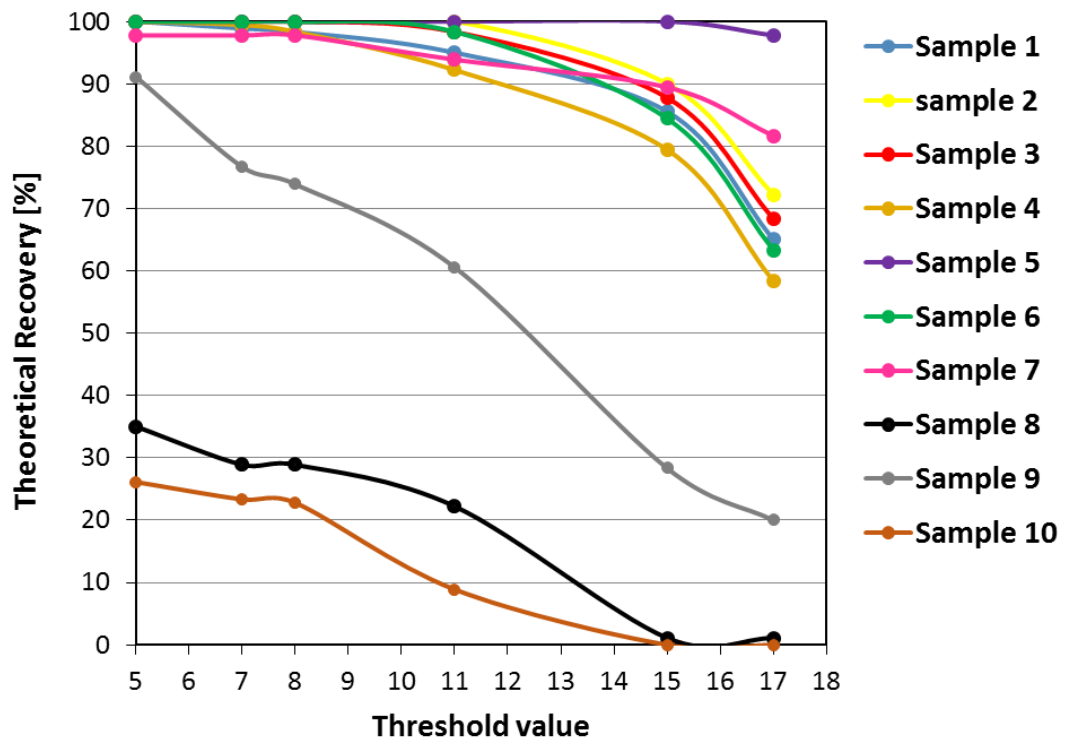


Figure 37. Effect of Threshold value on Recovery.

9.3 Sorting Results of Test Material 2

The measurement data of test material 2 is presented in Appendix VIII, similar to test material 1. With test material 2, attention was not paid to the effect of the different threshold values on the separation results, because its choice was very clear.

9.3.1 Recovery

The result of the actual recovery of each sample was compared with theoretical recovery, at threshold value five. This is shown in Figure 38 below.

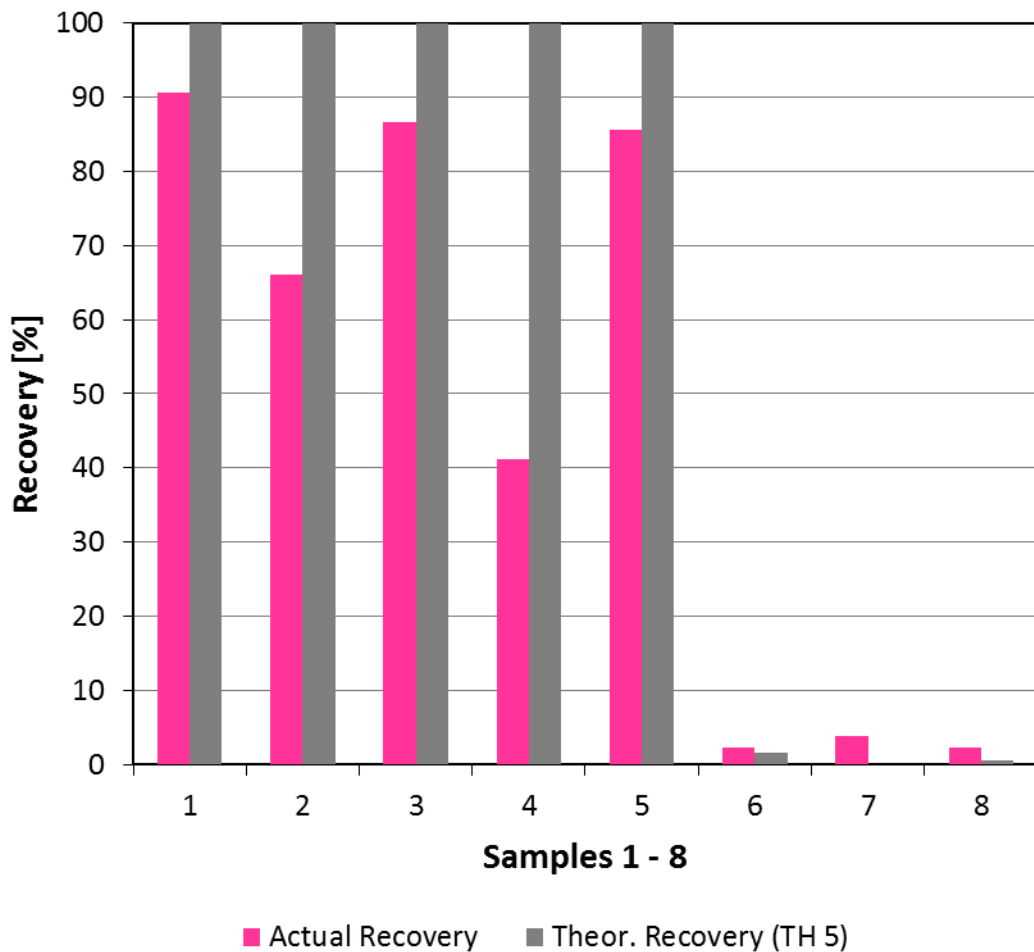


Figure 38. Actual and theoretical recovery at threshold value 5.

The effect of shape and size of the samples with similar chemical composition were studied with comparing the variation of pulse frequencies between different samples. Test material 2 included four different types of materials by chemical composition (Table 6; Samples 2 – 4 are considered very similar to each other). This pulse frequency variation between different sized samples is illustrated in Figures 39 and 42, where pulse distributions of samples 3 and 4 are given as an example. The results for the rest of the samples are given in Appendix IX.

Sample no. 4 also served as a good indicator when the vision of the camera was tested. The sample was placed at every detector line 30 times and it was noticed that the vision of the camera decreases from the central part of the conveyor towards the edges. The Recognition degree [%] of the camera on each detector line is shown in Table 10. The detectors measure only the samples that camera has first recognized.

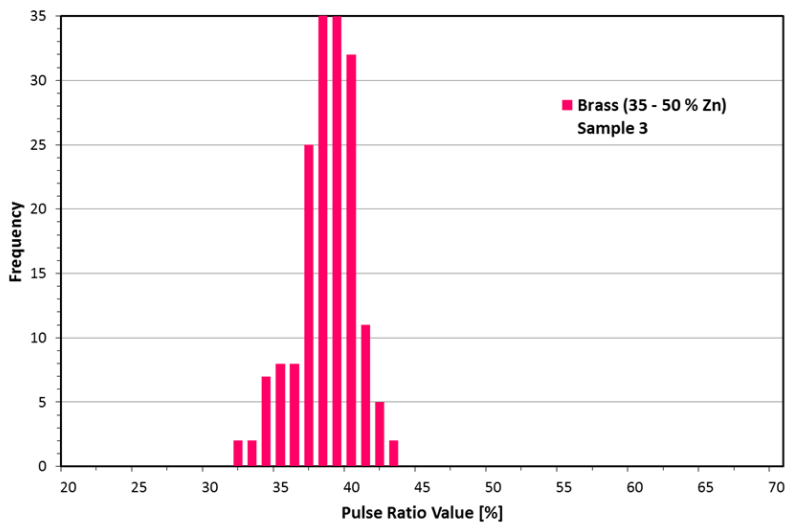


Figure 39. The pulse frequencies of test material 2, Sample 3 on all detectors.



Figure 40. Test material 2, Sample 3.

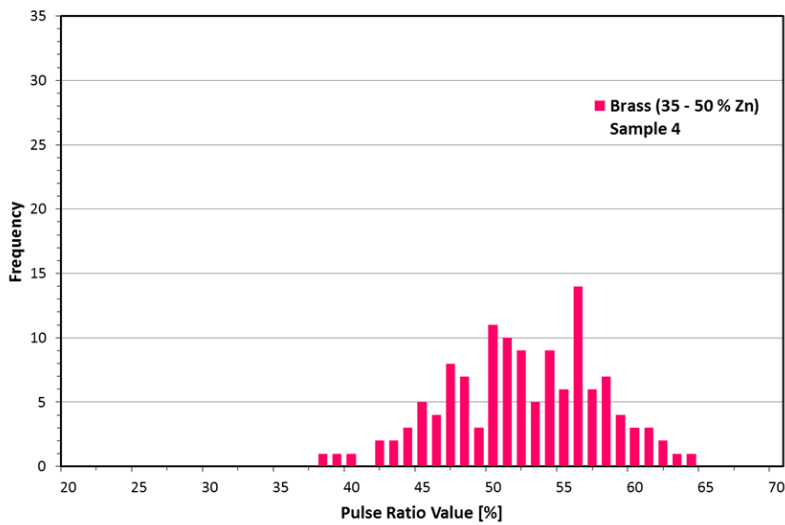


Figure 41. The pulse frequencies of test material 2, Sample 4 on all detectors.

Figure 42. Test material 2, Sample 4.

Table 10. Recognition degree of the camera on each detector line

Detector line	Line 1	Line 2	Line 3	Line 4	Line 5	Line 6
Sample 3	100 %	100 %	100 %	100 %	100 %	100 %
Sample 4	50 %	70 %	100 %	100 %	70 %	37 %

9.3.2 Grade

The objective was to separate brass from more pure copper. Therefore zinc and copper grades for both product fractions were calculated and they are presented in Tables 11 and 12 below. Theoretical separation result was calculated from the measured pulse values (Appendix VIII). Threshold value was set at 5.

Table 11. Zinc and copper grade of Eject

	Grade Cu [%]	Grade Zn [%]
Feed	79	17
Theoretical Grade at TH 5	57	39
Actual Grade	60	37

Table 12. Zinc and copper grade of Drop

	Grade Cu [%]	Grade Zn [%]
Feed	79	17
Theoretical Grade at TH 5	95	< 1
Actual Grade	90	6

9.4 Sorting Results of Test Material 3

The characterization results of element composition of test material 3, Au-coated RF-circuit board, are presented in Appendix X. The samples were all cut from one larger circuit board, so therefore only sample 1 was measured. The resolution of the handheld XRF analyser was not enough to identify gold at all. The coating thickness is app. 0.05 μm .

Test material 3 was not studied in the same way as materials 1 and 2. The examining was stopped when it was noticed that the camera does not identify the flattest parts. The results of pre-tests are shown in Appendix XI; two measurements with each detector were made. The spectra of a few samples were analysed with the software of the spectrometer manufacturer (Amptek), with measuring times of 5s and 0.3s. One measurement of each was included here in Figures 43 and 44, as an example. The L_{α} and L_{β} emission lines for gold are marked in figures. The peak data can be found in Appendix XII. The spectra were measured with detector 1. Note: The y-axis is on a logarithmic scale. In addition, in Figure 45 is shown three samples of test material 3, illustrating the measurement problem. The camera does not see the rightmost type of the pieces.

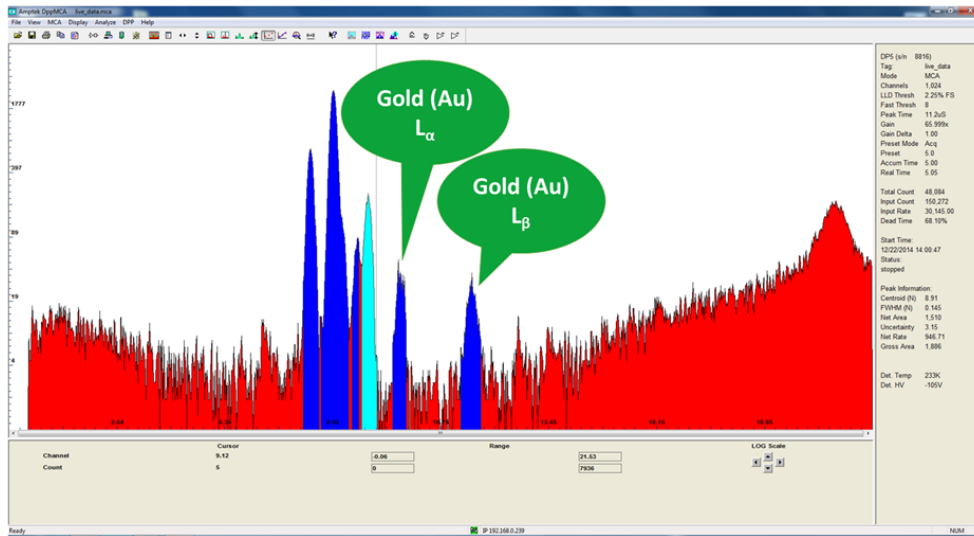


Figure 43. Spectrum of test material 3, sample 1. Measuring time 5s.

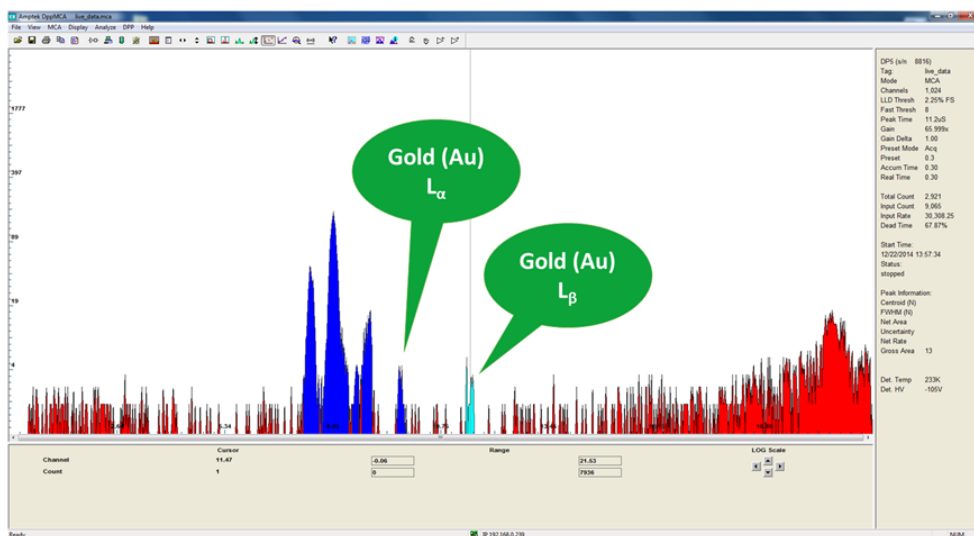


Figure 44. Spectrum of test material 3, sample 1. Measuring time 0.3s.

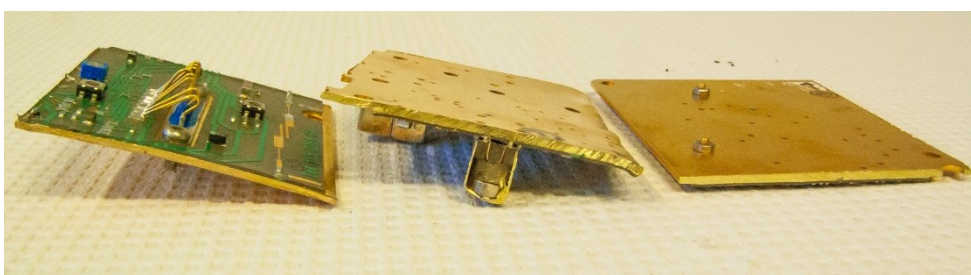


Figure 45. Test material 3, showing an example of the different angles.

10 Discussion

The main aim of the experimental part was testing of the Poly-XRF sorting equipment with selected samples. Therefore not only the separation results of three test materials are important but also the found errors and defects either on the functionality of mechanics or software. As the work proceeded, these faults that were preventing the testing were repaired several times. One of the biggest challenges was the slowness of data processing.

Examining the consistency between detectors was also one of the main objectives of the work (see Chapter 9.1). It was found that very little differences occur between the detectors; this was studied with test materials 1 and 2. The results of individual samples give consistent results with all detectors and the distributions followed the same trend fairly well.

During the experiments, it was found that factors limiting the final separation result the most, are the functionality of the camera and the success of the ejection. The performance of the camera decreases from the central part of the conveyor towards the edges. The camera is placed in the middle of the conveyor belt in the crosswise direction. Another problem is in the image processing algorithm that combines two separate particles into one piece according to a specific rule. Here the limit distance is about 23 mm. In other words, if the particles are too close to each other they are recognized as one. This condition causes problems also in the identification of small or flat shaped particles from which the camera sees only their edges.

In the Separation unit, a particle that contains the searched element is ejected in the product fraction called Eject. In the case of Poly-XRF, only one element can be search at a time. Re-circulation of the material is of course possible. A positive decision about the ejection is made when the measured pulse values are greater than the set threshold value.

An individual particle may still fall in the wrong product fraction caused by several factors, e.g.:

- The camera misreads the size or the place of a particle.
- Samples are fed too frequently. In this work it was found that with belt speed of 0.2 m/s the distance has to be at least 10 cm.
- The air blow event does not happen even though sufficient threshold value was exceeded. This happened in about 6 % of all single measurements in this work. This is one of the signal processing errors that still remained uncorrected.
- The shape or size of the sample is unfavourable.
- The object might hit the divider and fall into the wrong product fraction.
- Finally, the timing of the air jet is not correct. In the case of Poly-XRF, this may be adjusted on the basis of operator's visual observations.

The final separation degree differs from the theoretical separation degree. This can be seen from the results of test materials 1 and 2 in Figures 27 and 38. Thus it may be assumed that some of the factors affecting the final recovery are originated from the material characteristics. The effects of these variables on recovery were studied with test material 1, in Figures 28 - 31. The variables were the molybdenum content of a sample, mass, sample width, and the sample width – mass ratio. It is seen from the results that the elemental content (here molybdenum content) does not affect the recovery, when a certain material group is considered. The groups were acid proof steel (AISI 316) and common stainless steel (AISI 304). Furthermore, it can be seen from Figure 28 that the separation degree is low, when the Mo content is less than 0.5m-%.

Next it was studied if the deviation is caused by the sample mass. Figure 29 shows that there is no correlation between the pure mass and recovery. The samples were always placed on the conveyor in the same position. Thus the effect of the apparent sample width on the separation degree was examined next (Figure 30). It was found that the width of the sample affects the separation degree significantly. Also some correlation exists between the sample width-mass ratio and the recovery (Figure 31).

In addition, the effect of shape and size between samples with similar chemical composition on the form of the pulse frequency distribution was examined with test materials 1 and 2. Examples are given both in Figures 32 - 35 and 39 - 42. It was noticed that the size and shape affect the form of the distribution. On small or narrow samples more deviation appeared than with larger samples. This is probably due to the fact there is more back scattering, which interferes with the analysis.

The other sources of errors were dealt in Chapter 3.3; the results are influenced for example by time-dependent repeatability and the settling of the particle towards X-Rays and the detectors. In the experiments of the diploma work an attempt was made to minimize these sources of errors by feeding the individual samples manually. The samples were always placed in the same position on the conveyor and to certain lines, so that they would pass under the detectors as near as possible. Also an attempt was made to avoid possible calibration errors by calibrating the equipment every time just before the beginning of measurements.

Sorting Result of Test Material 1

The successful calibration is one of the key parameters when operating the Poly-XRF sorting equipment. This was noticed during the measurements of test material 1. The spectrometers were calibrated after first ten repetitions when the threshold value was also increased from 8 to 11. It can be seen from the results that small change in level of Pulse Ratio Values happened with AISI 304 samples. In other words, a possible calibration error may have occurred.

The actual recovery was compared with the theoretical recovery. The actual recovery was calculated by manually collecting the samples which had ended up in both output fractions and the theoretical recovery by counting the number of the pulse values which were either over or below the set threshold value.

The recovery, as well as the quality of the end product can be estimated from the theoretical Grade-Recovery curve (Figure 36 and Table 9), where threshold value has been used as a variable. Here the quality refers to the Molybdenum content of the final product. It is seen from the graph that the best recovery is achieved when the threshold value is set between 5 and 8. In that case the quality of the end product also remains homogeneous. The actual recovery rate remained at a lower level than the theoretical, but the quality of the end product was at the same level with the theoretical. The effect of the threshold value on the theoretical recovery was also observed with the help of Figure 37 from which it is seen that in theory the recovery decreases when threshold value is increased. It is seen also from this graph that suitable threshold value will be around 7-8, if the purpose is to maximise the final recovery.

It can be concluded that with test material 1, it is not possible to make a sharp cut due to large amount of deviation in the results. One option to reduce this error is the pre-treatment of the material e.g. with screening, in order to narrow the size distribution of the feed. The right threshold value is one of the key parameters in sorting, since the operator makes the final decision on which value is used. Thus the choice has big significance to the final results, at least in theory.

The obtained results can be roughly compared with an older XRF sorting device, which is in use at Kuusakoski Works Heinola. There this same material i.e. stainless steel is sorted for acid proof (EN 1.4432; AISI 316) and common stainless steel (EN 1.4301; AISI 304) fractions. An example of AISI 316 spectrum can be found in Chapter 3.4, Figure 11. This sorting device has only one X-Ray tube and detector and the expected capacity is around 1 ton an hour. The average results for recovery and grade in the years 2013 and 2014 are presented in Table 13 below. Thus it can be concluded that the Poly-XRF device has potential as a challenger of the old sorting device. In this work, capacity was not studied.

Table 13. Comparison of Poly-XRF and Kuusakoski Works Heinola XRF

	Average Recovery [%]	Average Mo [%]
Heinola 2013	75	2.2
Heinola 2014	69	2.0
Poly-XRF Sorting Equipment	79	2.0

Sorting Result of Test Material 2

Brass is an alloy of copper and zinc and both concentrations may vary a lot. Brass contains relatively large amount of zinc and this results as quite high $K\alpha$ emission line in the spectrum. A typical spectrum of Brass was presented in Chapter 3.1, Figure 5. The brass samples used in the experiments contain zinc from around 10 % up to 50 %. If the concentration was lower, the emission lines might get behind the lines of copper and therefore stay unidentified. The success of the calibration as well as setting of accurate limits to the searched fluorescence emission energies in Channels 1 and 2 becomes very important when copper and zinc are separated with this technique. If calibration error occurs it results in failed identification of elements and mixed product fractions.

The experiments for separation between copper and brass gave very promising results. However, it must be kept in mind that in reality the input would also contain other metals e.g. iron, lead and aluminium, which might disturb the analysis. For example, the emission lines of iron usually appear very strong and might disturb the separation. In that case recirculation of the material with more cleaning stages would be needed.

As a curiosity, interesting observations were made with Sample no. 4, which was rather small and flat shaped particle. It worked as a good indicator for testing the vision ability of the camera, which turned out to be the limiting factor of the whole system (discussed earlier). The sample was unnoticed in app. 30 % of times. When the

sample was measured, the Pulse Ratio Values were good. However in some cases, it still ended in the drop fraction due to failed ejection.

According to literature [5, 11] usually colour separation is used for separating brass and copper from each other into red and yellow metals. However, a lot of measuring errors occur and only a small part of the fraction correspond the colour requirements due to surface contamination, such as paint and dust. Often prewashing is needed. As XRF is an element-specific detection method, it does not give significance to the colour of the metal. Also the surface contaminations don't have that major effect on the results as with colour separation. Therefore, XRF sorting technique gives a promising option for colour sorting.

The comparison of actual and theoretical recovery has been given in Figure 38. It can be seen that samples number 2 and 4 differ the most from the theoretical values. This is due to the shape and size of the samples as already discussed earlier. The grade and recovery were calculated for both product fractions since both are interesting (Tables 11 and 12). In this context, the zinc containing samples were ejected. Only one element at a time can be identified. Thus it could also be thought as a reverse cleaning of the copper fraction.

The final results of grade and recovery for both fractions are excellent and the contents are fairly near the theoretical values. Thus it can be concluded that the Poly-XRF sorting device has potential for sorting this type of material.

Sorting Result of Test Material 3

Reason, that test material 3 was included in these experiments was its potential economic significance if the particles of this kind were detected and separated from heterogeneous input. However, examination of this material had to be stopped due to the malfunctioning of the camera. The sorting logic of Poly-XRF is that if *camera detects the particle, then the measurement result from the spectrometers is recorded*. The camera is unable to detect plate-like samples and in this case the shape of all the samples was flat. If these particles are settled in a small angle, then there is a greater

probability that they are detected. The differences in the angle are illustrated in the Figure 45, in Chapter 9.4.

However, the effect of the measurement time for the identification of gold was observed by measuring the spectrum of the sample in two different measurement times 5 s and 0.3 s (Figures 43 and 44). With the measurement time of five seconds both emission lines of gold, L_{α} and L_{β} , stand out quite well. With a shorter measurement time, the accuracy of the identification decreases significantly. The lines could mix with the baseline. In order to obtain a sufficient accuracy, the measuring time should be longer than 0.3 seconds. In this case, the overall capacity would be very low.

11 Conclusions

The main objectives of the thesis were to perform technical testing of XRF sorting equipment and to test the applicability of the sorter on selected process samples. The number of the test materials had to be limited to three, since the commissioning of the equipment and software testing took quite a lot of time. The aim was to separate two different steel grades from each other based on the differences in molybdenum content (test material 1), brass samples from more pure copper based on the zinc content (test material 2) and to analyse the gold coated copper-nickel circuit board having very thin coating (test material 3).

The consistency between the detectors was set as an indicator of the device functionality and it was examined through the results of test materials 1 and 2. The pulse value results from each detector were compared with each other and it was found that very little differences occur between the detectors and the distributions followed the same trend fairly well. The most limiting factors of the whole system are the functionality of the camera and the success of the ejection. The performance of the camera decreases from the central part of the conveyor towards the edges. The ejection of a particle may fail for several reasons, e.g. small or thin shape of the particle or the timing of the air jet is not correct.

The results of test materials 1 and 2 showed that the final separation degree differs from the theoretical separation degree. Therefore, different material based characteristics were compared with the actual recovery. The effects of these variables on recovery were studied mainly with test material 1. The variables were the molybdenum content of a sample, mass, sample width, and the sample width – mass ratio. It was found that mainly the sample width and sample width – mass ratio, affect the final recovery.

The sorting results of test materials 1 and 2 showed positive signs. The sorting of steel grades was a bit more difficult, since lot of variation occurred in the measured pulse

values. It was not easy to set the threshold value, because the pulse distributions were overlapping. The separation of brass from copper based on zinc content gave very good results. The difference between the actual sorting result and the theoretical was mainly due to the varying sample shape. With the gold coated circuit board sample (test material 3), the objective was to examine the capability of Poly-XRF to identify the energy that gold emits. The measurement time in on-line measurement is rather short and the coating is very thin. The examination was stopped due to the limitations of the camera.

The applicability of Poly-XRF sorting equipment on small or flat shaped particles was not found suitable on its present configuration. For example, this leaves out the printed circuit boards (BCPs) from WEEE, which usually goes through a crushing stage before sensor-based sorting process. The ideal feed material for Poly-XRF is multiple shaped and relatively large (> 4 cm) particles, e.g. metal scrap. Materials of this kind are easier to identify and eject. If Poly-XRF was moved to a suitable place in the production site e.g. at the Kuusakoski Heinola Works, it would at least require a better functioning feeding unit.

The further development of the device and testing the sorting of other process samples is recommended, also as pilot size tests. For instance, the test material 2, separation between copper and brass gave very promising results. In reality, this material fraction contains various amounts of other components such as zinc, aluminium, lead, electrical cables, as well as some non-metallic components. It would be interesting to examine if the other metals interfere the separation event and which of the product fractions they will end up. Additional cleaning stages could be needed. The purpose of using sorting technologies for recycled material is not producing too high quality material fractions if it is at the expense of economic aspects.

12 Suggestions for Further Research

Already at the beginning of this work, it has been taken into consideration that Poly-XRF is a prototype sorting equipment with unpredictable challenges; both in hardware set up and the functionality of the software. After all, the Poly-XRF was put into operation and the main errors of the software were corrected. Functionality still needs to be further improved in the future. Few suggestions are given in this chapter.

Two matters which restrict efficient and reliable separation the most were: the identification ability of the camera and optimization of the feeding system. In several cases, the camera proved to be the most limiting factor of the whole separation event. In that case re-adjustment of the camera and software optimization might help with the problem. The extreme case is to replace the camera to a totally new one with proven functionalities. When recycled material is in question, it may take any form one can imagine. Therefore, it is very important that all shaped particles are detected, also the thin plate-shaped ones. The correction need also depends on which application the equipment will be placed in the future.

The response time, i.e. how quickly a new particle can be measured on the same detector, also proved to be a very important issue. Therefore, it is essential to optimize the feeding system. With the current vibratory feeder and queuing system, the input material cannot be fed evenly enough. There needs to be a monolayer of material and sufficient distances between particles. In addition, different type or longer liners might help to direct the particles straight under a certain detector. The better use of liners might also stabilize the motion of objects that move easily on the conveyor due to their shape, e.g. round pieces.

Another option to prevent the small or round shaped particles from ending up in the drop fraction could be adding a second measurement point for the location, for example just before the air valve module. At the moment, the distance between the

camera and air valve block is 2.2 m and when the conveyor is on motion the particles may move from their original place resulting in failed ejection. In addition, if the focus was on ejecting small sized particles, it would be good to have a changeable air valve block with other type of valves.

The purpose of the current feeding system is to divide the input material into six fractions and transport the particles directly under the detectors. It would be good to check if the detectors cover the whole width of the conveyor, or if there is a blind area between the detector pares. The distance between the detectors and the conveyor affects the coverage area. If there are blind areas between the detector pares, then the improvement of the feeder system is essential. The test could be done using the thesis test materials, since there is already statistical information on the pulse values. These results could also show if the intensity of the pulses lower when distance between a particle and a detector increases. Also information on the coverage area is provided. There is a possibility to adjust the detector collimators that are at the moment set fixed.

The Poly-XRF device was commissioned and tested with a few recipes and test materials in the master's thesis. Further research suggestion includes finalizing the rest of the recipes that were originally agreed with VTT, but also finding proper process samples where these recipes can be utilized and optimized. When suitable materials are found, the applicability of Poly-XRF device to enrich these materials and possibly increase their economic value could be tested; also with larger material volumes.

References

1. Worrel, E. Reuter, M. *Handbook of Recycling, State-of-the-art for Practitioners, Analysts, and Scientists*. Elsevier, 2014. pp. 1 – 25. ISBN: 978-0-12-396459-5
2. Maul, A., Raulf, K., Köpcke, M. & Gaastra, M. *Sensor-based sorting in the recycling industries*. In the proceedings: Pretz, T., Quicker, P. & Wotruba, H. *Applications of Sensor-based Sorting in the Raw Material Industry*. Aachen, Germany: Shaker Verlag GmbH, 2011. 249 p. ISBN 978-3-8440-0585-1.
3. Raulf, K. & Gaastra, M. *Introduction*. In the proceedings: Nienhaus, K., Pretz, T. & Wotruba, H. *Sensor Technologies: Impulses for the Raw Materials Industry*. Aachen, Germany: Shaker Verlag GmbH, 2014. 477 p. ISBN 978-3-8440-2563-7.
4. Berwanger, M & Gaastra, M. *Fields of application for sensor technologies in the raw materials industry*. In the proceedings: Nienhaus, K., Pretz, T. & Wotruba, H. *Sensor Technologies: Impulses for the Raw Materials Industry*. Aachen, Germany: Shaker Verlag GmbH, 2014. 477 p. ISBN 978-3-8440-2563-7.
5. Weiss, M. *A new approach - An equipment supplier makes the case for using X-Ray fluorescence to sort shredded metals*. Recycling Today Magazine. [Online Magazine]. Vol 53 / No 1. 2015. Cited 03.02.2015. Available at: <http://www.recyclingtoday.com/rt0115-xray-fluorescence-sorting-metals.aspx>.
6. Neubert, K., Knapp, H. & Fietz, N. *Principles of X-ray fluorescence analysis*. In the proceedings: Nienhaus, K., Pretz, T. & Wotruba, H. *Sensor Technologies: Impulses for the Raw Materials Industry*. Aachen, Germany: Shaker Verlag GmbH, 2014. 477 p. ISBN 978-3-8440-2563-7.
7. Brouwer, P. *Theory of XRF, getting acquainted with the principles*. 2nd ed. The Netherlands. PANalytical B.V., 2006. 62 p. ISBN 90-9016758-7. Cited 28.10.2014. Available at: <http://www.panalytical.com/Technology-background/Theory-of-XRF-getting-acquainted-with-the-principles-booklet.htm>

8. Pretz, T., Quicker, P. & Wotruba, H. *Applications of Sensor-based Sorting in the Raw Material Industry*. Aachen, Germany: Shaker Verlag GmbH, 2011. 249 p. ISBN 978-3-8440-0585-1.
9. Reuter, M. A., Hudson, C., van Schaik, A., Heiskanen, K., Meskers, C. & Hagelüken, C. *UNEP Metal Recycling: Opportunities, Limits, Infrastructure, A Report of the Working Group on the Global Metal Flows to the International Resource Panel*. United Nations Environment Programme. 2013. Cited 09.11.2014. Available at: [http://www.unep.org/resourcepanel/Portals/24102/PDFs/Metal Recycling Full Report.pdf](http://www.unep.org/resourcepanel/Portals/24102/PDFs/Metal_Recycling_Full_Report.pdf).
10. Steinert GmbH. *Innovative Solutions, Sensor Sorting Systems, Magnetic Separators*. Germany, 2015. Cited 15.02.2015. Available at: [http://www.steinertglobal.com/fileadmin/user_upload/australia/brochures/STEINERT Product Range.pdf](http://www.steinertglobal.com/fileadmin/user_upload/australia/brochures/STEINERT_Product_Range.pdf).
11. Tomra Sorting Solutions Recycling, *Recycling Technology*. Cited 10.2.2015. Available at: www.tomra.com/en/solutions-and-products/sorting-solutions/recycling/recycling-technology.
12. TOMRA Sorting Solutions Recycling. *Non-Ferrous Metals*. Segment Guide. 2014.
13. ZenRobotics Ltd. *Advantages of ZenRobotics Recycler*. Cited 15.02.2015. Available at: <http://www.zenrobotics.com/product/advantages/>.
14. Gaustad, G., Olivetti, E. & Kirchain, R. *Review: Improving aluminum recycling: A survey of sorting and impurity removal technologies*. Journal of Resources, Conservation and Recycling. [Online Magazine]. Vol 58. pp. 79– 87. 2012. Cited 09.11.2014. DOI:10.1016/j.resconrec.2011.10.010.
15. TOMRA Sorting Solutions Recycling. *Meatball Sorting from Ferrous Line*. Application Report. 2014.

16. Pigorsch, E., Gärtner, G., Hollstein, F. & Meinschmidt, P. *Sorting of Waste Wood by NIR Imaging Techniques*. Proceedings of the Sensor-based Sorting 2014 International Conference and Exhibition, Aachen, Germany. 11-13.3.2014.
17. Fraktman, L. *Bromatut palonestoaineet ympäristössä*. Helsingin kaupungin ympäristökeskuksen julkaisuja. [Web document]. Vol. 2/2002. Cited 09.11.2014. Available at: <http://www.hel.fi/static/ymk/julkaisut/julkaisu-02-02.pdf>.
18. Wills, B. A. & Napier-Munn, T. *Mineral Processing Technology, An Introduction to the Practical Aspects of Ore Treatment and Mineral Recovery*, Seventh Edition. Oxford, Boston, USA: Butterworth-Heinemann, 2006. 457 p. ISBN 9780080479477 (E-Book). ISBN 9780750644501 (Print Book).
19. Redwave, a division of BT-Wolfgang Binder GmbH, *Sensor based sorting machines*. Cited 15.03.2015. Available at: <http://www.redwave.at/en/>.
20. Tomra Sorting Solutions Recycling, *Titech X-Tract with Duoline and Suppixx Technology*. 2014.
21. Wotruba, H. & Harbeck, H. *Sensor-Based Sorting*. Ullmann's Encyclopedia of Industrial Chemistry. Vol 32. pp. 395 – 404. 2012. Wiley-VCH Verlag GmbH & Co. KGaA, Weinheim. DOI: 10.1002/14356007.b02_18.pub2. ISBN: 9783527306732 (Online).
22. Kassouf, A., Maalouly, J., Rutledge, D. N., Chebib, H. & Ducruet, V. *Rapid discrimination of plastic packaging materials using MIR spectroscopy coupled with independent components analysis (ICA)*. Journal of Waste Management. [Online magazine]. Vol 34, pp. 2131-2138. 2014. Cited 15.03.2015. DOI: 10.1016/j.wasman.2014.06.015.
23. Neumann, K. & Hahn, M. *Principles of Laser Detection and Ranging*. In the proceedings: Nienhaus, K., Pretz, T. & Wotruba, H. *Sensor Technologies: Impulses for the Raw Materials Industry*. Aachen, Germany: Shaker Verlag GmbH, 2014. 477 p. ISBN 978-3-8440-2563-7.

24. Oxford Instruments. *Laser Induced Breakdown Spectroscopy – An Introduction to LIBS*. 2015. Cited 10.2.2015. Available at: <http://www.oxford-instruments.com/businesses/industrial-products/industrial-analysis/about-libS>.
25. Hein, K., Stein, D., Stadtschnitzer, M., Demming, M. & Kuls, J. *Recycling of Plastics with THz technology*. Proceedings of the Sensor-based Sorting 2014 International Conference and Exhibition, Aachen, Germany. 11-13.3.2014.
26. Amptek Inc. *X-RAY FLUORESCENCE (XRF)*. Cited 11.08.2014. Available at: <http://www.amptek.com/pdf/xrf.pdf>
27. Hou, X., He, Y. & Jones, B.T., *Recent Advances in Portable X-Ray Fluorescence Spectrometry*, Applied Spectroscopy Reviews, Vol. 39:1, 1-25, 2004. DOI: 10.1081/ASR-120028867.
28. Suoninen E. & Tuominen, P. *Röntgen- ja fotoelektronispektrometria I, Instrumenttialalytiikka 4*. Teknillisten tieteiden akatemia. Jyväskylä, Finland: K. J. Gummerus Oy, 1982. pp. 15 – 30. ISBN 951-20-1841-1.
29. Jaarinen, S. & Niiranen, J. *Laboratorion analyysitekniikka, Laatu, spektrometria, kromatografia*. 3. Edition. Helsinki, Finland: AEL-ammattitieto, Oy Edita Ab. 197 p. ISBN 951-37-1614-7.
30. Amptek Inc. *XRF Example: Brass*. Cited 28.10.2014. Available at: <http://www.amptek.com/pdf/brass.pdf>.
31. Kuusi, J., Pessa, M. & Visapää, A. *Röntgen- ja fotoelektronispektrometria II, Instrumenttialalytiikka 5*. Teknillisten tieteiden akatemia. Jyväskylä, Finland: K. J. Gummerus Oy, 1982. pp. 248 - 271. ISBN 951-20-1841-1.
32. Provencher, M.-E., Bouchard, M. & Anzelmo, J. A. *X-Ray Fluorescence Spectroscopy, Part I: The Educational Essentials*. 2013. Spectroscopyonline. [Online Magazine]. Vol 28, Issue 7. 2013. Cited 25.2.2015. Available at:

<http://www.spectroscopyonline.com/x-ray-fluorescence-spectroscopy-part-i-educational-essentials?id=&sk=&date=&pageID=2>.

33. Redus, R., *XRF Spectra and Spectra Analysis Software*. Amptek Application Note XRF-1 Rev B1. 2008. Cited 7.8.2014. Available at: http://www.amptek.com/pdf/xrf_2.pdf.

34. Oxford Instruments. *Products, X-Ray tubes and integrated sources*. 2015. Cited 1.2.2015. Available at: <http://www.oxford-instruments.com/products/x-ray-tubes-and-integrated-sources>.

35. Oxford Instruments. *Typical X-Ray Spectra by Anode Material*. X-Ray Technology Applications Notes. 3904006 Revision A. 2015. Cited 03.03.2015. Available at: <http://www.oxford-instruments.com/OxfordInstruments/media/x-ray-technology/application-notes/Typical-X-ray-Spectra-by-Anode-Material.pdf>.

36. Van Grieken, R. E., & Markowicz, A. A. *Handbook of X-Ray Spectroscopy, Methods and Techniques*. Vol 14. Practical Spectroscopy Series. 1992. 704 p. ISBN 0-8247-8483-9.

37. Amptek Inc. *X-Ray Detector Selection Guide*. Cited 25.2.2015. Available at: <http://www.amptek.com/x-ray-detector-selection-guide/>.

38. Oxford Instruments. *XRF – X-Ray Fluorescence analysis explained*. Cited 20.02.2015. Available at: <http://www.oxford-instruments.com/businesses/industrial-products/industrial-analysis/xrf>.

39. *XRF Metallien kierrätysessä*. Kuusakoski Oy Heinola. Oxford Instruments, Industrial Analysis. 2007. Confidential customer report between Kuusakoski Oy and Oxford Instruments. Not public source.

40. Amptek Inc. *XR-100SDD Silicon Drift Detector (SDD)*. Cited 06.03.2015. Available at: <http://www.amptek.com/products/xr-100sdd-silicon-drift-detector/>.

41. Online Article, *X-Ray Sorting System from Titech Boosts Copper Recovery Rates*. Waste Management World. 2010. Cited 15.01.2015. Available at: <http://www.waste-management-world.com/articles/2010/12/x-ray-sorting-system-from-titech-boosts-copper-recovery-rates.html>
42. Oxford Instruments. *Scrap Metal Analysis and Sorting*. 2015. Cited 15.1.2015. Available at: <http://www.oxford-instruments.com/industries-and-applications/metals/scrap-metal-sorting>
43. Hinterseer, R., Sales Manager at Steinert Elektromagnetbau GmbH, Widdersdorfer Straße 329–331, D-50933 Köln, Germany. Interviewed at the 14th International Electronics Recycling Congress IERC 2015 on 21.01.2015.
44. Köpcke, M., Wacholik, M. & Knapp, H. *Principles of X-ray transmission*. In the proceedings: Nienhaus, K., Pretz, T. & Wotruba, H. *Sensor Technologies: Impulses for the Raw Materials Industry*. Aachen, Germany: Shaker Verlag GmbH, 2014. 477 p. ISBN 978-3-8440-2563-7.
45. Close, W & van de Winkel, F. Non-Ferrous Metal Sorting using X-Ray Transmission Based Sorting Technology. In the proceedings: Pretz, T., Quicker, P. & Wotruba, H. *Applications of Sensor-based Sorting in the Raw Material Industry*. Aachen, Germany: Shaker Verlag GmbH, 2011. 249 p. ISBN 978-3-8440-0585-1.
46. Tomra Sorting Solutions Mining. *Diamonds*. Application Report, 2014. Cited 20.2.2015. Available at: https://www.tomra.com/~media/Documents/Mining%20Brochures/TSMI_11_Segment%20Guide%20-%20Diamonds_english_WEB.ashx
47. Mesina, M.B., de Jong, T.P.R. & Dalmijn, W.L., *Improvements in Separation of Non-Ferrous Scrap Metals Using an Electromagnetic Sensor*, 2003. Physical Separation in Science and Engineering, Vol 12, No. 2. pp. 87-101.

48. Habich, U. *Selective Sorting of Metals*, 2011, Steinert Elektromagnetbau GmbH, in the proceedings Pretz, T., Quicker, P. & Wotruba, H. Applications of Sensor-based Sorting in the Raw Material Industry. Aachen, Germany: Shaker Verlag GmbH, 2011. 249 p. ISBN 978-3-8440-0585-1.
49. Berwanger, M. & Maul, A. *Principles of VIS*. In the proceedings: Nienhaus, K., Pretz, T. & Wotruba, H. *Sensor Technologies: Impulses for the Raw Materials Industry*. Aachen, Germany: Shaker Verlag GmbH, 2014. 477 p. ISBN 978-3-8440-2563-7.
50. Tomra Sorting Solutions Recycling, *Titech Combisense with Fluidcool® Led Technology*. 2014. Cited 10.2.2015. Available at: <http://www.titech.com/assets/x/50530>
51. PixelLink®, *Industrial Machine Vision Cameras*, 2015. Cited 18.3.2015. Available at: <http://www.pixelink.com/products/industrial-machine-vision.aspx>.
52. Schropp, C., Raulf, K. & Robben, M. *Principles of near infrared*. In the proceedings: Nienhaus, K., Pretz, T. & Wotruba, H. *Sensor Technologies: Impulses for the Raw Materials Industry*. Aachen, Germany: Shaker Verlag GmbH, 2014. 477 p. ISBN 978-3-8440-2563-7.
53. Li-Chan, E., Chalmers, J. M. & Griffiths, P. R. *Applications of Vibrational Spectroscopy in Food Science*, Vol 1. 2011. John Wiley & Sons. ISBN 0470742992, 9780470742990.
54. Tomra Sorting Solutions Recycling, *Titech Autosort with Flying Beam Technology*. 2014.
55. Lotfi, A. *Plastic Recycling*. [Online document] 2009. Cited 17.3.2015. Available at: <http://www.lotfi.net/recycle/plastic.html>.

56. Lindweiler, *Treatment of remaining materials from e-scrap recycling with sensor technology*, STEINERT Elektromagnetbau GmbH Germany, 2014. Proceedings of the Sensor-based Sorting 2014 International Conference and Exhibition, Aachen, Germany. 11-13.3.2014.
57. Steinert Global, *UniSort PR with Hyper Spectral Imaging Technology*. Cited 01.03.2015. Available at: http://www.steinertglobal.com/fileadmin/user_upload/global/brochures/products_en/STE_UNI_PR_EN.pdf
58. Schenker, T., Negara, C. Vieth K.-U. & Gelo, S. *Quality Improvements of Wine due to Hyperspectral Analysis*. 2014. Proceedings of the Sensor-based Sorting 2014 International Conference and Exhibition, Aachen, Germany. 11-13.3.2014.
59. Micro-Epsilon. *Laser sensors for displacement and position*. Cited 19.3.2015. Available at: <http://www.micro-epsilon.com/displacement-position-sensors/laser-sensor/index.html>
60. Gaastra, M. & Küch, C., *Principles of laser-induced breakdown spectroscopy*. In the proceedings: Nienhaus, K., Pretz, T. & Wotruba, H. *Sensor Technologies: Impulses for the Raw Materials Industry*. Aachen, Germany: Shaker Verlag GmbH, 2014. 477 p. ISBN 978-3-8440-2563-7.
61. Feierabend, A., *LIBS-technology in use. Inline analysis of materials in industrial processes*. Secopta GmbH Laser Based Sensor Systems. 2014. Proceedings of the Sensor-based Sorting 2014 International Conference and Exhibition, Aachen, Germany. 11-13.3.2014.
62. Secopta GmbH. *Laser Based Sensor Systems*. Photonics Cluster. Cited 19.3.2015. Available at: <http://optik-bb.de/en/content/secopta-gmbh>.

63. Maul, A. & Nagel, M. *Principles of Terahertz technology*. In the proceedings: Nienhaus, K., Pretz, T. & Wotruba, H. *Sensor Technologies: Impulses for the Raw Materials Industry*. Aachen, Germany: Shaker Verlag GmbH, 2014. 477 p. ISBN 978-3-8440-2563-7.
64. Nüßler, D. *blackValue*. Fraunhofer Institute for High Frequency Physics and Radar Techniques FHR. 2015. Cited 15.3.2015. Available at: www.blackvalue.de.
65. Eriez Manufacturing Co., *Eriez/TORATEC EcoTowerSort*. Cited 15.03.2015. Available at: <http://www.eriez.com/Products/ResourceRecoveryEquipment/ecotowersort/>.
66. IMRO Maschinenbau GmbH. *Imro Products – Conveying and Sorting Equipment*. Cited 06.10.2014. Available at: <http://www.imro-maschinenbau.de/en/products.html>.
67. Pellenc selective technologies, *Products*. Cited 06.10.2014. Available at: <http://www.pellencst.com/products/>.
68. S+S Separation and Sorting Technology GmbH. *Recycling*. Cited 06.01.2015. Available at: <http://www.sesotec.com/en/profiler/recycling/1/100>.
69. BLUBOX Trading AG. *BLUBOX Plug & Recycle, Mixed Lamp and Flat Screen Recycling*. Cited 15.03.2015. Available at: <http://blubox.ch/technologies/blubox>.
70. MSS INC. Optical Sorters a Division of the CP Group. *Material Sorting Equipment*. Cited 15.03.2015. Available at: <http://www.magsep.com/material-sorting-equipment/>.
71. Viitanen, J. Professor. VTT Technical Research Centre of Finland LTD. Tekniikankatu 1, P.O. Box 1300, FI-33101 Tampere, Finland. Interviewed between August 15 and November 5, 2014.
72. Jokela M., Niemeläinen T., Saarinen M, Täppinen R. and Viitanen J. *Automaattinen lajittelu käyttäen XRF-fluoresenssia (PolyXRF); PolyXRF loppuraportti. 2*. Version. VTT Technical Research Centre of Finland. 2014. 67 p. VTT-R-01947-14. Confidential customer report between Kuusakoski Oy and VTT Technical Research Centre of Finland. Not public source.

73. Amptek, *K and L Emission Line Lookup Chart. XR-100CR / XR-100T-CdTe / GAMMA-8000 / X-123, X-Ray and Gamma Ray Detectors*. Cited 06.10.2014. Available at: <http://www.amptek.com/pdf/xraychrt.pdf>.

Appendices

Appendix I	Test Material 1 Data Sheet
Appendix II	Test Material 2 Data Sheet
Appendix III	Calibration of Poly-XRF Sorting Equipment
Appendix IV	Consistency Between Detectors, Test Material 1
Appendix V	Consistency Between Detectors, Test Material 2
Appendix VI	Measurement Data of Test Material 1
Appendix VII	Frequency Distributions for Test Material 1 Samples
Appendix VIII	Measurement Data of Test Material 2
Appendix IX	Frequency Distributions for Test Material 2 Samples
Appendix X	Test Material 3 Data Sheet
Appendix XI	Measurement Data of Test Material 3
Appendix XII	The Peak Data of Test Material 3 Measurements

Appendix I - Test Material 1 Data Sheet

All of the samples were characterized by weighing with a laboratory scale (METTLER TOLEDO, NewClassicMS) and analysing their element composition with a handheld XRF analyser (OXFORD INSTRUMENTS, X-MET 7500). These are shown in Tables 14 – 16.

Table 14. The masses of test material 1 samples

	Sample 1	Sample 2	Sample 3	Sample 4	Sample 5	Sample 6	Sample 7	Sample 8	Sample 9	Sample 10
Mass [g]	173.7	112.1	88.0	206.3	273.1	220.3	81.9	280.5	73.5	59.9

Table 15. Test material 1, element composition analysis, part 1

	SS Type	Fe [%]	Cr [%]	Ni [%]	Mo [%]
Sample 1	316	68	17	9.5	2.0
Sample 2	316	69	17	10	1.9
Sample 3	316	68	17	10	2.1
Sample 4	316	69	17	10	2.5
Sample 5	316	64	17	12	2.4
Sample 6	316	71	16	8.1	2.0
Sample 7	316	68	16	9.6	2.6
Sample 8	304	70	18	9.0	0.26
Sample 9	304	71	18	8.7	0.17
Sample 10	304	71	18	8.6	0.05

Appendix I - Test Material 1 Data Sheet

Table 16. Test material 1, element composition analysis, part 2

	Si [%]	Mn [%]	Zn [%]	Co [%]	Cu [%]	Ti [%]
Sample 1	1.6	1.2	0.36	0.34	0.14	-
Sample 2	1.0	0.91	0.00	0.00	0.23	-
Sample 3	1.4	1.3	0.06	0.28	0.15	-
Sample 4	2.2	1.7	0.10	0.32	0.16	0.10
Sample 5	1.7	1.6	0.18	0.44	0.46	0.33
Sample 6	1.3	1.9	0.23	0.18	0.25	-
Sample 7	1.4	1.4	0.39	0.33	0.24	-
Sample 8	0.57	1.4	0.00	0.15	0.11	-
Sample 9	0.56	1.1	0.00	0.34	0.08	-
Sample 10	1.1	0.96	0.10	0.29	0.13	-

Appendix II – Test Material 2 Data Sheet

All of the samples were characterized by weighing with a laboratory scale (METTLER TOLEDO. NewClassicMS) and analysing their element composition with a handheld XRF analyser (OXFORD INSTRUMENTS. X-MET 7500). These are shown in Tables 17 – 19.

Table 17. The masses of test material 2 samples

	Sample 1	Sample 2	Sample 3	Sample 4	Sample 5	Sample 6	Sample 7	Sample 8
Mass [g]	54.24	64.09	160.6	26.60	34.35	23.74	355.5	87.41

Table 18. Test material 2, element composition analysis, part 1

	Cu [%]	Zn [%]	Al [%]	Si [%]	P [%]
Sample 1	85	10	1.1	0.67	0.03
Sample 2	56	38	2.0	2.3	0.11
Sample 3	61	35	1.6	1.9	0.06
Sample 4	50	50	1.9	2.18	0.15
Sample 5	0.17	99	-	-	-
Sample 6	95	0.47	1.2	3.0	0.11
Sample 7	95	0.61	1.2	2.8	0.05
Sample 8	96	0.50	0.38	1.3	0.04

Appendix II – Test Material 2 Data Sheet

Table 19. Test material 2, element composition analysis, part 2

	Mn [%]	Fe [%]	Ni [%]	Pb [%]	Sn [%]	W [%]
Sample 1	0.01	0.24	0.01	0.03	0.0	-
Sample 2	0.01	0.90	0.21	4.54	1.8	-
Sample 3	0.01	0.65	0.0	0.01	0.03	-
Sample 4	0.02	0.32	0.21	0.25	0.35	-
Sample 5	-	-	0.01	0.0	0.0	0.67
Sample 6	0.01	0.68	0.0	0.0	0.0	-
Sample 7	0.02	0.90	0.03	0.0	0.0	-
Sample 8	0.01	0.57	0.01	0.0	0.0	-

Appendix III – Calibration of Poly-XRF Sorting Equipment

An example of a successful calibration of Poly-XRF is presented below in Figure 46. The figure is taken from the user interface made by VTT, the Technical Research Centre of Finland.

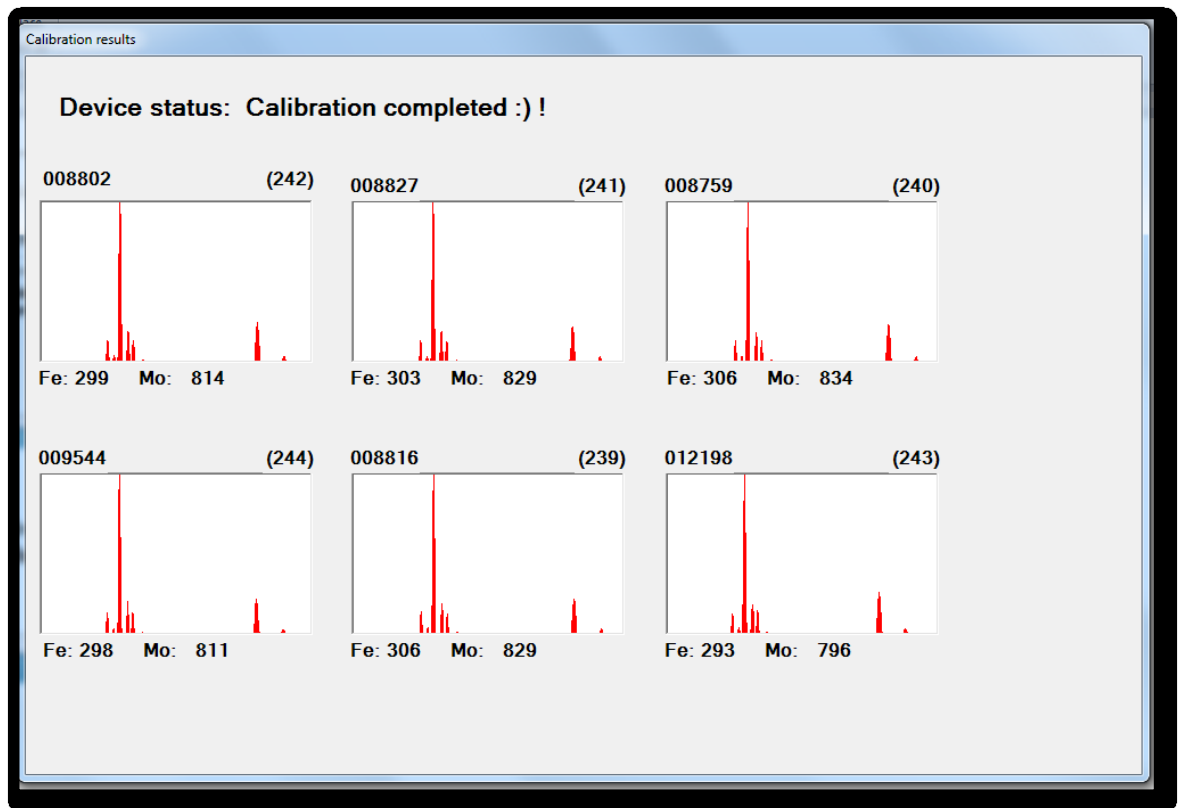


Figure 46. A calibration result of Poly-XRF sorting equipment.

Appendix IV – Consistency Between Detectors, Test Material 1

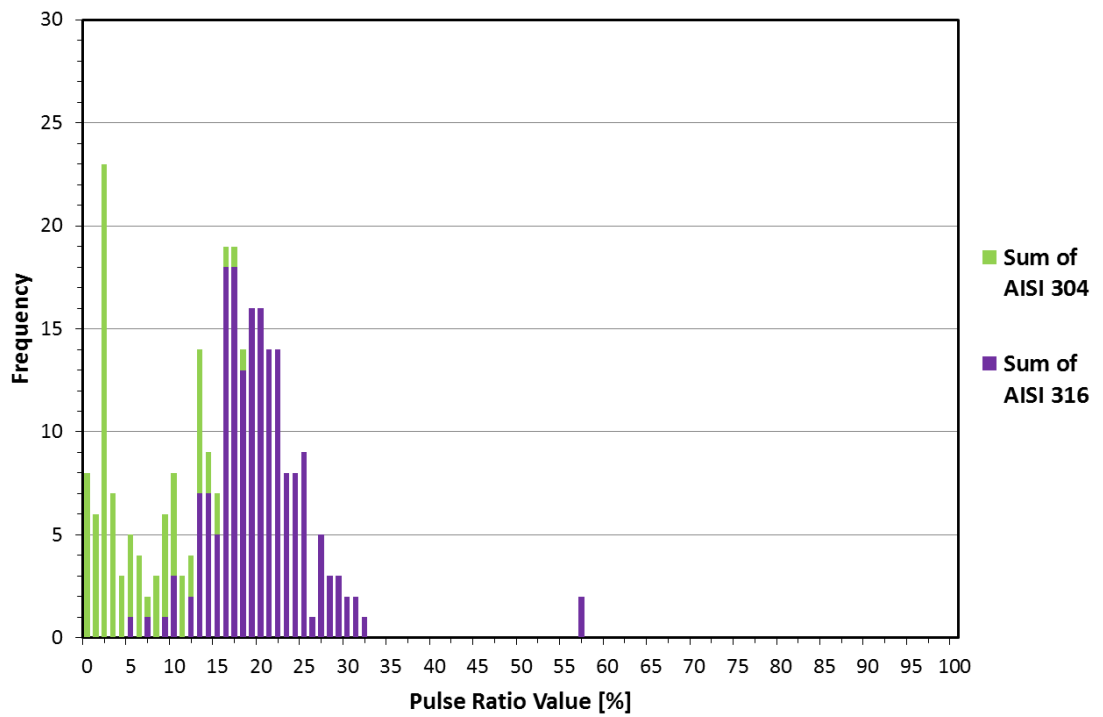


Figure 47. The pulse frequencies of test material 1 on detector 3.

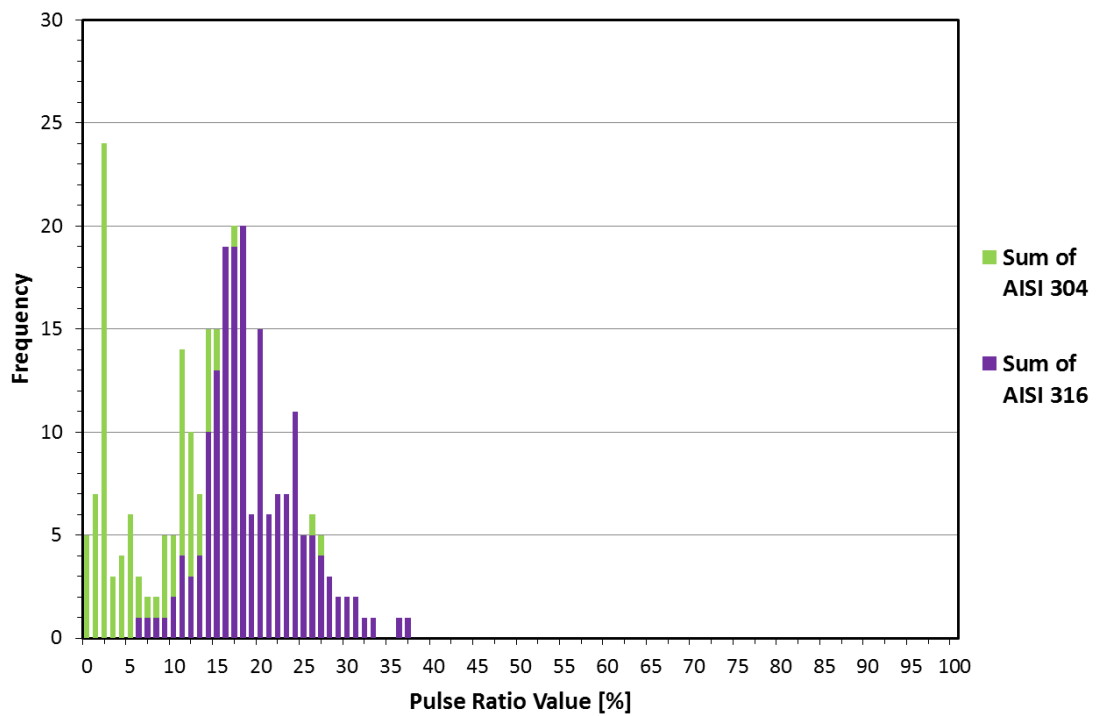


Figure 48. The pulse frequencies of test material 1 on detector 4.

Appendix IV – Consistency Between Detectors, Test Material 1

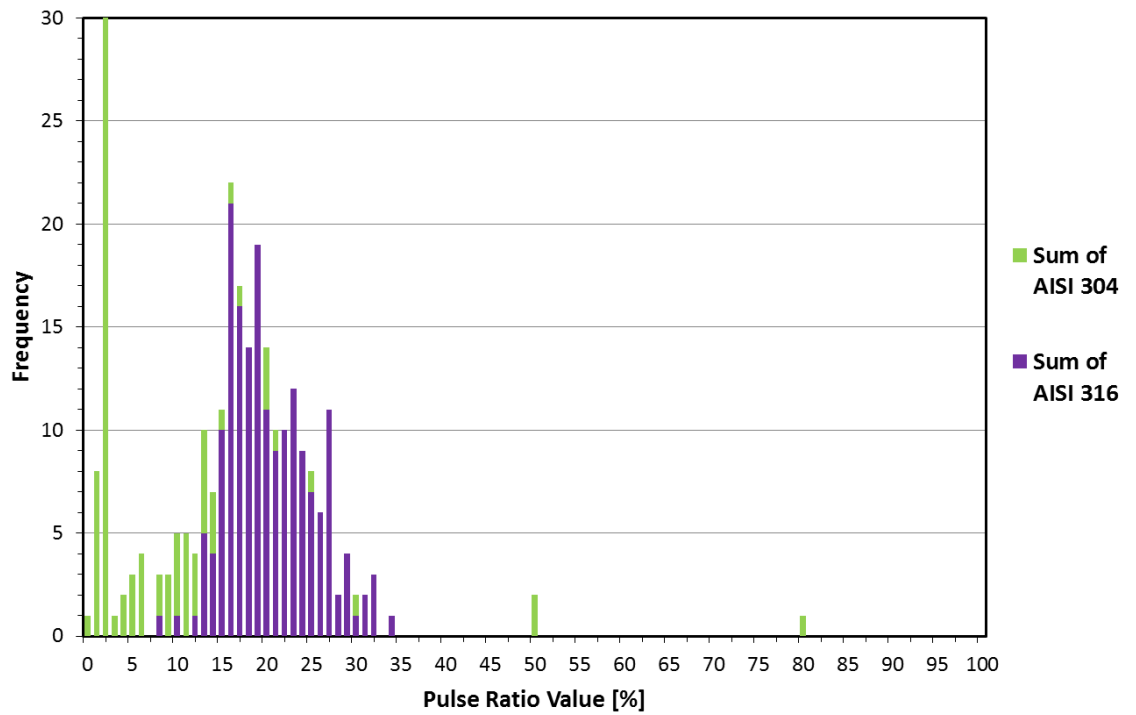


Figure 49. The pulse frequencies of test material 1 on detector 5.

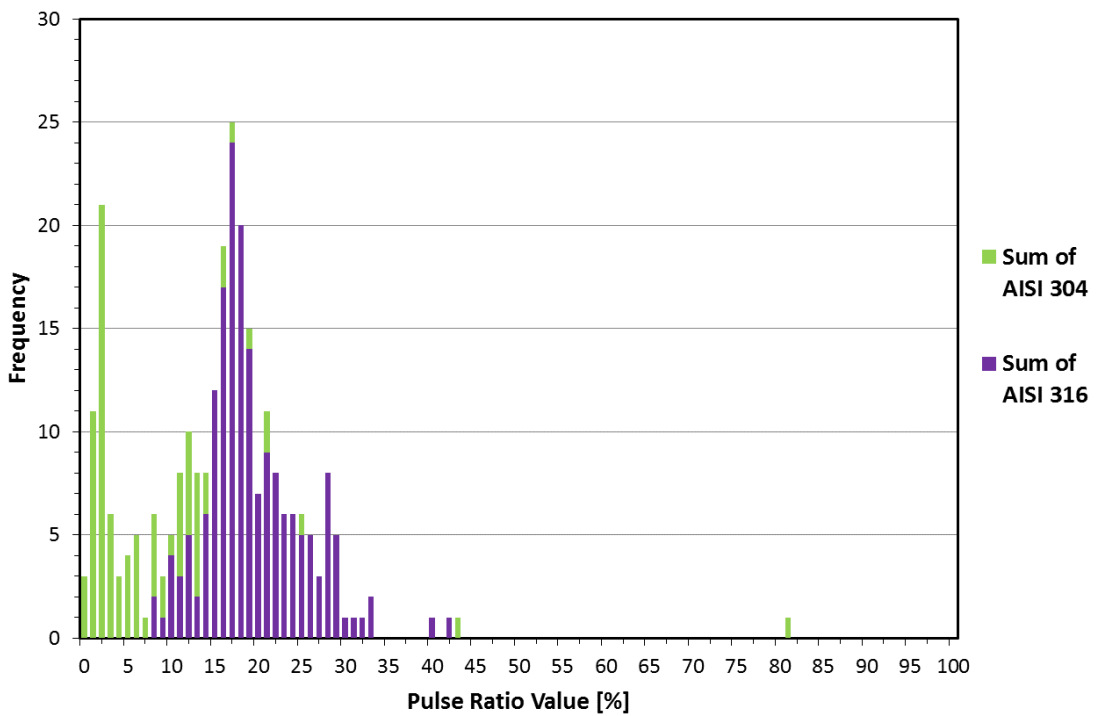


Figure 50. The pulse frequencies of test material 1 on detector 6.

Appendix V - Consistency between Detectors, Test Material 2

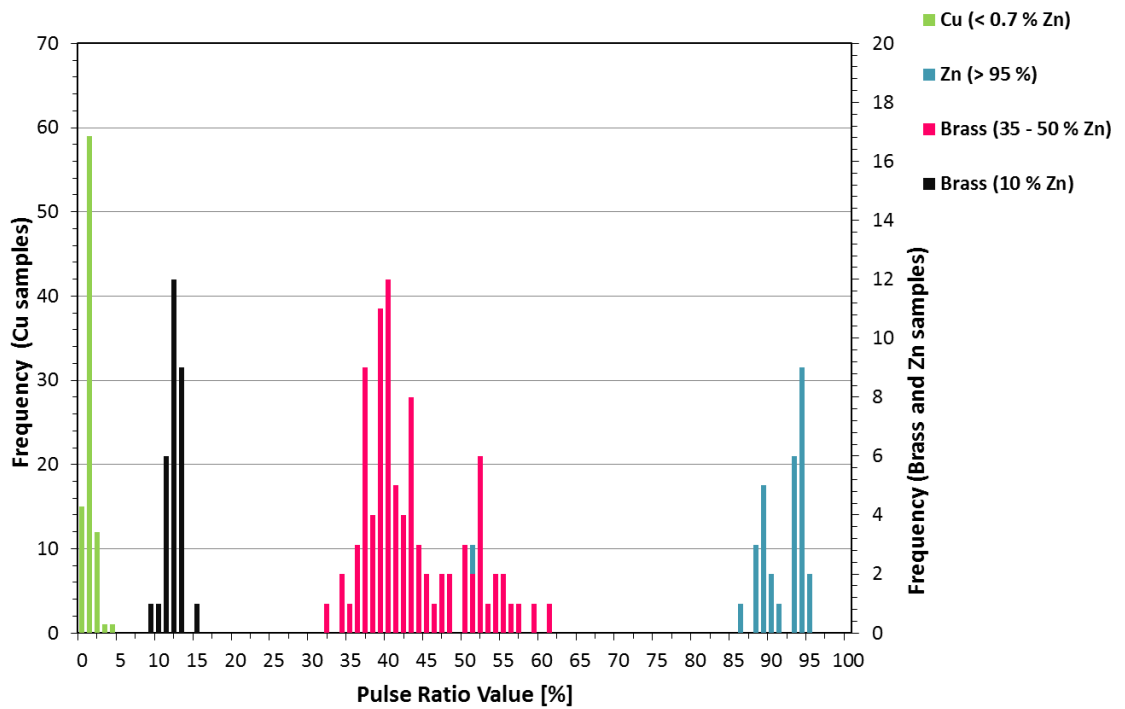


Figure 51. The pulse frequencies of test material 2 on detector 3.

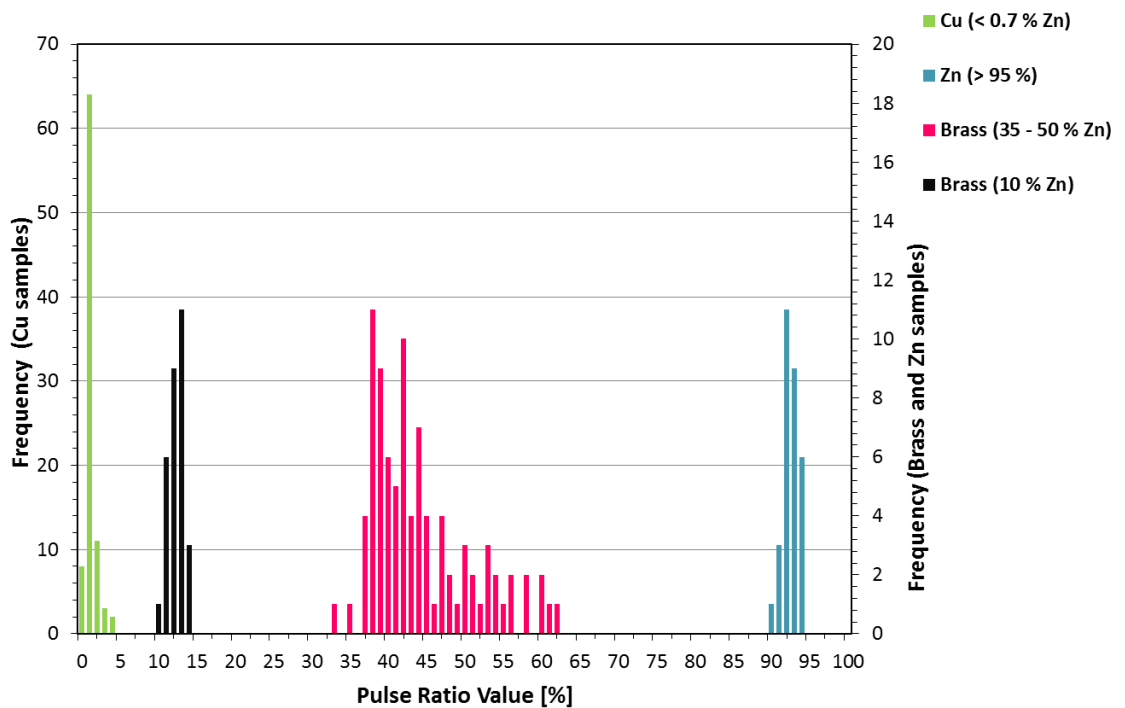


Figure 52. The pulse frequencies of test material 2 on detector 4.

Appendix V - Consistency between Detectors, Test Material 2

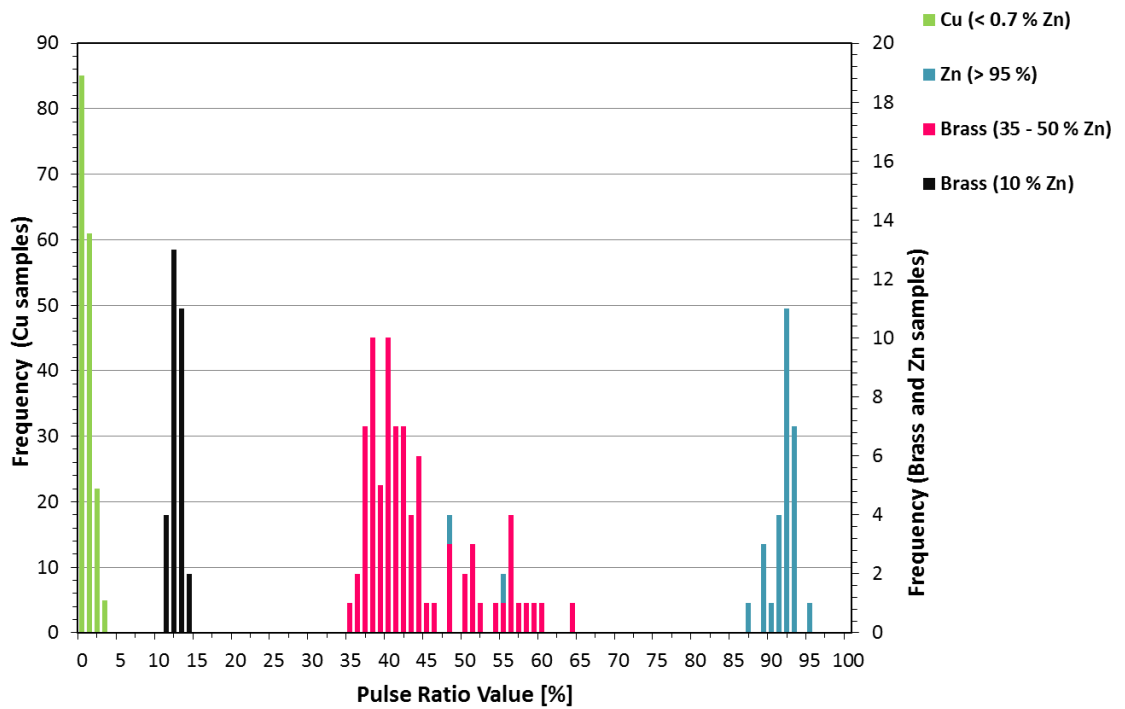


Figure 53. The pulse frequencies of test material 2 on detector 5.

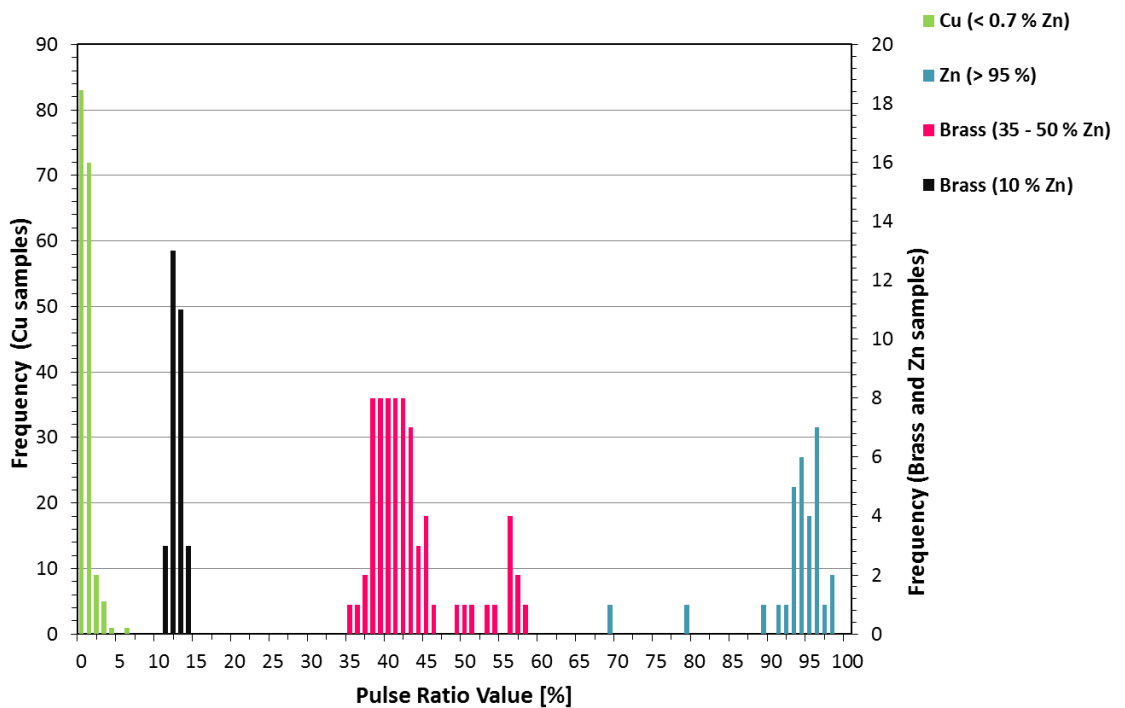


Figure 54. The pulse frequencies of test material 2 on detector 6.

Appendix VI – Measurement Data of Test material 1 on Detector 1

Test no.	1		2		3		4		5		6		7		8		9		10	
Specimen no.	Drop	Eject																		
1	14	15	17	17	17	17	16	16	17	17	16	16	16	14	14	20			16	16
2	15	15	16	16	16	16	16	16	19	15	15	15	17	18	18	12			20	20
3	15	15	14	17	14	17	17	17	17	17	15	19	17	17	22				32	32
4	15	18	17	16	16	16	16	16	16	16	16	16	23	16	16				12	12
5	18	18	796	19	18	19	19	19	18	18	18	18	17	17	18	22			21	21
6	16	14	15	15	18	18	18	18	18	18	13	18	18	17	17	19			19	19
7	17	22	18	20	18	18	20	20	18	20	20	17	17	15	14				22	22
8	12	13	13	10	11	14	10	10	11	14	14	14	14	12	2				1	1
9	15	11	11	14	12	14	14	14	12	12	12	13	11	11	21				5	5
10	9	9	10	9	8	9	9	9	8	10	10	10	9	9	2				0	0

Test no.	11		12		13		14		15		16		17		18		19		20	
Specimen no.	Drop	Eject																		
1	17	17	16	10	10	23	19	21	16	20	9	21	21	17	17	56			50	50
2	17	17	17	17	17	17	17	19	20	20	21	17	17	21	X				20	20
3	15	15	17	17	17	17	9	9	19	19	12	12	25	31	13				12	12
4	27	15	22	19	22	19	19	19	10	10	7	7	17	15	279				31	31
5	22	29	24	29	24	29	29	29	22	22	15	15	26	24	23				29	29
6	20	13	28	11	13	11	11	11	13	13	11	17	17	16	16				19	19
7	21	32	24	19	24	19	19	19	25	25	40	22	22	22	26				33	33
8	1	2	8	2	8	2	2	2	8	8	1	2	2	3	4				2	2
9	6	100	13	10	10	10	10	10	10	10	21	12	12	75	30				15	15
10	2	2	2	1	1	1	1	1	1	1	1	1	1	2	2				0	0

Test no.	21		22		23		24		25		26		27		28		29		30	
Specimen no.	Drop	Eject																		
1	34	17	32	18	18	20	18	17	20	20	23	23	20	13	31				21	21
2	18	17	17	17	22	17	17	17	16	16	17	17	13	16	19				15	15
3	14	14	12	18	12	12	12	12	12	12	15	15	13	16	23				16	16
4	27	14	12	25	12	16	12	12	16	16	16	22	19	16	16				26	26
5	22	23	28	25	23	23	25	25	23	23	28	28	25	24	21				21	21
6	25	14	12	16	12	12	16	16	23	23	18	18	21	20	17				19	19
7	24	31	15	28	13	13	28	28	13	13	19	19	18	33	19				4	4
8	1	1	12	1	1	1	1	1	1	1	1	1	1	2	2				9	9
9	19	5	15	5	15	0	5	5	0	0	13	13	7	9	16				17	17
10	1	1	2	2	2	0	2	2	0	0	1	1	1	2	1				2	2

	No air jet, even though TH value was exceeded
	Pulse Ratio Max Value 100 % was exceeded
	Otherwise false Pulse Ratio Value
X	Camera did not see the sample
Drop	1. Sample Fraction
Eject	2. Sample Fraction

Appendix VI – Measurement Data of Test material 1 on Detector 2

Test no.	1		2		3		4		5		6		7		8		9		10		
	Specimen no.	Drop	Eject																		
1	18		17		16		16	17		16		15		18		21	19		23		
2		18		18		16		18		17		16		17		26		21		15	
3		15		16		15		20		15		16		16		13		20		18	
4		15	17		15		15		17		18		18		20		22		19		
5		19		18		18		18		17		17		20	40		23		20		
6		16		18		15		18		17		17		17		15		16		20	
7		19		19		18	18		20		21		16		36		21		12		
8		12		10		11	12		13		11		12	2	6		6		1		
9		14		14	16		13		13		13		13		21	6	6		6		
10		9		11	9		10		10		10		11	2	1		1		2		

Test no.	11		12		13		14		15		16		17		18		19		20			
	Specimen no.	Drop	Eject																			
1	25		26		11		17		30		30		18		168		49		25			
2		22		27		19		17		13		11		24		27		25		35		
3		20		35		26		19		16		12		22		21		21		32		
4		24		20		17		11		9		25		22		33		29		34		
5		28		29		25		32		29		25		23		28		29		36		
6		23		20		23		22		22		18		248		13		20		16		
7		26		25		4		31		25		17		22	48		42		88			
8		2		1		10		2		2		2		4		3		2		3		
9		14		7		6		60		4		11		11		100		9		27		
10		2		2		3		3		0		3		6		3		3		0		

Test no.	21		22		23		24		25		26		27		28		29		30			
	Specimen no.	Drop	Eject																			
1	19		20		20		11		21		15		17		24		162		30			
2		18		20		23		15		21		23		19		19		17		18		
3		16		19		12		24		21		21		18		14		8		33		
4		21		24		22		5		18		26		14		20		11		15		
5		23		23		24		32		26		20		34		21		22		22		
6		25		16		16		12		29		22		15		16		12		17		
7		20		10		26		26		28		13		49		27		33		32		
8		2		2		2		2		3		2		3		1		1		3		
9		14		13		8		6		12		11		0		18		0		15		
10		2		2		4		7		2		3		2		2		0		2		

	No air jet, even though TH value was exceeded
	Pulse Ratio Max Value 100 % was exceeded
	Otherwise false Pulse Ratio Value
X	Camera did not see the sample
Drop	1. Sample Fraction
Eject	2. Sample Fraction

Appendix VI – Measurement Data of Test material 1 on Detector 3

Test no.	1		2		3		4		5		6		7		8		9		10		
	Specimen no.	Drop	Eject																		
1		17		18	14		17		17		14		23		15		29		12		12
2		17		16	16		16		17		20		19		19		14		20		20
3		18		16	18		16		18		16		22		25		27		21		21
4		17		16	16		17		17		16		13		32		14		23		23
5		17		20	19		18		19		27		22		23		21		25		25
6		17		20	18		18		13		19		15		24		21		16		16
7		21	3932		16		15		18		28		28		8		24		18		18
8		13		10	14		11		12		100		6		2		0		10		10
9		13		13	13		13		12		5		10		100		18		6		6
10		8		8	10		11		11		2		9		2		3		1		1

Test no.	11		12		13		14		15		16		17		18		19		20		
	Specimen no.	Drop	Eject																		
1		10		16	23		22		23		15		15		21		22		25		25
2		20		24	13		22		21		13		21		18		17		20		20
3		21		18	24		15		20		16		21		19		21		28		28
4		19		17	16		24		29		9		23		17		25		7		7
5		26		19	25		20		57		30		20		20		27		28		28
6		17		18	21		31		57		22		13		21		21		24		24
7		46		29	101		33		29		24		4		27		9		30		30
8		2		2	5		0		3		5		2		4		2		2		2
9		17		5	9		15		15		6		8		16		9		100		100
10		2		2	4		1		2		3		2		2		0		2		2

Test no.	21		22		23		24		25		26		27		28		29		30		
	Specimen no.	Drop	Eject																		
1		19		5	14		16		23		13		22		20		17		25		25
2		20		19	22		14		14		22		25		21		16		20		20
3		17		22	18		18		18		17		28		30		20		24		24
4		22		10	24		19		20		12		20		16		16		19		19
5		22		29	31		25		19		21		25		19		27		27		27
6		13		19	10		24		22		17		16		23		19		22		22
7		22		26	17		34		22		30		11		19		23		23		23
8		6		2	2		0		3		14		2		4		1		3		3
9		10		3	0		9		0		0		13		13		9		7		7
10		2		1	2		1		2		1		2		0		2		2		2

	No air jet, even though TH value was exceeded
	Pulse Ratio Max Value 100 % was exceeded
	Otherwise false Pulse Ratio Value
X	Camera did not see the sample
Drop	1. Sample Fraction
Eject	2. Sample Fraction

Appendix VI – Measurement Data of Test material 1 on Detector 4

Test no.	1		2		3		4		5		6		7		8		9		10	
	Specimen no.	Drop	Eject																	
1			18	15		16	15	16	16	16	15	17	17	16	16	16	15	15	10	
2			17	18		18	16	16	16	16	16	17	17	16	19	18	18	15	15	
3			17		17	18	18	18	16	16	20	15	15	18	18	21	16	16	16	
4			17		14	15	14	14	16	16	16	16	16	14	14	30	19	19	19	
5			20		18	19	19	18	20		20	17	17	18	21	15	15	15	15	
6	16				18	16	16	17	16		17	17	17	17	13	14	14	14	14	
7			17		14	22	16	16	17		18	20	20	18	18	29	26	26	26	
8			14		12	13	11	11	12		12	11	11	13	2	4	4	4	4	
9			12		15	14	14	14	11		17	14	14	11	4	0	0	0	0	
10			11		10	11	11	11	11		11	11	11	9	1	2	2	2	2	

Test no.	11		12		13		14		15		16		17		18		19		20	
	Specimen no.	Drop	Eject																	
1			26	25	37	15	15	29	29	32	23	118	20	15	15	15	15	15	15	
2			22	24	15	16	17	17	17	20	22	118	11	24	24	24	24	24	24	
3			23	14		22	17	15	15	21	25	21	25	24	85	85	85	85	85	
4			18	29		12	25	24	24	18	9	11	12	12	12	12	12	12	12	
5			24	28		28	27	27	27	25	21	24	20	22	22	22	22	22	22	
6			18	19		20	18	17	17	16	23	14	24	18	18	18	18	18	18	
7			20	26		15	22	20	20	31	40	17	35	20	20	20	20	20	20	
8	1		4		3	5	5	5	5	1	2	10	2	2	2	2	2	2	2	
9	9		10			26	5	6	6	8	6	27	4	4	4	4	4	4	4	
10	5		2		2	2	2	2	2	0	1	2	1	1	1	1	1	1	1	

Test no.	21		22		23		24		25		26		27		28		29		30	
	Specimen no.	Drop	Eject																	
1			26	23	33	16	16	7	20	14	18	27	31	6	6	6	6	6	6	6
2			22	20		22	17	20	20	22	17	20	17	13	13	13	13	13	13	13
3			24	13	30	19	11	11	11	10	26	18	16	23	23	23	23	23	23	23
4			13	36	11	18	8	8	14	8	17	23	17	14	14	14	14	14	14	14
5			24	25	27	31	24	24	24	20	28	26	26	23	23	23	23	23	23	23
6			14	19	24		16	20	20	20	21	18	12	20	20	20	20	20	20	20
7			23	18	19	11	11	59	16	16	26	10	24	24	24	24	24	24	24	24
8	0		0	0	2	2	2	2	1	1	2	2	1	1	1	1	1	1	1	1
9	9		5	5	7	0	0	12	9	9	12	12	14	15	15	15	15	15	15	15
10	2		2	2	5	2	2	2	3	3	2	3	2	2	2	2	2	2	2	2

	No air jet, even though TH value was exceeded
	Pulse Ratio Max Value 100 % was exceeded
	Otherwise false Pulse Ratio Value
X	Camera did not see the sample
Drop	1. Sample Fraction
Eject	2. Sample Fraction

Appendix VI – Measurement Data of Test material 1 on Detector 5

Test no.	1		2		3		4		5		6		7		8		9		10			
	Specimen no.	Drop	Eject																			
1			17	15	15	16		17	17	16	21		18	14		17	14		17		17	
2			16	16	16		18	18	18	19		19	14		18	19		19		18		18
3			20	17	17		17	17	19	17		17	22		22	20		20		23		23
4			15	16	17		16	16	16	15		15	17		23	16		16		12		12
5			19	18	17		18	18	16	16	24		24	19		19		19		26		26
6			17	18	16		16	16	16	16		16	14		14	16		16		17		17
7			18	17	18		19	19	16	17		17	54		17	15		15		23		23
8			11	13	12		12	12	13	11	2		2	1	2		1					
9			20	12	14		14	14	13	11	4		17	10		17	10					8
10			9	9	10		11	11	11	10	2		1	2		1	2					2

Test no.	11		12		13		14		15		16		17		18		19		20			
	Specimen no.	Drop	Eject																			
1			27	27	22		18	18	20	25		29	24		24	19		19		15		15
2			20	18	13		23	23	24	18		17	19		19	19		19		22		22
3			28	20	26		22	22	18	27		15	17		17	20		20				19
4			21	15	20		25	25	23	23		32	8		22	22		22				28
5			20	27	26		27	27	24	27		29	27		27	22		22				29
6			27	13	21		13	13	20	19		19	24		24	16		16				18
7			27	0	54		22	22	36	37	62		15	27		15	27					27
8			2	2	2		2	2	2	1	2		2	2		2	2					6
9			13	14	25		15	15	80	50		20	16		16	20						6
10			1	2	2		2	2	2	2	0		2	2		2	2					2

Test no.	21		22		23		24		25		26		27		28		29		30			
	Specimen no.	Drop	Eject																			
1			16	25	22		23	23	27	19		23	25		25	19		19		24		24
2			22	13	18		19	19	21	23		23	25		25	19		19		21		21
3			22	24	24		23	23	26	19		19	31		31	23		23		15		15
4			29	25	14		21	21	32	20		20	23		23	19		19		15		15
5			10	17	25		26	26	27	27		27	26		26	32		32		30		30
6			72	21	17		16	16	23	19		18	19		19	16		16		15		15
7				32	38		18	18	50	32		25	28		28	32		32		32		32
8			2	2	10		2	2	2	1		3	2		2	2		2		1		1
9			5	13	21		8	8	50	5		5	9		9	6		6		30		30
10			2	1	2		2	2	2	2		6	4		4	2		2		2		2

	No air jet, even though TH value was exceeded
	Pulse Ratio Max Value 100 % was exceeded
	Otherwise false Pulse Ratio Value
X	Camera did not see the sample
Drop	1. Sample Fraction
Eject	2. Sample Fraction

Appendix VI – Measurement Data of Test material 1 on Detector 6

Test no.	1		2		3		4		5		6		7		8		9		10		
	Specimen no.	Drop	Eject																		
1		17	18	17	16	16	17	15	15	16	16	16	16	16	15	15	15	22	25	25	18
2		16	17	16	16	16	16	17	17	17	17	17	17	20	14	14	25	18	15	18	15
3		17	19	16	16	16	15	18	15	17	17	17	14	17	19	25	18	16	15	18	18
4		18	16	16	16	16	18	18	15	17	17	17	17	22	28	20	20	20	29	16	16
5		19	18	18	17	17	19	18	17	17	17	17	16	16	16	18	18	18	29	16	16
6	18		18	17	18	18	17	17	17	15	15	15	16	16	16	18	18	18	29	16	16
7		17	17	18	18	18	18	17	17	18	18	18	38	38	22	20	39	20	39	20	39
8		13	12	12	10	10	13	12	12	13	13	13	0	1	2	2	2	2	2	2	2
9		13	17	14	11	11	14	16	16	11	11	6	6	7	6	6	6	6	6	6	11
10		12	11	11	11	11	12	9	9	X	X	2	2	1	1	2	2	2	1	1	1

Test no.	11		12		13		14		15		16		17		18		19		20		
	Specimen no.	Drop	Eject																		
1	14		12	15	21	19	10	12	287	8	33	12	12	12	12	12	21	21	42	42	
2		19	15	16	13	13	18	10	19	19	23	16	16	16	15	15	29	29	13	13	13
3		19	17	10	10	10	10	10	30	16	16	26	26	26	15	15	31	17	17	17	17
4		9	26	26	27	28	28	24	17	21	21	28	28	21	11	27	26	26	26	26	26
5		23	19	19	20	20	24	24	24	24	24	14	14	21	23	29	29	29	29	29	29
6		17	20	20	25	25	22	22	17	12	12	14	14	14	15	18	18	18	18	18	18
7		28	20	20	25	25	22	22	23	16	16	20	20	20	18	25	25	25	25	25	25
8		1	4	3	3	3	1	1	1	6	6	1	1	6	2	2	2	2	2	2	2
9		13	8	5	5	5	9	9	13	4	4	21	21	19	0	0	0	0	0	0	0
10		1	2	2	2	2	2	2	2	2	2	2	2	2	3	3	3	3	3	3	3

Test no.	21		22		23		24		25		26		27		28		29		30		
	Specimen no.	Drop	Eject																		
1		32	11	22	20	20	18	16	21	21	25	19	19	22	22	15	15	11	11	11	11
2		24	22	22	22	22	20	20	19	19	23	14	14	24	24	28	28	18	18	18	18
3		18	28	28	22	22	20	20	15	15	19	12	12	26	26	28	28	17	17	17	17
4		17	18	18	18	18	19	19	8	8	18	17	17	17	17	17	17	17	17	17	17
5	22		26	23	28	28	23	23	18	18	24	22	22	28	28	22	22	34	34	34	34
6		14	23	13	16	16	10	10	21	21	19	40	40	20	20	21	21	17	17	17	17
7		21	13	13	36	36	10	10	10	10	33	29	29	32	32	10	10	15	15	15	15
8	8		2	2	1	1	4	4	3	3	3	81	81	1	1	2	2	0	0	0	0
9		21	8	8	14	14	6	6	5	5	12	81	81	43	43	3	3	25	25	25	25
10	2		3	3	1	1	2	2	8	8	2	5	5	2	2	2	2	2	2	2	2

	No air jet, even though TH value was exceeded
	Pulse Ratio Max Value 100 % was exceeded
	Otherwise false Pulse Ratio Value
X	Camera did not see the sample
Drop	1. Sample Fraction
Eject	2. Sample Fraction

Appendix VII – Frequency Distributions for Test Material 1 Samples

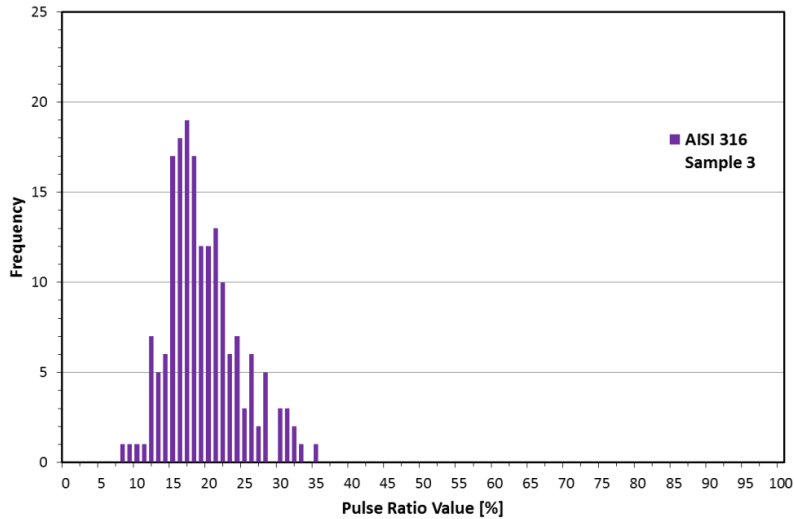


Figure 55. The pulse frequencies of test material 1, Sample 3 on all detectors.



Figure 56. Test material 1, Sample 3.

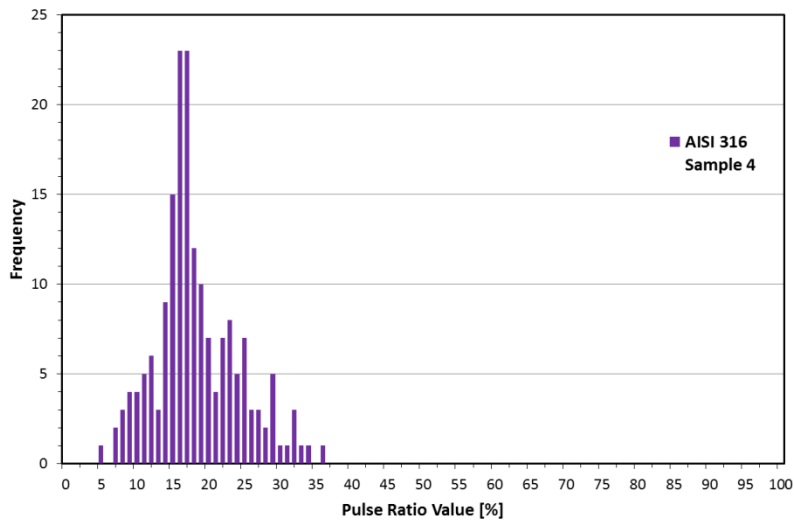


Figure 57. The pulse frequencies of test material 1, Sample 4 on all detectors.



Figure 58. Test material 1, Sample 4.

Appendix VII – Frequency Distributions for Test Material 1 Samples

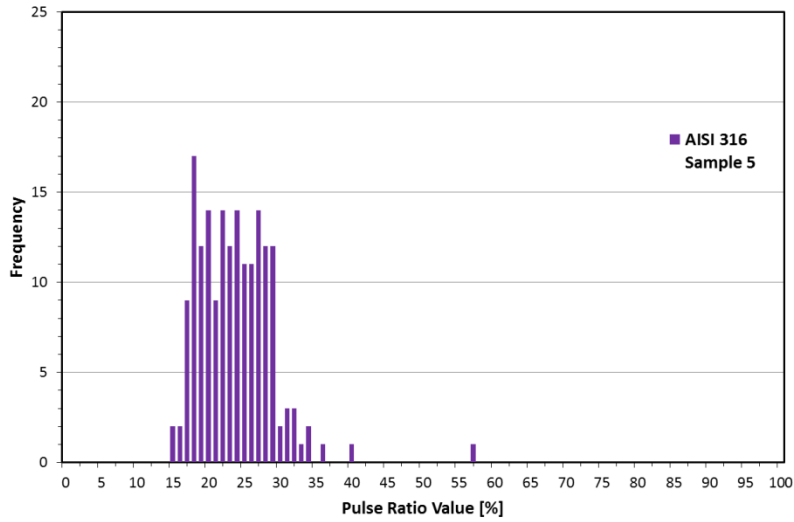


Figure 59. The pulse frequencies of Sample 5 on all detectors.



Figure 60. Test material 1, Sample 5.

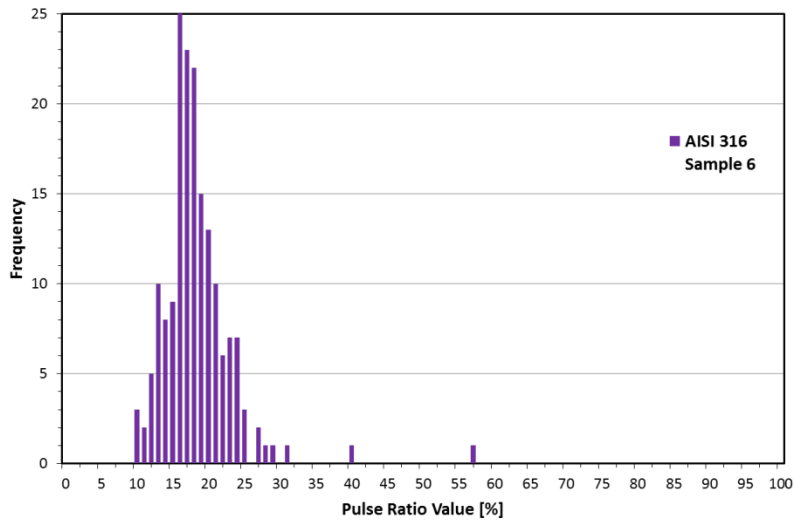


Figure 61. The pulse frequencies of Sample 6 on all detectors.



Figure 62. Test material 1, Sample 6.

Appendix VII – Frequency Distributions for Test Material 1 Samples

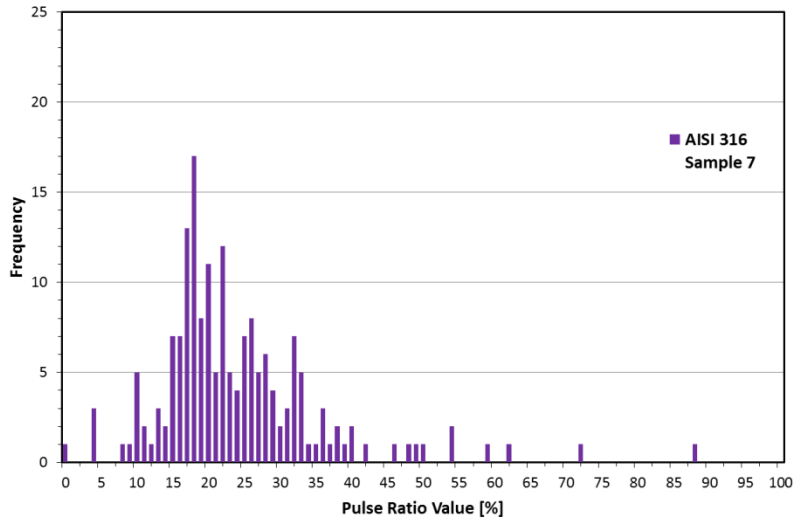


Figure 63. The pulse frequencies of test material 1, Sample 7 on all detectors.



Figure 64. Test material 1, Sample 7.

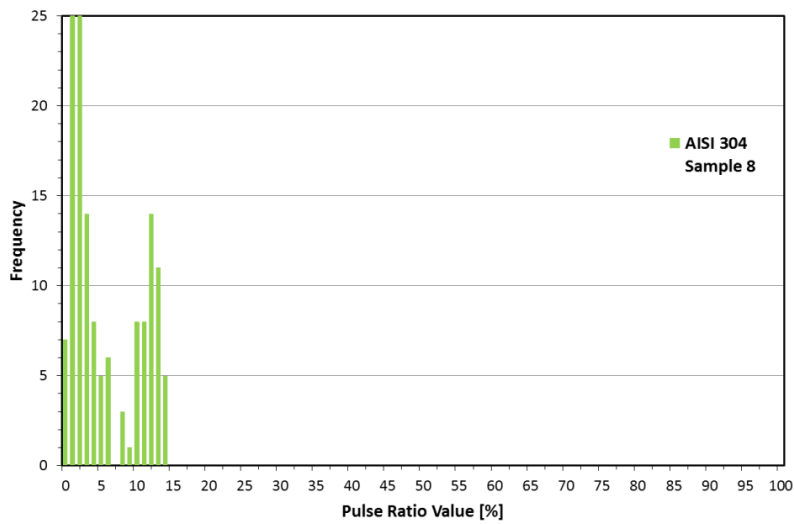


Figure 65. The pulse frequencies of test material 1, Sample 8 on all detectors.



Figure 66. Test material 1, Sample 8.

Appendix VII – Frequency Distributions for Test Material 1 Samples

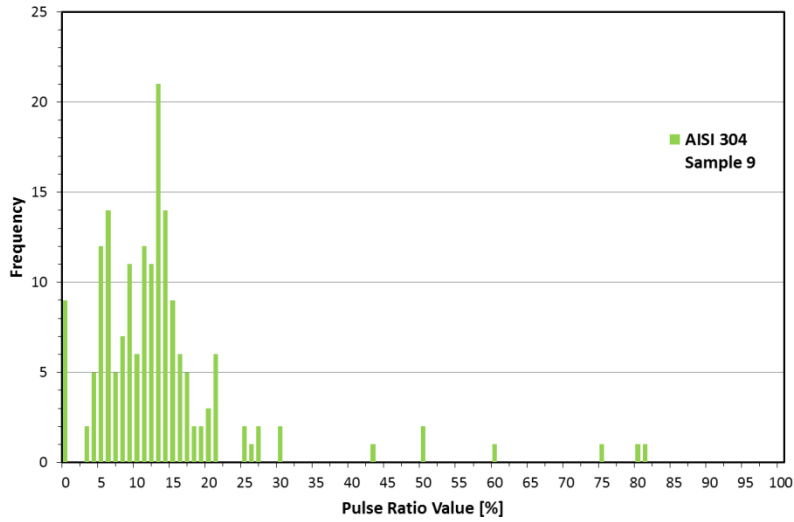


Figure 67. The pulse frequencies of test material 1, Sample 9 on all detectors.



Figure 68. Test material 1, Sample 9.

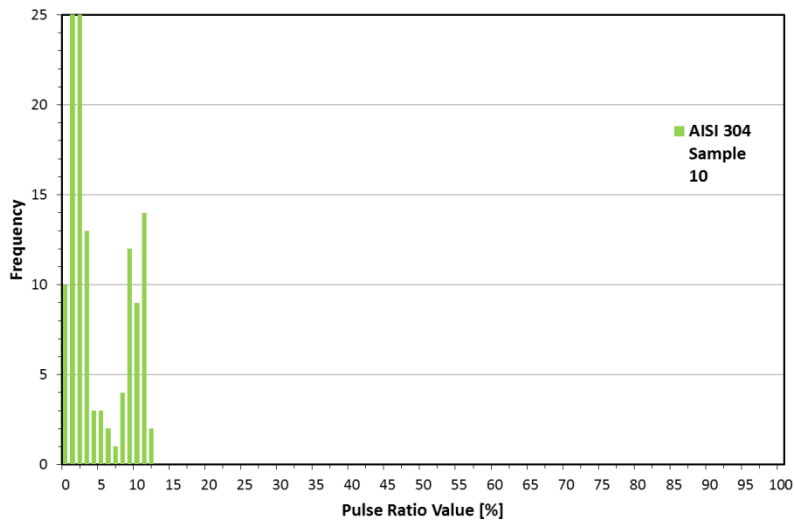


Figure 69. The pulse frequencies of test material 1, Sample 10 on all detectors.



Figure 70. Test material 1, Sample 10.

Appendix VIII – Measurement Data of Test Material 2 on Detector 1

Test no.	1		2		3		4		5		6		7		8		9		10	
Specimen no.	Drop	Eject																		
1		12		12		14		12		11		12		13		11		11		12
2	40		44		40		43		46		43		44		40		40		44	
3		41		37		39		40		40		40		38		40		39		39
4	46		X		X		54		X					55		59		62		56
5	95		95		94		94		92		96		95		95		96		96	
6	1		0.4		1		0.4		0.4		1		1		3		1		1	0.8
7	0.9		0.8		0.9		1		0.7		0.6		1		0.8		0.8		0.8	
8	0.3		0.8		0.5		1		0.7		0.6		2		1		2		2	0.4

Test no.	11		12		13		14		15		16		17		18		19		20	
Specimen no.	Drop	Eject																		
1		12		12		11		13		11		11		11		13		12		10
2	42			42	40			38		38		41		41		39		39		37
3		39		40		37		34		37		33		36		34		35		36
4	X		X		49		56		47		58		X		50		X		X	
5		95		92		86		84		83		88		84		85		84		86
6	1		1		1		0.7		2		1		1		2		2		2	
7	2		0.5		1		0.4		0.5		0.9		0.5		0.6		0.5		0.7	
8	2		0.8		0.7		2		0.5		1		0.2		0.6		1		0.8	

Test no.	21		22		23		24		25		26		27		28		29		30	
Specimen no.	Drop	Eject																		
1		13		10		11		10		11		11		9		11		12		10
2		39		38		39		39		38		37		42		41		34		36
3	37			38		37		35		34		35		32		35		34		34
4	48			43		X		47		X		X		X		X		X		X
5	87			87		84		89		86		88		85		89		87		86
6	1		1		0.3		0.7		1		0.4		1		4		1		0.9	
7	0.8		0.5		0.8		0.6		0.5		0.5		0.1		0.6		0.8		0.8	
8	0.4		0.3		0.4		0.5		0.5		1		0.5		1		0.5		1	

	No air jet, even though TH value was exceeded
	Pulse Ratio Max Value 100 % was exceeded
	Otherwise false Pulse Ratio Value
X	Camera did not see the sample
Drop	1. Sample Fraction
Eject	2. Sample Fraction

Appendix VIII – Measurement Data of Test Material 2 on Detector 2

Test no.	1		2		3		4		5		6		7		8		9		10	
Specimen no.	Drop	Eject																		
1		13	38	45	12	12	42	12	41	12	11	13	43	13	43	13	39	45	12	14
2		38		41	43		38		37		40	43		40		38		38		39
3	38			X	X		38		X		X	57		58		45		X		39
4	X			X	X		94		96		93		94		94		95		95	95
5		94		93	2		1		0.9		1		0.4	3		1		1		2
6	0.4			0.4	1		0.3		1		0.5		1	1		0.7		0.5		
7	1			0.8	0.4		0.3		0.1		0.4		1	0.8		0.7		0.6		
8	0.3			0.7																

Test no.	11		12		13		14		15		16		17		18		19		20	
Specimen no.	Drop	Eject																		
1		12		12	11		14		12		11		14		12		13		13	
2	42			45	43		41		42		43		42		44		44		41	
3		40		39	40		40		42		38		41		36		41		40	
4	46			49	52		46		47		51		54		59		X		X	
5		93		93	95		95		92		93		94		95		95		94	
6	2			1	0.4		2		2		0.4		2		1		7		1	
7	1			1	0.7		0.8		0.9		0.6		1		0.7		0.8		1	
8	1			0.4	0.7		0.6		1		0.5		0.9		0.5		0.9		0.8	

Test no.	21		22		23		24		25		26		27		28		29		30	
Specimen no.	Drop	Eject																		
1		14		12	13		14		12		12		13		12		12		12	
2		45		48		39		43		42		44		41		39		47		44
3		38		38	39		39		38		38		39		38		40		40	
4	63			47	61		54		51		58		X		55		57		56	
5		92		94	95		94		93		92		93		93		95		93	
6	2			150	X		1		1		1		1		0.4		1		0.9	
7	0.7			0.5	0.9		0.2		0.4		0.5		0.4		0.7		1		0.9	
8	0.6			0.4	1		0.4		0.2		1		0.8		1		0.1		0.9	

	No air jet, even though TH value was exceeded
	Pulse Ratio Max Value 100 % was exceeded
	Otherwise false Pulse Ratio Value
X	Camera did not see the sample
Drop	1. Sample Fraction
Eject	2. Sample Fraction

Appendix VIII – Measurement Data of Test Material 2 on Detector 3

Test no.	1		2		3		4		5		6		7		8		9		10	
Specimen no.	Drop	Eject																		
1		13		12		11		12		13		12		11		12		12		13
2		43		36		42		43		44		41		39		39		42		44
3		35		40		40		40		41		37		40		37		40		39
4		50		52		55		51		59		50		46		47		52		53
5		94		93		93		93		94		94		94		94		94		95
6	1		2		0.6		0.7		2		1		0.3		0.8		2		1	
7	0.9		0.3		0.6		0.8		0.8		0.8		0.4		0.5		0.8		0.3	
8	0.7		0.3		0.4		0.9		2		0.5		0.7		0.7		0.4		1	

Test no.	11		12		13		14		15		16		17		18		19		20	
Specimen no.	Drop	Eject																		
1		15		12		12		10		12		12		11		13		11		12
2		41		39		39		37		37		40		43		41		40		39
3		39		38		37		37		34		38		37		34		32		36
4		57		52		51		39		43		52		42		48		50		40
5		95		93		91		89		89		89		88		89		86		88
6	0.4		93		2		1		1		1		1		2		1		1	
7	1		0.6		0.9		0.5		0.9		0.6		0.7		1		0.6		0.6	
8	1		0.7		0.3		0.5		0.8		0.2		1		0.5		0.2		0.3	

Test no.	21		22		23		24		25		26		27		28		29		30	
Specimen no.	Drop	Eject																		
1		11		12		9		13		13		12		13		13		11		13
2		40		41		39		42		47		43		40		43		44		43
3		39		36		37		38		40		40		37		39		40		43
4		48		55		45		54		52		54		52		56		45		61
5		89		90		88		93		93		51		94		94		90		94
6	1		X		1		0.4		2		1		1		3		4		0.9	
7	0.4		0.3		0.5		0.8		0.7		0.8		0.9		0.9		1		1	
8	0.5		0.6		0.7		2		1		0.9		2		1		2		0.6	

	No air jet, even though TH value was exceeded
	Pulse Ratio Max Value 100 % was exceeded
	Otherwise false Pulse Ratio Value
X	Camera did not see the sample
Drop	1. Sample Fraction
Eject	2. Sample Fraction

Appendix VIII – Measurement Data of Test Material 2 on Detector 4

Test no.	1		2		3		4		5		6		7		8		9		10	
Specimen no.	Drop	Eject																		
1	10	14	12	13	13	13	12	13	13	13	13	13	13	13	12	12	13	13	12	12
2		42	43	44	45	44	43	44	47	44	47	41	43	41	43	44	44	44	41	41
3		38	38	40	39	37	38	39	39	39	39	39	39	39	38	38	39	39	38	38
4		47	53	50	53	49	49	53	60	60	55	62	62	62	50	50	60	60	56	56
5		92	93	93	93	93	93	93	92	92	93	94	94	94	94	94	94	94	93	93
6	0.8	3	2	4	2	4	4	4	0.7	2	2	0.8	0.8	1	1	3	3	1.9	1.9	
7	0.9		0.6				1	1	1	0.8	0.8	1	1	1	1	1	1	0.6	0.6	
8	0.6		0.4				1	1	1	1	1	0.9	0.9	0.6	0.6	2	2	0.7	0.7	

Test no.	11		12		13		14		15		16		17		18		19		20	
Specimen no.	Drop	Eject																		
1		13	11	14	14	14	13	14	12	12	11	11	14	11	11	12	12	11	11	11
2		41	41	42	42	42	42	42	40	40	39	45	45	43	43	46	46	42	42	42
3		37	38	38	38	38	40	37	38	38	38	40	40	41	41	37	37	33	33	33
4		54	58	44	44	44	53	52	58	58	58	45	45	51	51	44	44	50	50	50
5		91	94	92	92	92	92	92	92	94	94	94	94	93	93	92	92	92	92	92
6	2	0.8	0.7	1	0.7	1	1	1	1	0.7	2	2	2	2	4	4	4	0.8	0.8	
7	1	0.4	0.8	1	0.8	1	1	1	0.7	1	1	1	1	1	1	1	1	1	1	1
8	1	0.6	2	0.5	2	0.8	1	1	0.8	1	1	0.4	0.4	2	2	0.2	0.2	1	1	1

Test no.	21		22		23		24		25		26		27		28		29		30	
Specimen no.	Drop	Eject																		
1		11	11	12	12	12	13	13	13	13	13	13	13	13	12	13	13	12	12	12
2		40	42	42	42	42	42	42	45	44	44	42	44	44	42	43	43	42	42	42
3		40	38	38	38	38	38	38	39	35	35	39	39	39	38	38	39	39	39	39
4		56	51	47	47	47	61	47	47	53	53	54	54	48	48	48	48	42	42	42
5		93	93	92	92	92	92	92	91	91	91	91	90	93	93	92	92	92	92	92
6	2.0	0.3	1	1	1	2	2	2	0.9	0.9	0.9	1	1	0.7	0.7	2	2	X	X	X
7	1.3	0.9	0.2	0.9	0.2	0.9	0.9	0.9	1	1	1	1	0.9	0.7	0.7	0.8	0.8	1	1	1
8	0.1	0.3	1	0.8	1	0.8	0.8	0.8	1	1	1	1	0.8	0.7	0.7	0.5	0.5	0.9	0.9	0.9

	No air jet, even though TH value was exceeded
	Pulse Ratio Max Value 100 % was exceeded
	Otherwise false Pulse Ratio Value
X	Camera did not see the sample
Drop	1. Sample Fraction
Eject	2. Sample Fraction

Appendix VIII – Measurement Data of Test Material 2 on Detector 5

Test no.	1		2		3		4		5		6		7		8		9		10	
Specimen no.	Drop	Eject																		
1		12		13	13			12		13		13		12		11		12		11
2		44		42		41		43		38		41		44		41		43		42
3		38		37		37		39		37		38		38		39		39		35
4		56	X			48	X		52		X			56	X		X		55	
5		92		93		95		92		92		91		91		93		91		91
6	1		1		1		3		1		1		2		0.8		1		2	
7	1		1		2		1			2	0.6		1		0.8		1		1	
8	1		0.7		0.8		1		0.8		2		2		1		0.8		1	

Test no.	11		12		13		14		15		16		17		18		19		20	
Specimen no.	Drop	Eject																		
1		12		13		12		13		12		11		13		13		12		13
2		48		40		46		41		44		42		43		40		41		43
3		40		38		40		38		39		40		38		40		37		41
4		64		58	56		X		44		44			51	50			59		51
5		92		92		92		92		93		92		93	93			92		93
6	3		1	1	1		1		3		2		2		0.8		0.8		0.4	
7	1		1		0.9		1		1		1		1		1		1		1	
8	2		0.6		0.8		2		0.7		1		1		1		0.5		0.8	

Test no.	21		22		23		24		25		26		27		28		29		30	
Specimen no.	Drop	Eject																		
1		12	12		14		13		12		14		12		13		12		11	
2		44	44		38		40		40		42		42		40		42		41	
3		38	37		40		39		37		38		42		36		36		37	
4	X		48		45		56		50		51		X		54				60	
5		93	48		89		92		90		92		89		55		87		89	
6	1		0.7		1		2		2		2		1		1		2		1	
7	0.8		2		2		1		0.8		1		1		1		1		0.8	
8	2		1				1		1		0.6		1		1		1		0.3	

	No air jet, even though TH value was exceeded
	Pulse Ratio Max Value 100 % was exceeded
	Otherwise false Pulse Ratio Value
X	Camera did not see the sample
Drop	1. Sample Fraction
Eject	2. Sample Fraction

Appendix VIII – Measurement Data of Test Material 2 on Detector 6

Test no.	1		2		3		4		5		6		7		8		9		10	
Specimen no.	Drop	Eject																		
1		13		13		13		12		12		14		12		14		13		14
2		42		44		42		40		42	49		46		43		43		45	
3		41		40		42		41		41	39		43		36		39		39	
4	X			56	X			56		56	56		X		51		X		X	
5		97		93		96		98		96		96		96		96		96		98
6	0.8		1		0.9		1		0.3		1		1		1		2		1	
7	0.8		1		0.6		1		1		1		1		0.9		1		1	
8	1		0.5		0.6		0.8		0.7		2		1		0.9		2		0.5	

Test no.	11		12		13		14		15		16		17		18		19		20	
Specimen no.	Drop	Eject																		
1		13		12		13		12		13		13		12		12		12		13
2		40		44		43		41		43		40		42		41		45		39
3		38		42		38		40		40		35		40		42		38		37
4	X			X		X		X		X		X		X		X		50		X
5		95		92		95		69		96		95		94		94		94		91
6	0.8		0.7		1		3		3		1		0.9		1		0.7		0.8	
7		4		1		0.9		3		0.7		1		0.7		0.6		1		0.6
8	0.5		1		0.8		0.9		2		2		1		1		1		0.5	

Test no.	21		22		23		24		25		26		27		28		29		30	
Specimen no.	Drop	Eject																		
1		13		12		13		12		11		11		11		12		12		12
2		42		45		43		41		40		41		45		43		44		37
3		38		38		38		39		38		39		41		39		39		38
4		57		57		X		54		58		53		X		X		X		X
5		79		93		93		94		95		93		94		94		89		93
6	0.4		1		1		0.6		3		3		2		2		2		1	
7	0.6		0.5		0.8		2		0.9		1		0.6		1		1		1	
8	0.8			5	1		0.5		1		0.6		1		0.7		0.5		0.7	

	No air jet, even though TH value was exceeded
	Pulse Ratio Max Value 100 % was exceeded
	Otherwise false Pulse Ratio Value
X	Camera did not see the sample
Drop	1. Sample Fraction
Eject	2. Sample Fraction

Appendix IX – Frequency Distributions for Test Material 2 Samples

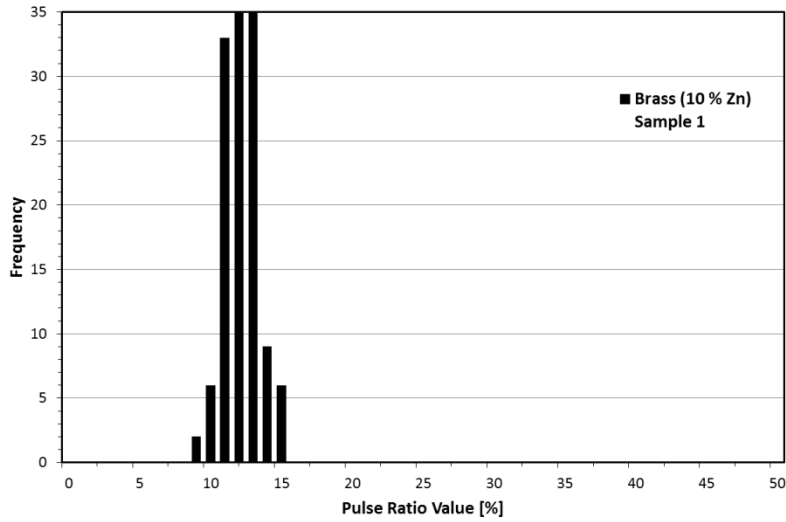


Figure 71. The pulse frequencies of test material 2, Sample 1 on all detectors.



Figure 72. Test material 2, Sample 1.

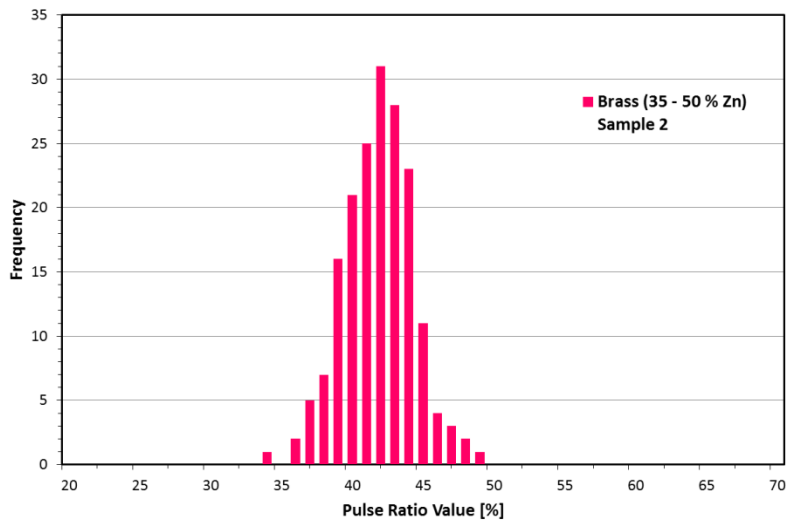


Figure 73. The pulse frequencies of test material 2, Sample 2 on all detectors.



Figure 74. Test material 2, Sample 2.

Appendix IX – Frequency Distributions for Test Material 2 Samples

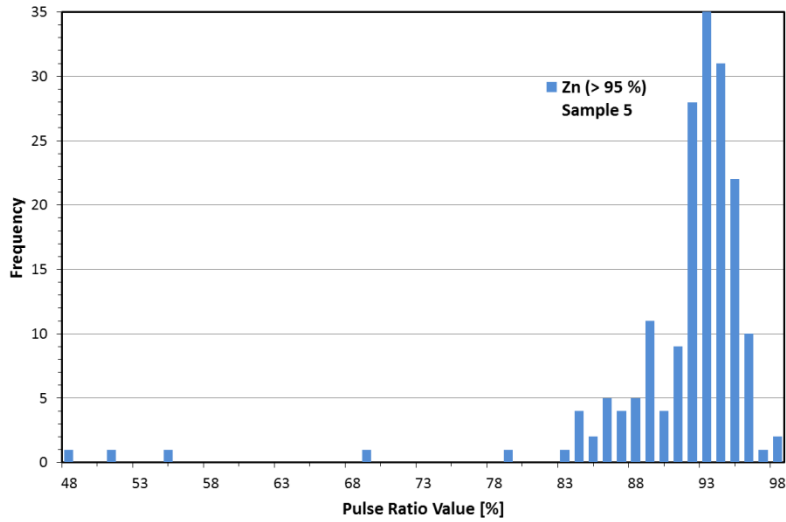


Figure 75. The pulse frequencies of test material 2, Sample 5 on all detectors.

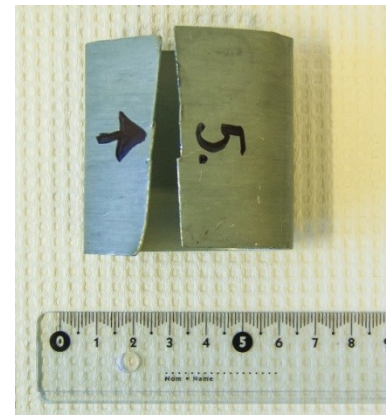


Figure 76. Test material 2, Sample 5.

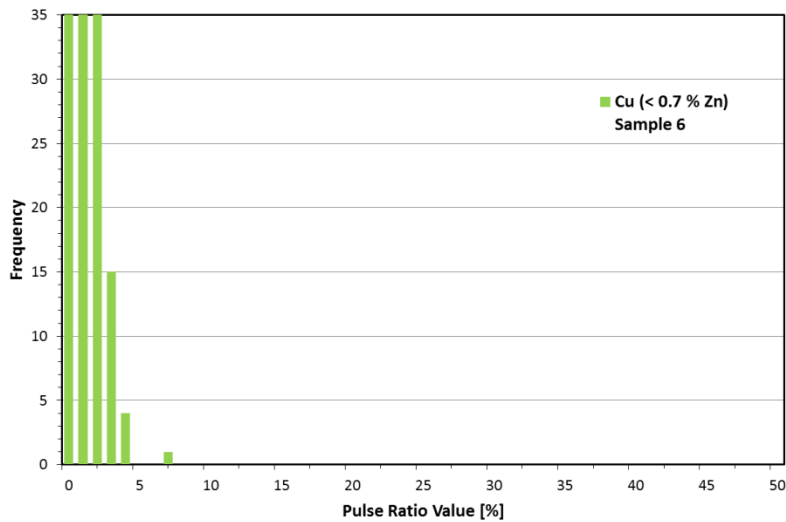


Figure 77. The pulse frequencies of test material 2, Sample 6 on all detectors.



Figure 78. Test material 2, Sample 6.

Appendix IX – Frequency Distributions for Test Material 2 Samples

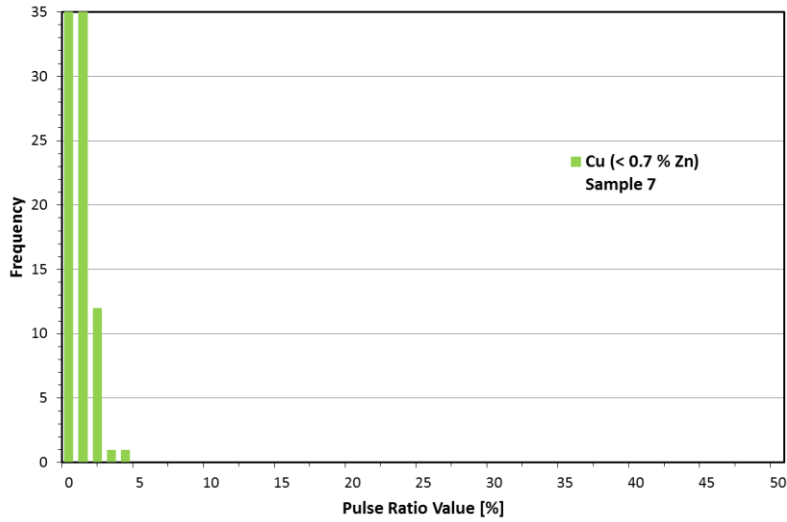


Figure 79. The pulse frequencies of test material 2, Sample 7 on all detectors.



Figure 80. Test material 2, Sample 7.

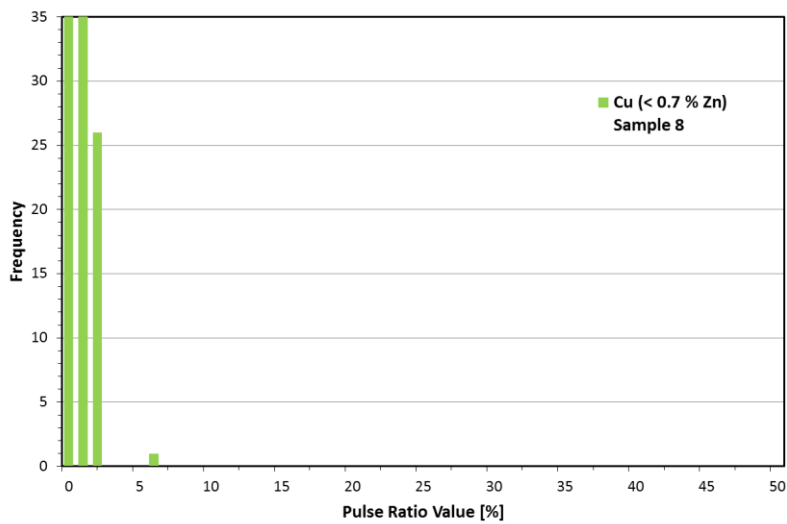


Figure 81. The pulse frequencies of test material 2, Sample 8 on all detectors.



Figure 82. Test material 2, Sample 8.

Appendix X – Test Material 3 Data Sheet

The samples of test material 3 were all cut from one larger circuit board. Therefore only one sample was measured and the results are presented in Table 20 below. The handheld XRF analyser did not identify gold at all. The coating thickness is app. 0.05 μm .

Table 20. Test material 3, element composition analysis

Element	[%]
Cu	69.61
Ni	28.48
Zn	0.76
Al	0.52
Si	0.83
P	5.39
Se	0.21
Pb	0.01

Appendix XI – Measurement Data of Test Material 3

The results of test material 3 pre-tests are shown in Table 21 below. Two measurements with each detector were made.

Table 21. The results of pre-tests of test material 3

Sample	Det. 1	Det. 1	Det. 2	Det. 2	Det. 3	Det. 3	Det. 4	Det. 4	Det. 5	Det. 5	Det. 6	Det. 6
1	12	25	17	23	28	33	15	10	16	33	24	36
2	X	X	X	X	X	X	X	X	X	X	X	X
3	X	X	X	X	X	X	X	X	X	X	X	X
4	X	16	X	5	5	8	20	3	6	2	X	8
5	8	9	4	4	14	12	13	11	8	10	29	X
6	X	X	X	X	X	X	X	X	X	X	X	X
7	13	19	11	30	26	23	15	21	12	X	15	21
8	X	X	X	X	X	X	X	X	X	X	X	X

X Camera did not identify the sample

Appendix XII – The Peak Data of Test Material 3 Measurements

Two spectra were measured from test material 3 with measuring times of 5 s and 0.3s. These were presented in Chapter 9.4, in Figures 43 and 44. The peak data from these spectra is given below in Tables 22 and 23.

Table 22. The peak data of test material 3, sample 1 spectrum (5 s)

Start	End	Net Area	Gross Area	Centroid (N)	Status
7.31	7.67	5003	5379	7.47	GOOD
7.75	8.4	22648	23128	8.05	GOOD
8.53	8.66	0	308	-0.06	BAD
8.76	9.12	1510	1886	8.91	GOOD
9.54	9.84	201	363	9.72	GOOD
11.25	11.72	248	363	11.5	GOOD

Table 23. The peak data of test material 3, sample 1 spectrum (0.3 s)

Start	End	Net Area	Gross Area	Centroid (N)	Status
7.31	7.67	289	337	7.48	GOOD
7.75	8.4	1283	1388	8.05	GOOD
8.53	8.66	0	14	-0.06	BAD
8.76	9	55	110	8.91	MARGINAL
9.65	9.84	0	19	-0.06	BAD
11.38	11.57	0	13	-0.06	BAD